Modelling the Laser Treatment of Vascular Lesions.

A thesis
submitted for the degree of
Doctor of Philosophy in Physics
in the
University of Canterbury
by

John W. Pickering

University of Canterbury
February 1990

CONTENTS

Abstract 1

1 Introduction 3
- 1.1 Incidence and Psychology . . . 3
- 1.2 Treatments Prior to the Laser . . . 5
- 1.3 The Physics of Laser Treatments . . . 5
- 1.4 The First Laser Treatments . . . 7
- 1.5 The Status Quo in 1987 . . . 8
- 1.6 The 20 W Copper Vapour Laser . . . 9
- 1.7 An Introduction to the Contents of this Thesis . . . 9
  - 1.7.1 Chapter 2. Physiology of human skin. . . . 10
  - 1.7.2 Chapter 3. Histology. . . . 10
  - 1.7.3 Chapter 4. Techniques and results. . . . 11
  - 1.7.4 Chapter 5. Automatic scanning. . . . 11
  - 1.7.5 Chapter 6. Radiative transfer. . . . 11
  - 1.7.6 Chapter 7. The model. . . . 11
  - 1.7.7 Chapter 8. The optimal treatment. . . . 12
  - 1.7.8 Chapter 9. The clinical treatment. . . . 12
  - 1.7.9 Chapter 10. Discussion. . . . 13

2 Physiology of human skin 15
- 2.1 Epidermis . . . 15
- 2.2 Dermis . . . 18
- 2.3 Blood Vessels . . . 18
- 2.4 Telangiectasia and Spider Naevi . . . 20
- 2.5 Port Wine Stains . . . 22

3 Histology 27
- 3.1 Non-yellow Light Lasers . . . 27
  - 3.1.1 Carbon dioxide . . . 27
  - 3.1.2 Argon . . . 28
- 3.2 Yellow Light Lasers . . . 29
  - 3.2.1 Pulsed dye . . . 29
  - 3.2.2 Continuous wave dye . . . 33
  - 3.2.3 Copper vapour . . . 33
- 3.3 Melanin Absorption . . . 34

4 Techniques and Results **35**
- 4.1 Clinical Technique . . . 35
- 4.2 Clinical Results . . . 36
- 4.3 Questionnaire . . . 37

5 Automatic scanning **39**
- 5.1 Why A Robot? . . . 39
- 5.2 The Design . . . 40
- 5.3 The Operation . . . 40

6 Radiative transfer **43**
- 6.1 The Nature of Scattering . . . 43
- 6.2 The Transport Equation . . . 45
- 6.3 Solutions to the Transport Equation . . . 46
  - 6.3.1 Beer's law . . . 46
  - 6.3.2 Kubelka-Munk . . . 47
  - 6.3.3 The diffusion approximation . . . 47
  - 6.3.4 Seven flux model . . . 50
  - 6.3.5 The modified Henyey-Greenstein phase function . . . 50
  - 6.3.6 Monte Carlo calculations . . . 52
  - 6.3.7 Summary of solutions to the transport equation . . . 53

7 The Model **57**
- 7.1 Yellow Light . . . 57
- 7.2 Treatment Modalities . . . 58
- 7.3 The Numerical Calculations . . . 59
  - 7.3.1 Previous models . . . 59
  - 7.3.2 Assumptions . . . 61

8 The Optimal Treatment **65**
- 8.1 The Damage Criteria . . . 65
- 8.2 Individual Vessels . . . 66
  - 8.2.1 Vessel size . . . 66
  - 8.2.2 Coagulation temperature and endothelial cell thickness . . . 66
- 8.3 Damage Integral . . . 67
  - 8.3.1 The integral . . . 67
  - 8.3.2 Haemoglobin as a protein . . . 69
- 8.4 Scattered Light . . . 72
- 8.5 Vessel Depth . . . 78

9 The Clinical Treatment 83
9.1 Illumination Times 83
9.1.1 Long illumination times (Blanching) 83
9.1.2 Short illumination times (Purpura) 85
9.1.3 Comparison between illumination times 87
9.2 A New Optimal Wavelength? 87
9.2.1 585 and 590 nm with short illumination times 89

10 Discussion 95
10.1 Conclusion 1: The 20 Watt Copper Vapour Laser 95
10.2 Conclusion 2: The Optimal Damage 95
10.3 Conclusion 3: The Model of the Physics 96
10.4 Conclusion 4: Understanding the Treatment Protocols 96
10.5 Summary 97

References 99

A Pickering et al. 1989a 109

B Walker et al. 1989 111

C Pickering et al. 1989b 113

D Pickering et al. 1990a 115

E Pickering et al. 1990b 117

F Thermal relaxation time calculations 119

G Acknowledgements 123

List of Figures

2.1 The epidermis 16
2.2 Melanin absorption 17
2.3 Blood vessel plexus 19
2.4 Haemoglobin absorption 21
2.5 Facial cutaneous nerve regions 23
2.6 Typical port wine stains 24

5.1 The scanner 41

6.1 Irradiance per unit area 44
6.2 The diffusion approximation 48
6.3 The diffuse distribution 49
6.4 Seven flux 51
6.5 Henyey-Greenstein light distribution at 100 and 500 μmdepths . . . 52
6.6 Approximations to space irradiance 54

8.1 Optimal temperature profile 70
8.2 Optimal damage profile 70
8.3 Absorption of haemoglobin as a function of temperature 71
8.4 Temperature profile with haemoglobin denaturation 73
8.5 Damage profile with haemoglobin denaturation 73
8.6 Incident light on vessels of differing depths 74
8.7 Absorption within a vessel according to the diffusion approximation 75
8.8 Temperature profile with collimated incident light 76
8.9 Temperature profile with diffuse incident light 77
8.10 Comparison of collimated and diffuse incidence 77
8.11 Monte Carlo temperature profile at 300 μm 80
8.12 Monte Carlo temperature profile at 500 μm 80
8.13 Monte Carlo temperature profile at 150 μm 81

9.1 Temperature profile for 30 ms illumination 84
9.2 Damage profile for 30 ms illumination damage 84
9.3 Temperature profile for 0.45 ms, 4660 W/cm^2 (2.1 J/cm^2), no vaporisation 86
9.4 Temperature profile for 0.45 ms, 4660 W/cm^2 (2.1 J/cm^2), vaporisation 86
9.5 Temperature profile for 0.45 ms, 4660 W/cm^2 (2.1 J/cm^2), vaporisation and central cross section 87

9.6 Comparison between long, optimal, and short illumination times . . 88
9.7 Comparison of optimal and purpura producing (with vaporisation) illumination times 88
9.8 Wavelength, depth, and vessel size 90
9.9 Short pulse length temperature profile without vaporisation at 577 nm 91
9.10 Short pulse length temperature profile without vaporisation at 585 nm 91
9.11 Short pulse length temperature profile without vaporisation at 590 nm 92
9.12 Short pulse length temperature profile with vaporisation at 577 nm . 92
9.13 Short pulse length temperature profile with vaporisation at 585 nm . 93
9.14 Short pulse length temperature profile with vaporisation at 590 nm . 93
9.15 Cross section comparisons without vaporisation 94
9.16 Cross section comparisons allowing vaporisation 94

List of Tables

2.1 Skin types 18
2.2 The distribution of lesions as presenting for treatment as a function of nerve regions 25

3.1 Pulsed dye laser histology 30
3.1 Pulsed dye laser histology (continued) 31
3.2 Continuous wave yellow light laser histology 32

4.1 The treatments 37

7.1 Optical properties of skin and blood 64

8.1 Damage integral constants 68
8.2 Optical parameters used in Monte Carlo calculations 79
8.3 Variation in irradiance with depth 79

ABSTRACT

This thesis investigates four aspects of the laser treatment of vascular lesions. The first is the use of a copper vapour laser at a wavelength of 578 nm as a means for removal of these lesions. The second is an evaluation of the physiological conditions that lead to the removal of the ectatic vessels. The third is a numerical model that predicts the optimal treatment parameters. The fourth is an evaluation of the current treatment protocols.

A copper vapour laser at a wavelength of 578 nm has been used to treat over 500 vascular lesions. The chosen technique has been constrained by the available technology, but where possible has been based on histology, clinical investigation, and theoretical modelling of the physics of light interaction with vascular lesions. The treatment has been successful in the vast majority of cases and is at least as effacious as other reported techniques. The results of a patient survey indicated an emphatic approval of the treatment, with most patients feeling their treatment has resulted in a good change in appearance.

Histology has established that specific damage to the ectatic vessels of these vascular lesions is achieved to a greater extent than with the wavelengths of the argon laser. This also illustrated histological differences to the pulsed dye lasers which produce purpura rather than blanching. A model of the physics of the copper vapour laser treatment suggests the damage to the ectatic vessels is thermal rather than mechanical, this is supported by the histology. The optimal damage criteria has yet to be established, but is likely to be somewhere between the part thermal/part mechanical damage caused by the pulsed dye lasers and the totally thermal damage caused by the copper vapour laser.

A numerical model of the physics of illuminating ectatic blood vessels has been developed. Several criteria for optimal damage have been discussed. The model is used to produce optimal treatment parameters based on the damage criteria. These parameters are a wavelength of 577/578 nm, an irradiance of 400 to 3000 W/cm^2 and an illumination time of 1 to 10 ms.

Additionally, this model has been applied to the present treatment protocols. The results suggest that there is likely to be vaporisation of haemoglobin and a minimum of thermal damage with the short pulses from the pulsed dye lasers. The longer illumination times of the continuous wave lasers are likely to restrict the thermal damage to vessel lumen surroundings.

585 nm has been modelled as an alternative wavelength for pulsed dye laser technique. This wavelength produces greater coagulation of individual vessels and coagulation deeper within the dermis than at 577 nm.

Five papers on this work have been accepted for publication and are included in the appendices. Other parts of the work are discussed within the main body of this thesis.

CHAPTER 1 INTRODUCTION

A bright red lesion that covers a substantial portion of one side of a face is most likely to be a port wine stain (naevus flammeus), that is, a vascular birthmark consisting of ectatic (enlarged) blood vessels within the skin. The greater volume of blood within these vessels gives rise to the pink, red, or purple colour. Some other vascular lesions appear long after birth. These include; spider naevus, a small red spot, and facial rosacea or telangiectasia, ectatic vessels visible on the cheeks and nose. This thesis is concerned with the development of a methodology to remove these lesions. An integral part of this methodology has been a copper vapour laser, used to treat over 300 port wine stain patients. We wish to optimise the input treatment parameters so as to obtain the most satisfactory clinical result. This result may be defined in terms of the damage done to the ectatic vessels. The optimal damage is unknown. We have had to assume a damage criteria based on our knowledge of protein denature and cell necrosis. The treatment parameters include those of wavelength, illumination time, and irradiance. To find the optimal parameters which produce this damage we have constructed a numerical model. This model is based on the physics of the interaction of light with skin and blood, and on the thermal processes that take place within the skin as a result of this interaction.

1.1 Incidence and Psychology

A large proportion of infants are born with an abnormally coloured part of their body (50% or greater, Jacobs and Walton 1976). Often these take the form of salmon coloured patches on the eyelids or the nape of the neck[1]. Most of these salmon patches resolve in very early life. Some lesions such as the strawberry birthmark may persist for 5 to 7 years. The port wine stain usually appears a few days after birth and does not spontaneously resolve. Two studies of approximately 1000 infants recorded 3 (Jacobs and Walton 1976) and 4 (Pratt 1954) instances of port wine stains. The incidence of these lesions has often been quoted as 0.3 to 0.5% (Carruth and McKenzie 1986). Clearly, because of the rarity of these birthmarks, only two

[1] A patch on the eyelid is commonly known as an "angel's kiss" and one on the neck as a "stork bite".

studies of 1000 infants each leave a large margin for error in the percentage of those with these particular birthmarks. A port wine stain usually appears a few days after birth as a clearly defined pale salmon-pink patch. The colour is a consequence of the greater volume of blood within the lesion due to abnormally large blood vessels within the skin. The colour tends to darken with age sometimes becoming very purple and nodular. The rate of darkening depends on the individual.

In 1 to 2% of cases the central nervous system is involved, and this may result in mental retardation (the Sturge-Weber syndrome). Where the lesion extends into the sub-cutaneous tissue limb overgrowth may occur (Klippel-Trenaunary-Weber syndrome). The most common complication is glaucoma due to involvement of the intra-ocular area. Glaucoma occurs in 45% of those whose port wine stains involve this area (Carruth and McKenzie 1986). Unfortunately, involvement around the eye appears to be reasonably common, at least with those who have presented for treatment (14% of our patients).

Of the other cutaneous (of the skin) vascular lesions the strawberry birthmark is the most common in infants, but as it tends to spontaneously resolve we have not treated many of these lesions. Other lesions may develop later in life, in particular spider naevi and facial telangiectasia are very common in middle age.

Although benign, and usually providing no physical hindrance, port wine stains are often devastating to an individual. This is especially so with facial birthmarks. I am sure we all remember the taunts during our school days that were thrown at individuals who were in any way slightly out of the ordinary. The social pressures for personal attractiveness continue throughout adult life and have so for thousands of years. In medieval times a birthmark was thought of as evidence of service to the devil. Some societies believed a birthmark was a sign of reincarnation of someone who had previously had a similar birthmark. Now we may not display such superstition but the stigma remains and is perpetuated by such things as a multi-billion dollar cosmetics industry and the recording of birthmarks in passports and police records. As a consequence many of those with port wine stains are hindered in their self image and personal relationships. Lanigan and Cotterill (1989) have shown that feelings of self worthlessness often continue throughout adult life without the individual accepting the situation as *c'est la vie*. We have also noted the low self image amongst our patients (Pickering *et al.* 1990b, included in this thesis as appendix E).

Port wine stain recipients are not the only people who are affected psychologically. Parents often have feelings of guilt over some accident during pregnancy that they think may have caused the birthmark. Even if they realise that this was not the reason for the birthmark, they have to cope with having a child who is not viewed by society as normal, but as deformed.

1.2 Treatments Prior to the Laser

Many different treatment methods were tried prior to the advent of the laser as a dermatological tool. None of these methods had been consistently successful and many had damaging side effects. It is now known that two methods, X-ray and radiocative phospherous (^{32}P) treatments, have potentially lethal side effects. Other methods attempted have included: tattooing with a white pigment such as titaniumdioxide, electric cautery, cryotherapy, dermabrasion, and skin grafting. While some of these treatments may successfully remove the lesion (especially skin grafting) the result may not be an aesthetic improvement on the original lesion.

The majority of those with port wine stains have not undergone any of the above treatments. Instead they have been forced to learn to live with their lesion. Ways of living with their lesion may include: avoiding public situations, tailoring their dress so as not to draw attention to themselves or their lesions, and sometimes covering their lesion. The use of heavy "theatrical" makeup is common among females. However, this makeup is expensive and difficult to apply.

1.3 The Physics of Laser Treatments

I have written this thesis with the intention of presenting an overview of the status of laser treatment of vascular lesions as well as presenting the results of my research. Therefore, I shall outline some of the basic physics and units used, so that those unfamiliar with their use may gain some insight before proceeding to the rest of the thesis, and in particular the papers included in the appendices.

Light has long been known to be a cause of some medical conditions and a treatment for others. For example, melanoma is known to be due to excessive exposure to ultraviolet light. On the other hand ultraviolet light is used as a treatment for jaundice in infants[2].

Lasers as sources of light are useful in surgery and medicine because of the potential to obtain well directed, high intensity, monochromatic light beams.

Light is described in terms of its wavelength, quoted in billionths of a metre (nanometres, nm), its power (watts, W) which is the energy (joules, J) per second, and its intensity, or radiance, which is the power per square centimetre (W/cm^2). Often the intensity of a collimated beam (all the light is moving in the one direction) incident on the skin surface is called the incident irradiance. The irradiance is also the integral of the intensity over all angles, thus where the light is not collimated, such as within the skin, the magnitude of the intensity and the irradiance may differ. When considering the light distribution within the skin I shall differentiate between the intensity and the irradiance. Sometimes the total input of energy per square centimetre is as part of a description of laser treatment. This is the fluence (J/cm^2).

[2]Supposedly this treatment was discovered accidently when infants with jaundice recovered when left in the sunlight.

The light incident on the skin is usually a beam of circular cross-section. This we describe as the incident spot of a particular diameter. For any given laser power the intensity increases proportionally to the square of the decrease in diameter of the spot (for example if the spot diameter halves the intensity will quadruple). The light will not necessarily be an even intensity across the whole of the spot. For example many lasers produce a spot that has a beam profile rather like a ten gallon hat, greatest in the centre and least on the outside (a gaussian profile).

The method of delivering the light to the lesion is often via a fibre optic. This is a solid glass or quartz tube through which the light is transmitted. The end of the fibre is held at a certain distance above the lesion so that the spot on the lesion will be of a predetermined diameter and, having made a measurement of the light power as it emerges from the fibre, the incident irradiance is known. The length of time the light is on any one spot on the lesion we have called the illumination time. This time may be controlled in one of two ways. The first is to mechanically, optically, or electronically pulse the light so that at each spot there is a predetermined illumination time. Normally only one pulse of light is incident on any one point of the lesion, thus the illumination time is the same as the pulse length of the laser. The second method is to use a continuous wave or quasi-continuous wave laser and to move the light in a scanning fashion across the lesion. This is much like "colouring in" an area. The length of illumination time is determined by the speed at which the spot is scanned across the skin and the size of the spot. We define the scan rate as the time, on average, taken to scan the light across one square centimetre of lesion. I quote all illumination times in thousandths of a second (milliseconds, ms).

The light incident on the skin will either be reflected from the surface of the skin or will penetrate into the first skin layer, the epidermis. Within the epidermis some the light will be scattered or absorbed. Scattering occurs when there is an interaction of a photon with a molecule or atom. The probability of scattering events depends on the nature of the tissue. We note this probability in terms of the scattering coefficient which has the units of inverse centimetres (/cm) for that medium. Similarly at each event there is a probability of the photon being absorbed by the molecule or atom. This probability is expressed in terms of the absorption coefficient, again in units of inverse centimetres.

Within the epidermis the most likely absorber is the chromophore melanin. Melanin is a black substance that gives us our tanned or black skin colouring. Most other epidermal tissue is more likely to scatter the photon. Deeper within the skin is the dermis which contains the blood vessels (I give the measurements of all the cutaneous structures in terms of millionths of a metre, that is micrometres, μm). These blood vessels contain the chromophore haemoglobin which is contained within the erythrocytes (red blood cells). At most of the wavelengths used for laser treatment the haemoglobin is the primary absorber.

The absorption of photons by the melanin and haemoglobin leads to the generation and conduction of heat. It is this conduction of heat around the blood vessels

that we wish to model so as to attain an estimate of the temperatures around a blood vessel at any given time during and after illumination with the light. When we know this temperature distribution we are able to estimate the extent of damage to the proteins within and surrounding the vessels. The process of absorption of light within one specific structure so as to cause thermal damage to that structure has been called selective photothermolysis (Anderson and Parrish 1983).

1.4 The First Laser Treatments

The first dermatological use of a laser for the removal of vascular lesions was reported by Solomon *et al.* (1968). The lasers used were Ruby, Nd:YAG and Argon. Since then many other lasers have been used in the treatment of vascular lesions. I shall categorise these lasers according to the results of histology:

Non selective All cutaneous tissue types are approximately equally damaged by the light. In this category are the Ruby (694.3 nm), the Carbon Dioxide (10600 nm) and the Nd:YAG (1060 nm) lasers.

Semi selective Some tissues (chromophores) absorb a greater proportion of the incident light than others. This results in greater heating within and surrounding the absorbing structures in comparison to the non-absorbing tissues. For port wine stains the target chromophore is the haemoglobin within the ectatic vessels. At some laser wavelengths the difference between absorption by haemoglobin and absorption by other cutaneous tissues and chromophores (in particular melanin, the yellow/brown/black pigment of the skin) is small. In this category are the Argon ion lasers both untuned (488 to 514.5 nm) and tuned (usually to 514.5 nm).

Selective The absorption characteristics are such that the heat is able to be maintained close to or within the target vessels so that the damage done is only therapeutic. In this category are the pulsed dye lasers (577, 585 nm), the continuous wave dye lasers (540, 575, 577 nm), the copper vapour laser (578 nm) and the frequency doubled NdYag (530 nm).

The argon laser was originally accepted as the laser of choice. Its then potential rivals, the CO_2 and Nd:YAG lasers, both produce gross non specific damage in a similar fashion to dermabrasion. The argon was able to spare damage to some of the dermis through selective absorption of the argon wavelengths by the blood chromophore, that is haemoglobin. This laser has produced a large proportion of desirable results (Goldman *et al.* 1976, Apfelberg *et al.* 1976, Cosman 1980, Arndt 1984, Touquet and Carruth 1984, Craig *et al.* 1985, Apfelberg *et al.* 1987). However, there are a number of complications, the greatest of which is scarring (5 to 30% of the patients, see the previous papers referenced in this section and the comments in

Dixon *et al.* 1984a,b and Olbricht *et al.* 1987). Other common complications are hyperpigmentation and hypopigmentation. One of the causes of these complications was damage to the epidermis (the outer most skin layer) and upper dermis due to absorption of light by melanin. The concentration of melanin within the epidermis of an individual may vary from place to place on the individual and vary over a period of time. Thus, any one individual may respond to the treatment in a different manner depending on the site of the lesion and on the time of illumination. Obviously the melanin concentration also differs between individuals. These variations make obtaining a consistent treatment very difficult. The adverse effects are particularly difficult to avoid with children. As a consequence many clinicians do not treat children under the age of 12 to 14.

In 1981 Anderson and Parrish first discussed the use of 577 nm light to selectively target the ectatic vessels (Anderson and Parrish 1981b). This thesis is primarily concerned with the use of this yellow light (at 577 and 578 nm).

1.5 The Status Quo in 1987

I began research for this thesis in September 1987. I am indebted to the efforts of Mr Chris van Halewyn, Dr Phil Butler, and Mr Peter Walker who had conducted the previous research within the department (van Halewyn 1985 and van Halewyn 1987).

In 1982 plastic and reconstructive surgeon Mr Peter Walker began to utilise the physics department solid state group's argon laser for the treatment of birthmarks. From 1982 to 1985 this laser produced some encouraging results for what was a previously "untreatable" condition. During this time Mr Walker found the lesions responded better when the laser was tuned to 514.5 nm as opposed to 488 nm. Soon the physicists took interest and began to investigate the reasons for the efficacy of the treatment. Mr Chris van Halewyn undertook an Honours part three project in 1985 and later an MSc. Together with Dr Phil Butler he designed a prototype automatic scanning device to direct the light to the skin (see chapter 5). They also realised the potential of yellow light and as a consequence obtained a copper vapour laser. At the time I began this thesis the copper laser had been used for approximately 270 treatment sessions on a variety of lesions. It has now been used for over 1570 treatment sessions.

Dr Butler and Mr van Halewyn had developed an analytical model to attempt to determine the "optimal" treatment parameters. The most important of these parameters are those of laser wavelength, illumination time (the time over which a point within the lesion is illuminated) and the irradiance (power per unit area). The status quo in 1987 was an agreement of yellow (577/578 nm) light with an illumination time of:

1. less than the thermal relaxation time of the vessel (Anderson and Parrish

1981b)

2. 1 to 10 ms (van Gemert *et al.* 1986)

3. 1 ms (Butler *et al.* 1987, unpublished)

The optimal fluence had only been approximated by Anderson and Parrish (1981b) as 2 to 4 J/cm^2 (with a 1 ms illumination time that is an irradiance of 2000 to 4000 W/cm^2). Using different arguments Butler *et al.* (1987, unpublished) calculated a similar optimal incident dose. Van Gemert *et al.* (1986) did not propose a specific optimal fluence or irradiance but established a criteria for determining this (see section 7.3.1).

The concept of "optimal treatment parameters" is important for the clinician who is attempting to obtain the best clinical result. This research has been dedicated to determining these optimal parameters using a numerical model and investigating the experimental (clinical results and histology) evidence to see if there is support for the the model results. I shall be investigating these optimal parameters in later chapters (7 to 10, note also Pickering *et al.* 1989a,b, included in this thesis as appendices A and C).

1.6 The 20 W Copper Vapour Laser

Throughout this thesis, unless stated otherwise, the copper vapour laser I refer to is a Quentron™ QM91C. This laser lases at wavelengths of 510.55 nm (60% of the power) and 578.21 nm (40% of the power). Maximum output from this laser has been about 28 W. The light is discharged as a rapid pulse train at a rate of 16 kHz. Each pulse is 0.00005 ms long.

During the course of research for this thesis the laser has gradually undergone considerable modification which has resulted in more consistent and greater power. These technological advances have resulted in an improvement in the treatment, the reasons for which I discuss with the aid of our numerical model results.

A repetition rate of 16 kHz means a duration of 0.067 ms between pulses. I shall show (chapter 7) this inter-pulse duration is short in comparison to the total illumination time and to the time over which a blood vessel will lose a significant quantity of heat. Consequently, for most of our purposes, this laser may be thought of as continuous.

1.7 An Introduction to the Contents of this Thesis

Most of the research conducted for this thesis is contained within five papers which have been published or accepted for publication. These five papers are presented in

appendices A to E and are, in order of publication:

Appendix A. Pickering JW, Butler PH, Ring BJ, and Walker EP, (1989a); *Thermal profiles of a blood vessel heated by a laser.*, Australasian Physical and Engineering Sciences in Medicine, **12**, 11-15.

Appendix B. Walker EP, Butler PH, Pickering JW, Day W, Fraser R, and van Halewyn CN, (1989); *Histology of port wine stains after copper vapour laser treatment.* British Journal of Dermatology, **121**, 217-223.

Appendix C. Pickering JW, Butler PH, Ring BJ, and Walker EP, (1989b); *Computed temperature distributions around ectatic capillaries exposed to yellow (578 nm) laser light.* Physics in Medicine and Biology, **34**, 1247-1258.

Appendix D. Pickering JW, Butler PH, Ring BJ, and Walker EP, (1990a); *Copper vapour laser treatment of port wine stains: A patient questionnaire.* Lasers in Medical Science, accepted October 1989.

Appendix E. Pickering JW, Walker EP, Butler PH, and van Halewyn CN, (1990b); *Copper vapour laser treatment of port wine stains and other vascular malformations.* British Journal of Plastic Surgery, accepted November 1989.

I shall outline my contribution to each of these papers as I introduce each of the chapters within this thesis.

1.7.1 Chapter 2. Physiology of human skin.

An understanding of the physiology of the skin is helpful for the later discussions of the treatment process. I introduce some of our observations on port wine stains and comment on the circumstantial evidence that points to a possible cause of these lesions.

1.7.2 Chapter 3. Histology.

One method of assessing the efficacy of the treatment is to microscopically examine the results of the treatment. Histology were taken by Mr Peter Walker and analysed by pathologists Mr Anthony Day and Professor Robin Fraser. Most of the results are presented in Walker *et al.* (1989, included in this thesis as appendix B). I compiled this paper and contributed the discussion. In this discussion I described the physical processes that result in selective damage to the blood vessels. I also discuss the physics of the treatment with respect to the differences between the copper vapour laser, argon laser, and pulsed dye laser histologies.

1.7.3 Chapter 4. Techniques and results.

With any medical treatment there is an obligation to study the clinical response to the treatment. We have attempted to fulfill this obligation by assessing our clinical results using the measurements of colour and area change as functions of the treatment parameters. The illumination time is calculated from the measurement of the area of the spot as incident on the skin and the rate at which the light is applied to the skin (here the term rate is used loosely as we normally measure the scan rate in s/cm^2). The irradiance is a function, once again, of the spot area and of the laser power incident on the skin (measured by a calibrated integrating sphere). Where possible we have made objective measurements of the clinical results to which we have applied statistical analysis. The results of this analysis aid the formation of an hypothesis which suggests certain treatment parameters will give the most desirable clinical results. The results of this analysis are presented in Pickering *et al.* 1990a (included in this thesis as appendix D).

As the treatment is designed to improve the quality of life rather than to cure a physical illness, no amount of objective measurement can give a true indication of the effectiveness of the treatment. The patient's psychological response must be taken into account. To do this Brendan Ring, as part of an Honours part three project (Ring 1988), designed a questionnaire that was based on a questionnaire for argon laser patients (Dixon 1984a). I later analysed the responses to this questionnaire, the results of which appear in Pickering *et al.* 1990b (included in this thesis as appendix E).

1.7.4 Chapter 5. Automatic scanning.

A continuing project during my research has been the development of the automatic scanner. This scanner, as I have discussed, was designed by Mr Chris van Halewyn and Dr Philip Butler. My contribution to this area of research has been limited to some input into the features of the design, the computer software, and the testing of equipment.

1.7.5 Chapter 6. Radiative transfer.

One of the current difficulties with modelling light interaction with tissue is the lack of an accepted standard optical model that describes scattering and absorption within any tissue. In this chapter I discuss the present light distribution models and their applicability to our own modelling.

1.7.6 Chapter 7. The model.

A task of Brendan Ring's Honours part three project was to produce a numerical model to describe the thermal response of blood vessels to collimated incident light.

The need for this model arose from discussions on the current state of the analytical models available and our dissatisfaction with them. Details of the numerical model have been published in Pickering *et al.* 1989a,b (included in this thesis as appendices A and C). We have utilised this model to discuss a variety of treatment parameters for a variety of lesion conditions. In this chapter I discuss the various assumptions we have made and how any deviation from these assumptions may affect the model output.

1.7.7 Chapter 8. The optimal treatment.

Our ultimate goal is to provide the best possible treatment for the patients. In pursuing this goal we need to know what the (optimal) treatment parameters are that will produce this result. We have used our numerical model to attempt to define these treatment parameters (specifically the illumination time and the irradiance). We made an initial assumption as to the thermal conditions required for optimal therapeutic damage. Then we applied our model to a variety of vessel sizes (Pickering *et al.* 1989a, included in this thesis as appendix A). To investigate further the influence of the assumptions concerning optimal damage we applied our model for a variety of possible damage criteria (Pickering *et al.* 1989b, included in this thesis as appendix C). A solution to one aspect of the damage criteria (the peak vessel wall temperature required) was to calculate the damage to the protein as a function of time and temperature . In this chapter I discuss the results of applying this calculation which is called the damage integral.

Light fluence and spatial distribution variations at varying depths within a port wine stain may affect the optimal treatment parameters. I discuss some of the optical distribution models of chapter 6 and apply a Monte Carlo model designed by Mr Derek Smithies to vessels at different depths.

1.7.8 Chapter 9. The clinical treatment.

To date, the optimal treatment parameters discussed in chapters 7 and 8 have not been applied clinically. This has been due to the nature of the available technology. In particular illumination times both shorter and longer than the optimal have been utilised. These two sets of illumination times produce a quite different histological and clinical response. The short illumination times produce purpura, the blue/grey appearance of the skin, and the long illumination times produce blanching, the whitening of the skin. I have applied our numerical model to both these sets of illumination times. In Pickering *et al.* 1989b (included in this thesis as appendix C) I also discuss the shorter illumination times and their clinical response. A recent suggestion was to use a slightly different wavelength (585 nm) with these short illumination times. This appears to improve the treatment of the darker coloured lesions. Our model gives an insight into why this wavelength may be an improvement

at this illumination time.

1.7.9 Chapter 10. Discussion.

This chapter is a summary of the results of the research. Four conclusions are reached. First, the copper vapour laser at 578 nm provides an effective tool for removal of vascular lesions. Second, the necrosis of ectatic vessels requires at least some thermal denaturation of endothelial cells, the extent of denaturation has not been established. Third, the optimal treatment parameters are a wavelength of 577/578 nm, an irradiance of 400 to 3000 W/cm^2 at the skin surface and an illumination time of 1 to 10 ms. Fourth, the illumination times shorter than optimal will result in some vaporisation of haemoglobin and those longer will denature protein beyond the endothelial cells.

CHAPTER 2 PHYSIOLOGY OF HUMAN SKIN

An understanding of the structure of skin is necessary to enable discussion about the interaction of laser light with the skin. We shall outline in this chapter the structure of the epidermis, the dermis, and the vascular plexus, as well as commenting on the malformations that give rise to port wine stains, telangiectasia, and spider naevi.

2.1 Epidermis

This is the outermost (top) layer of the skin and is itself constructed of four layers (figure 2.1). From the innermost layer they are: the basal layer, the stratum spinosum, the stratum granulosum, and the stratum corneum or keratin layer.

The cells of the basal layer divide and migrate outwards towards the stratum granulosum. Here they lose their nuclei and die. The cell remnants within the stratum corneum form into a tough protein called keratin. This protein protects us from most knocks and wear. Eventually the keratin is shed. The whole process from formation of basal cells to the shedding of keratin takes 45 to 75 days depending on the thickness of the epidermis (usually 60 to 100 μm). There is no system of blood vessels within the epidermis. As a consequence nutrients are obtained by diffusion from the capillaries within the papillary dermis immediately below the basal layer.

There are two types of cells formed at the basal layer (1 cell thick), melanocytes and keratinocytes. The melanocytes produce small egg shaped sacks (0.3 by 1 μm) called melanosomes that contain the chromophore melanin. These melanosomes are distributed by the melanocytes throughout the keratinocytes. It is the melanin which gives us our yellow, brown, or black pigmentation and protects us from ultraviolet and visible radiation . Thus, melanin also provides a barrier to laser light penetrating further into the skin. One of the reasons for using the yellow 577/78 nm light rather than the blue green 488 to 514.5 nm light from the argon laser is that there is approximately one third less absorption by melanin within the dermis at 577/578 nm than at 514.5 nm, and a much smaller fraction in than at 488 nm (figure 2.2). The quantity of light that penetrates the epidermis may vary by a large percentage between any two sites on the skin of an individual depending on the melanin concentration at each site. At any one site the melanin concentration may change over a period of days or months depending on the degree of exposure to the sun the skin receives. Between individuals the variation in melanin concentration

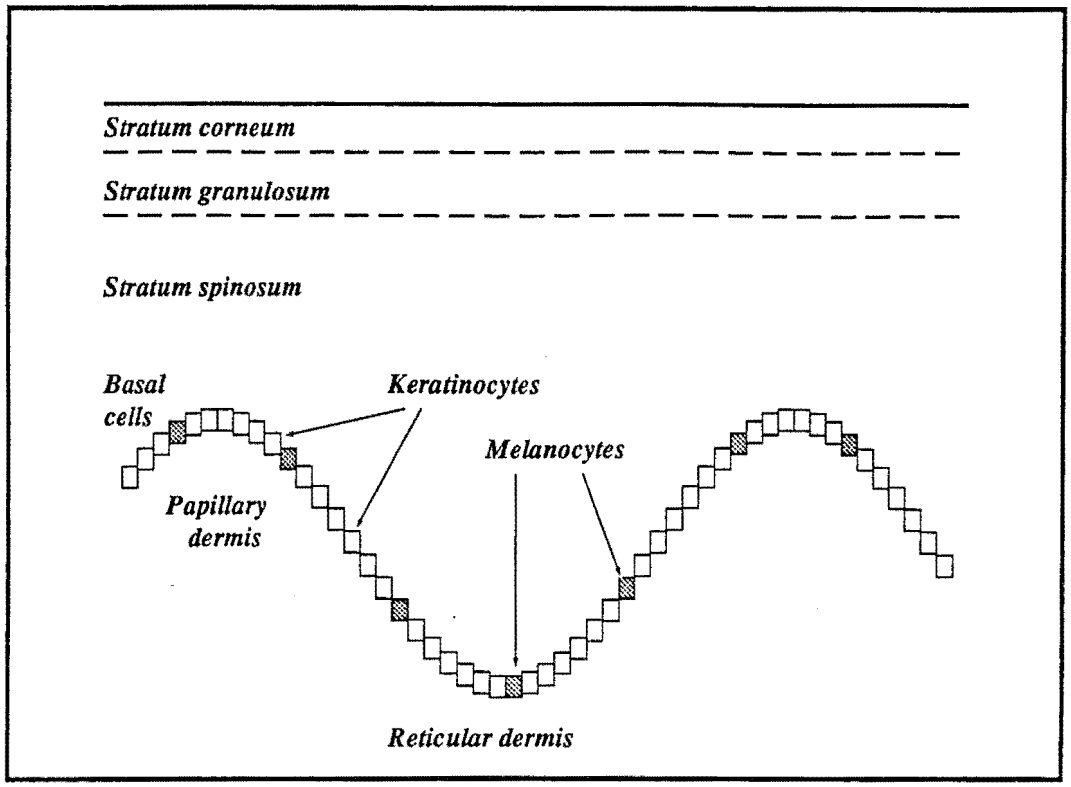

Figure 2.1: The four layers of the epidermis, and the two layers of the dermis.

may be even greater. Some individuals react much more to sunlight than others and may for example have a fair complexion. A person with this complexion who readily burns when exposed to sunlight has been classified as a type I skin (see table 2.1, from Tan *et al.* 1984). It is expected that this person's skin would also allow a greater percentage of the light to penetrate through to the dermis. A number of the studies with the pulsed dye lasers have used principally type I or II patients (Garden *et al.* 1986, Glassberg *et al.* 1988). Tan *et al.* (1984) showed that considerably greater irradiance was required for the treatment of more tanned skin. As New Zealanders most of our patients are type III or IV skin and several, being Maori, Asian, or Polynesian, have been type V.

Not only is the collimated laser light attenuated due to absorption by melanin, it is attenuated through scattering within the epidermis. At 578 nm approximately 20% of the incident collimated light will have been scattered before it reaches the dermis. As will be seen in chapter 6 much of the scattered light is scattered forward and thus transmitted into the dermis.

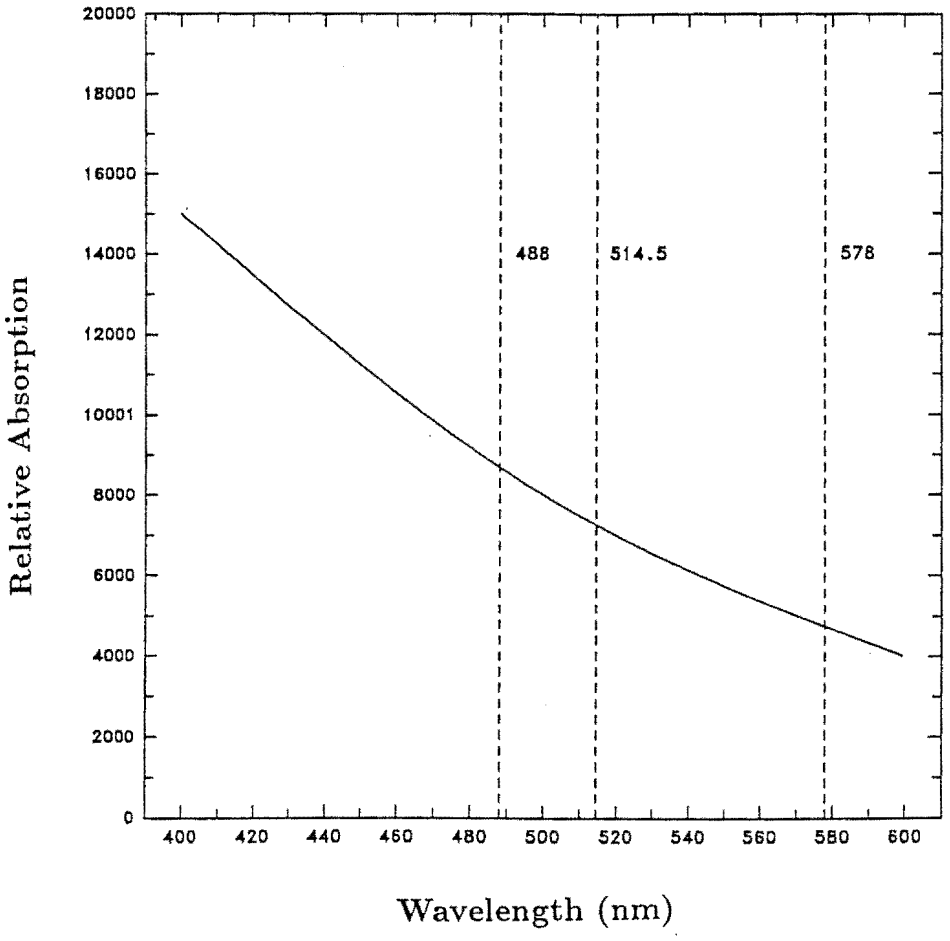

Figure 2.2: The relative wavelength dependence of absorption of light by melanin (Anderson and Parrish 1981a). The quantitative absorption at any skin site depends on the concentration of melanin within that site.

Table 2.1: Skin types. From Tan *et al.* 1984.

Type	*Colour and reaction*
0	Vitiligo
I	Always burn, never tan
II	Always burn, then slight tan
III	Sometimes burn, always tan
IV	Never burn, always tan
V	Heavily pigmented
VI	Black

2.2 Dermis

The bulk of the skin lies between the epidermis and a layer of fat. This, the dermis, is normally at least 1000 μm thick. The epidermal basal layer and the top of the dermis form the epidermal/dermal junction. This junction is characterised by undulations which may protrude up to 100 μm into the dermis. Between each of the protrusions is the region known as the papilla. At the level of the troughs of the protrusions is the arbitrarily defined boundary between the two layers of the dermis. The top layer, the papillary dermis, contains the capillaries that provide the nutrients for the epidermis. Below this is the reticular dermis which extends inwards to the fatty layer. The bulk of the dermis is composed of a fibrous connective protein called collagen. Within the papillary dermis the collagen forms long thin loosely connected strands. Within the reticular dermis the strands of collagen are coarse, tightly bundled, and linearly orientated. Also within the dermis are a number of adnexal structures such as hair follicles, sebaceous glands, and endocrine glands.

Light within the dermis is slightly more strongly scattered than within the epidermis. At argon, dye, and copper vapour laser wavelengths most of the attenuation of light is due to absorption by the haemoglobin within the blood vessels.

2.3 Blood Vessels

A tree-like structure approximates the distribution of the blood vessels within the dermis[1] (figure 2.3). An artery of around 100 μm diameter enters the lower dermis through the subcutaneous fat. This artery may branch once or twice before reaching the mid-dermis where the branches (now called arterioles) are approximately 50 μm in diameter. Continued branching occurs as the vessels extend outwards until they

[1] see Ryan 1973 for a more detailed discussion of the blood vessels of the dermis

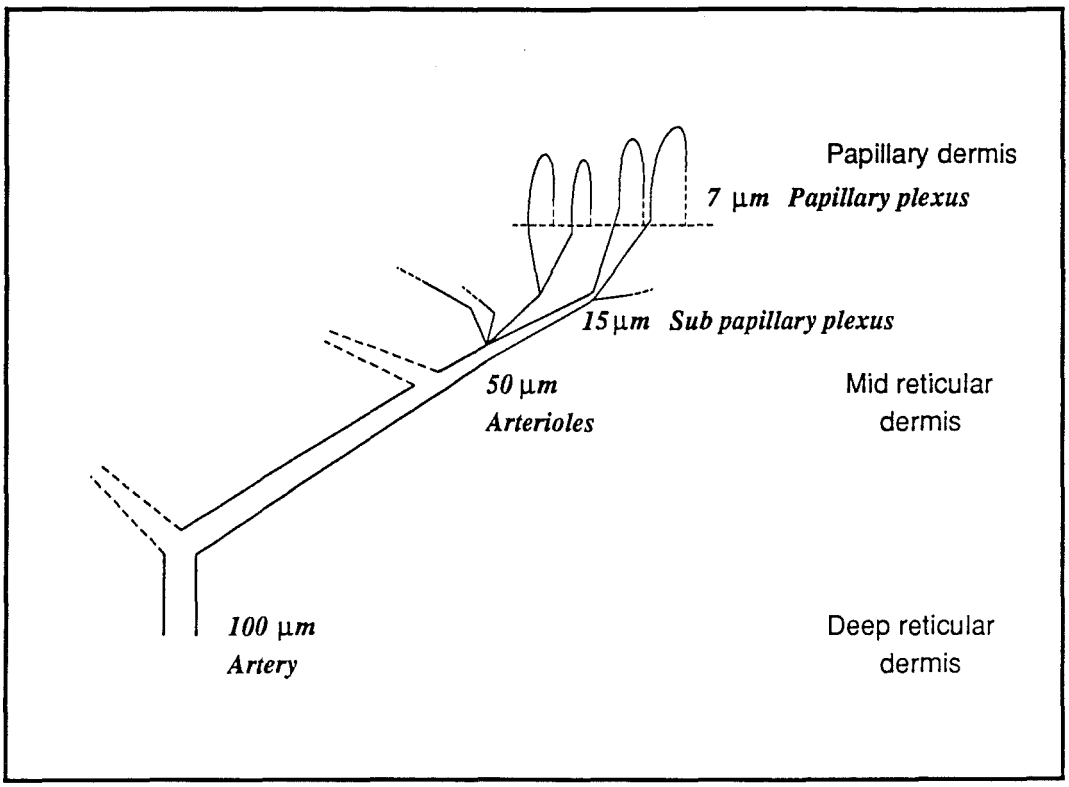

Figure 2.3: The blood vessels form a tree like structure within the dermis. Near the top of the dermis there is usually one or two plexi of horizontal capillaries. It is often these capillaries that are ectatic.

begin to form one or two plexi (the sub-papillary plexi) of small branches (capillaries) that lie approximately parallel to the surface. Extending from these plexi into the papilla (usually only one vessel per papilla) are the smallest capillaries, often only 5 to 10 μm in diameter. Such small diameter vessels force the erythrocytes to flow through them in single file. It is from these capillaries that the epidermis receives its nutrients. These capillaries loop around and drain into venules which in turn drain into larger and larger veins deeper and deeper within the dermis.

Capillaries are normally comprised of entwined endothelial cells. Ryan (1973) describes the endothelial cell as a lightly fried egg rolled over to form a tube. The yolk represents the nucleus and is an inflexible disk shape. However, the egg white represents the cytoplasm of the cell and may be found in almost any shape or form including having bubbles within it. It is the spreading of the cytoplasm into inter-connective tissue gaps that leads to the formation of new vessels. The volume encased by these cells is known as the vessel's lumen. Arterioles and larger vessels have pericytes and smooth muscle which serve to control blood flow.

The blood within the vessels is 45% by volume erythrocytes (red blood cells). This density of erythrocytes is such that they will be almost continually in contact with one another. These erythrocytes are bi-concave discs of around 7 μm in diameter and consist mainly of haemoglobin and a supporting framework. It is the haemoglobin that is our "target" chromophore. At 577/578 nm haemoglobin absorbs more strongly than at 514.5 nm (see figure 2.4) which allows quicker heating and less overall heat conduction. Together with comparitively low absorption by other cutaneous chromophores (principally melanin) these are the underlying principles of selective photothermolysis as applied to vascular lesions. Thus, the hypothesis is formed that 577/578 nm light is the optimal wavelength for the treatment of vascular lesions.

2.4 Telangiectasia and Spider Naevi

Telangiectasia is the prominent redness of the lower legs, neck, cheeks, and nose that is usually most notable in late middle age. Often individual vessels may be seen. These vessels are normally dilations of the sub-papillary plexus and are associated with a loss of papillary capillaries (Ryan 1973).

Similarly spider naevi originate in a very localised part of the sub-papillary plexus and are also associated with a loss of papillary capillaries. The dilated plexus is pushed upwards and has a characteristic red spot (the "body") with radiating "legs". They are not usually permanent and are manifest mostly in the young and in the pregnant.

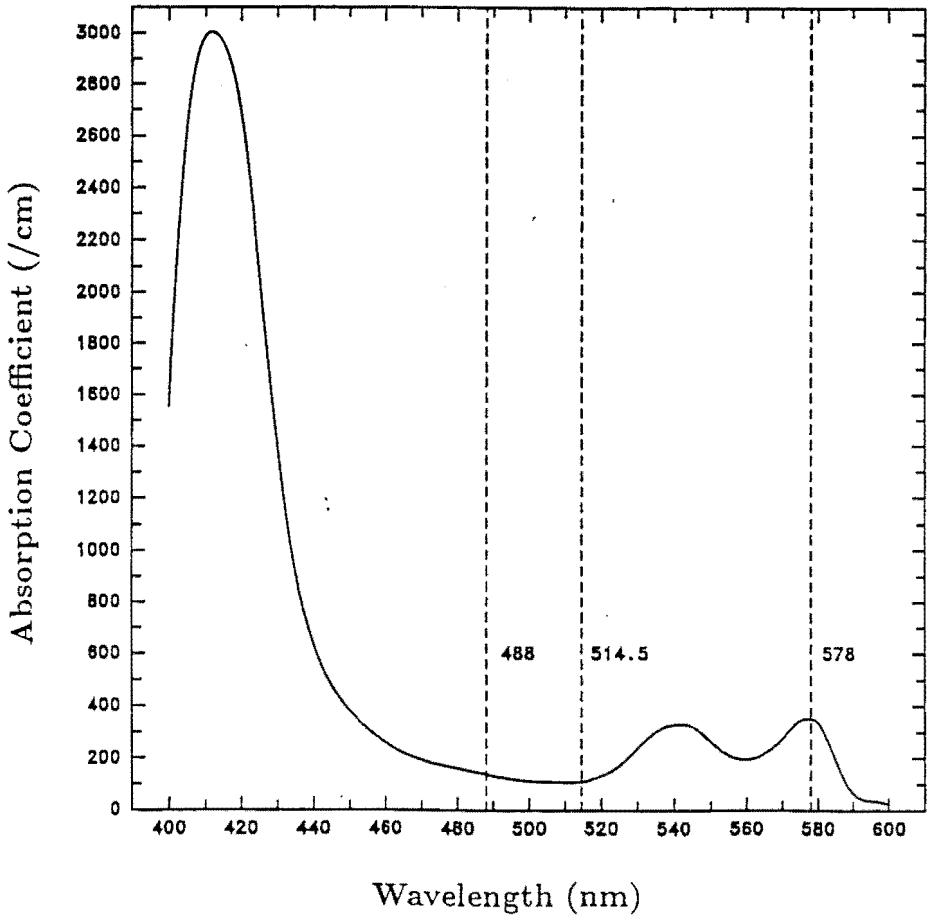

Figure 2.4: The absorption spectrum of haemoglobin. From van Gemert *et al.* 1989b

2.5 Port Wine Stains

Most of my research has been dedicated to improving the treatment to remove port wine stains. These lesions may vary in size from a few square centimetres to over 10% of the body surface area (2000 cm^2) and vary in colour from a light salmon pink to a dark red/purple colour.

Port wine stains have been classified by histology into four classes: constricted, intermediate, dilated, and deeply located (Noe *et al.* 1980, Ohmori and Huang 1981, see table 1 Pickering *et al.* 1989a). The constricted and intermediate classes have ectatic vessels within the papillary dermis. The dilated and deeply located classes have ectatic vessels of larger diameter deeper within the dermis and sometimes within the sub-cutaneous tissue. These vessels may be up to 150 μm in diameter. Ohmori and Huang (1981) and Barsky *et al.* (1980) illustrated that the colour of the stain was principally due to the size of the ectatic vessels and their percentage fullness of erythrocytes. The density of vessels within a port wine stain are approximately the same as the density of vessels within normal skin. Barsky *et al.* (1980) also measured the thickness of the endothelial cells and found this to be between 4 and 6 μm for all ectatic vessels. The vessels tend to become more ectatic with age. The greater blood volume results in a darkening of the stain. One possible reason for the progressive ectasia is the collagen degeneration with age. But, as some young patients have an "aged" lesion and vice versa, this can only be a contributing factor.

What is the cause of the ectasia? There is a small tendency for port wine stains to be hereditary (Carruth and McKenzie 1986). However, the physical reason for the cause of the ectasia has not been established. As a congenital defect there must be some additional or missing factor during the formation of the skin plexus. This takes place after the third inter-uterine month. There has been a suggestion that the ectatic capillaries are associated with an abnormality of the cutaneous nervous system (Smoller and Rosen 1986). We have noted that the lesions tend to involve singular or adjoining nerve regions of the skin (figure 2.5). Table 2.2 lists the numbers of our patients that involve the areas or combinations of areas that are illustrated by figure 2.5. Although most of our patients lesions involve the face, and most of these the maxillary division of cranial nerve V, table 2.2 only shows the lesions presenting for treatment. It is likely that the lesions are much more evenly distributed across the whole body . Note that there are very few port wine stains that have any continuity across the dividing line between left and right face. Figure 2.6 illustrates a typical (and well known) and an atypical port wine stain. Gaylarde *et al.* (1987) noted the differences in the vascular reflex function of two patients with port wine stains covering a large area of the leg. Smoller and Rosen (1986) had previously suggested that a cause of the ectasia may be a lack of nerves to the muscular tissue that serves to contract the arteries and arterioles. They performed some histology that indicated a lower than normal number of these nerves.

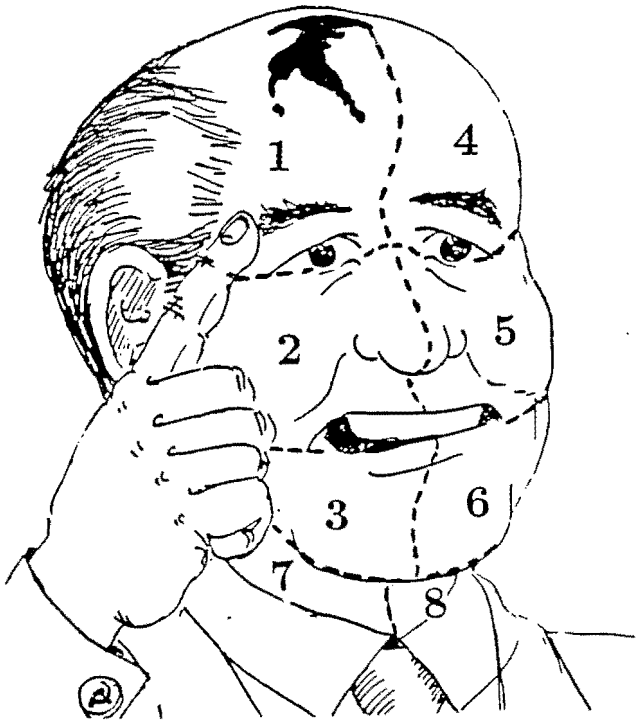

Figure 2.5: A schematic of the nerve regions of the face. 1 and 4 are the right and left opthalmic division of cranial nerve V, 2 and 5 are the right and left maxillary division of cranial nerve V, 3 and 6 are the right and left mandibular division of cranial nerve V, and 7 and 8 are the right and left cervical plexus. Cartoon by Stone 1989.

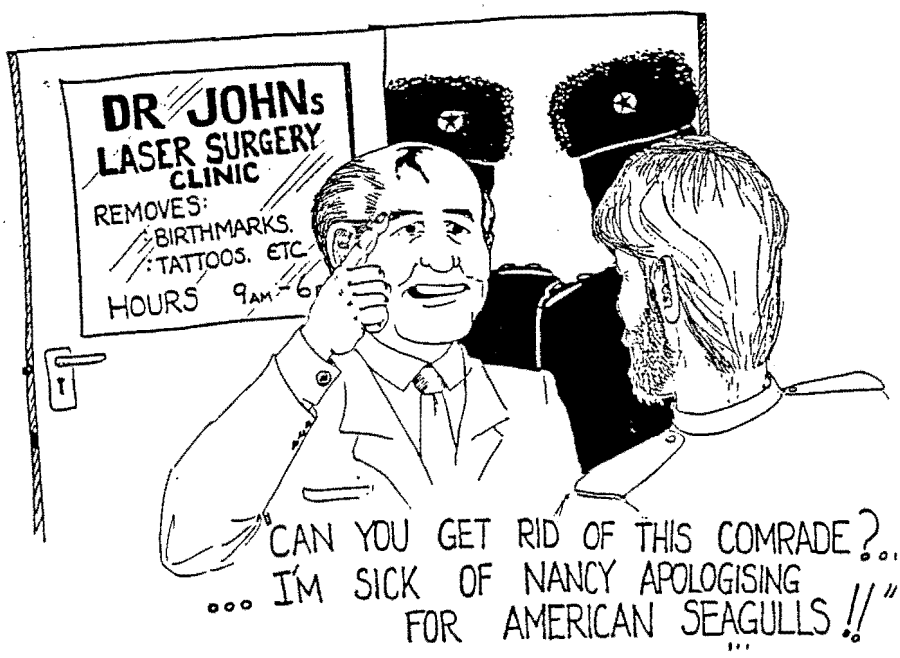

A

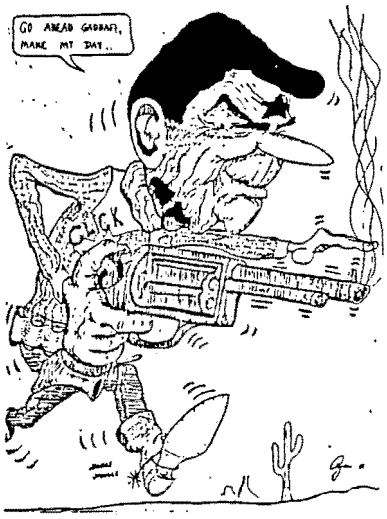

B

Figure 2.6: An example of a typical (A) and an atypical (B) port wine stain. Most port wine stains occupy one or two nerve regions on one side of the face and are usually adjacent to one another. Example A occured with 10 of the patients. No patients had a port wine stain of the manner of example B. Cartoon A by Stone 1989.

Table 2.2: The distribution of lesions as a function of nerve regions

Region	*Numbers*
1	10
2	54
3	6
4	9
5	50
6	7
7	3
8	8
1,2	10
1,5	1
2,3	2
2,7	1
3,7	7
4,5	6
5,6	2
5,8	2
6,8	3
1,2,3	2
1,2,7	2
2,3,7	3
3,5,7	1
4,5,6	1
5,6,7	1
5,6,8	2
1,2,3,7	2
1,2,4,5	1
1,2,5,6	2
2,3,6,7	2
3,6,7,8	1
4,5,6,8	1
1,2,3,5,6	1
2,3,5,6,7,8	1
2,4,5,6,7,8	1
LIMBS etc.	27

CHAPTER 3 HISTOLOGY

Our theoretical model predicts certain physiological changes within the skin after exposure to laser light. One goal of this research has been to attempt to define more precisely these changes and what the criteria are for inducing permanent change (therapeutic damage) to the ectatic vessels. These changes depend on the wavelength of the light, the irradiance, the illumination time, the type of laser, and the particular physical characteristics of the port wine stain. One method to assess the effect of any variations in these parameters is to examine the lesion after treatment with the aid of a biopsy and light or electron microscopy. We have undertaken histology of port wine stains exposed to 578 nm light from the copper vapour laser. The results show some initial temporary damage to the epidermis, only minor temporary damage to non vascular structures and selective therapeutic damage to the blood vessels.

3.1 Non-yellow Light Lasers

3.1.1 Carbon dioxide

Some use of the carbon dioxide (CO_2) laser at 10600 nm has been made for the treatment of port wine stains, but with contradictory reports on its success. Ratz and Bailin (1987) argue the case for this laser on the basis that it can vaporise the skin down to the level of the ectatic vessels (because this wavelength is strongly absorbed by water) and create minimal thermal damage below this level. They argue that the wound is similar to that caused by a dermabrasion or partial thickness graft and will usually heal in a similar manner without scar formation. To the contrary, van Gemert *et al.* (1987a) argue against the use of the CO_2 laser because of its propensity for scar formation (10% of patients – van Gemert *et al.* 1987a, 0-30% – Olbricht *et al.* 1987, 8% – Ratz and Bailin 1987). They argue that scarring will be at least as common as for the semi-selective argon laser and will be far in excess of the selective short pulsed dye lasers at 577 nm.

Histology immediately after treatment with the CO_2 laser indicate complete epidermal and part dermal necrosis (Buecker *et al.* 1984 and Tan *et al.* 1986). Healing requires complete epithelialization of the epidermis and formation of new fibrous tissue within the papillary and upper reticular dermis. Often this healing process may result in a lack of melanocytes and consequent hypopigmentation and/or

formation of scar tissue within the dermis (Tan *et al.* 1986). Olbricht *et al.* (1987) surveyed 85 specialists for their opinions on the complications of cutaneous laser surgery. They commented that:

> "It appears that some less-than-optimal outcomes, such as atrophic scarring and unexpected pigmentary change following the use of the argon laser and *atrophic or hypertrophic scarring after procedures performed with the carbon dioxide laser, occur so frequently that these were not considered complications...*"(my Italics)(Olbricht *et al.* 1987 page 349).

3.1.2 Argon

The argon laser was the preferred laser for treatment of port wine stains for a number of years and is still often used. The laser has been used both untuned (488 to 514.5 nm) and tuned (usually to 514.5 nm) and with a power ranging from 0.5 to 5 watts. Unlike the light from the CO_2 laser, the light from the argon laser is specifically absorbed by the chromophores of the skin. However, using the argon laser to produce the necessary coagulation of ectatic capillaries the exposure required is often long. This long exposure time allows for conduction of heat to non-vascular structures which may result in hypertrophic scar formation. Furthermore, epidermal damage may result from the absorption of light by the melanin. The attenuation of light by melanin before it reaches the haemoglobin and the relatively poor absorption of the light by haemoglobin (an average size ectatic vessel absorbs less than 50% of the light incident upon it) causes the need for long exposure times.

The histology of Greenwald *et al.* (1981), Finlay *et al.* (1984) and Tan *et al.* (1986) show marked dermal necrosis of collagen, adnexal structures and blood vessels. The damage was greatest in the papillary dermis. The extent of damage depended on the light fluence. The first two used an exposure time of 200 ms while Tan *et al.* (1986) does not state the exposure time but there are suggestions in the introduction that this was also several hundred milliseconds. After healing had taken place (1 to 6 months) the damaged tissue had been replaced by scar tissue with plump fibroblasts (Tan *et al.* 1986). The ectatic blood vessels had been replaced by scar tissue.

Heating within the epidermis may result in damage to the epidermal cells and/or damage to the papillary dermis due to the so called "iron heater" effect. That is, damage as a result of heat conduction from the epidermis. The basal cell layer shows the most pronounced damage, namely nuclear and cellular pyknosis (shrinkage solidification), vertical elongation of keratinocytes, cellular vacuolation (forming a cavity within the protoplasm of the cell which is indicative of steam formation) and separation of the epidermis from the dermis. Finlay *et al.* (1984) thought the melanin to be more obvious, probably as a result of cell water loss. Re-epithelialization takes place over a number of months. Often there are pigmentary changes which,

as Olbricht *et al.* (1987) indicated (section 3.1.1), are not always recognised as complications.

3.2 Yellow Light Lasers

3.2.1 Pulsed dye

Because of the relatively high absorbtion of yellow light by haemoglobin and relatively low absorbtion by melanin, in comparison to the argon laser the pulsed dye laser at 577 nm was expected to produce damage more specific to the vasculature. This damage was expected to be confined to the blood vessel and its immediate surroundings. A series of histological studies by members of the Department of Dermatology, Harvard Medical School, on normal human skin (Anderson and Parrish 1981b, Greenwald *et al.* 1981, Nakagawa *et al.* 1985) and on port wine stains (Morelli *et al.* 1986, Tan *et al.* 1986) at a variety of pulse widths, all illustrate the specificity of yellow light. Independently Hulsbergen Henning *et al.* (1984) also showed selective vascular damage with a 0.001 ms (1 μs) pulse at 575 nm. All these studies have illustrated little or no epidermal damage immediately after illumination (table 3.1). However, Anderson and Parrish (1981b) reported full thickness epidermal necrosis and sub-epithelial blister formation at 48 hours with their larger fluences.

Clinically this treatment produces purpura some 5 to 15 minutes after illumination. Purpura appears as a blue/grey colour within the skin and is by definition extravasation of blood (see for example Miller and Keane 1987). Purpura appears with all of these short pulse lengths. The shortest pulse length histologies (0.0003 to 0.02 ms) showed the effects of vaporisation of blood near the top of the vessels resulting in mechanical damage to the vessels and the extravasation of blood. The mechanical damage is the tearing of the vessel walls as a result of pressure waves within the lumen that are created by steam formation within the erythrocytes. At the longer pulse lengths (from 0.2 to 0.45 ms) similar extravasation has not been observed, although purpura is still observed.

The common features of the histology are selective vascular damage, particularly to the superficial vascular plexus within the papillary dermis, lack of epidermal damage, agglutination of erythrocytes, rupture and haemorrhage (see table 3.1). Hulsbergen Henning *et al.* (1984) commented that the vascular damage seen immediately after illumination was not evident at 48 hours, indicating that healing had taken place. This is probably because the initial damage was not thermal but due to the rupture of the vessel which resulted in the observed extravasation of erythrocytes.

Table 3.1: A Summary of Pulsed Dye Laser Histology.

Pulse length *Comments*

0.0003 ms With normal skin, a 1 mm diameter spot, and 577 nm light. Within 10 minutes of illumination the epidermis begins to show some epithelial cell necrosis and basal cell vacuolation with a fluence of 3 J/cm^2. At 5 J/cm^2 full thickness necrosis of the epidermis and subepithelial blisters are apparent 48 hours after illumination.

The dermis exhibits no change for the irradiances used.

With 2-4 J/cm^2 the response of the vascular plexus within 10 minutes of illumination is damage to the superficial vascular plexus. There is a mass of agglutinated erythrocytes. The endothelial cells often have ruptured and haemorrhage results. 48 hours later some of the vessel walls have been replaced by fibrin although there is some reconstitution of endothelial cells. The vessels are still inflamed, however the haemorrhage is less obvious.

Contributing papers: Anderson and Parrish 1981b, Greenwald *et al.* 1981, and Paul *et al.* 1983.

0.001 to 0.02 ms With normal skin, a 2 to 3 mm diameter spot, and 577 nm light. At threshold fluences (2-3 J/cm^2 which produce purpura across the whole spot) cutaneous damage was very similar to that produced with the 0.0003 ms pulse length. At suprathreshold fluences vacuolation of cells within the basal layer was enhanced and the dermis showed degeneration of fibroblasts that were adjacent damaged blood vessels.

With port wine stains and 575 nm light similar results were reported including subepithelial blisters, substantial melanin pigmentation in the basal cell layer, and, 48 hours after illumination, marked perivascular infiltrate with erythrocyte extravasation down to 900 μm and normal looking endothelium.

Contributing papers: Hulsbergen Henning *et al.* 1984, Nakagawa *et al.* 1985, and Garden *et al.* 1986.

0.056 to 0.02 ms With normal skin, a 3 mm diameter spot, and 577 nm light there was in comparison to the shorter pulse lengths, less microvascular rupture and haemorrhage, and an increase in the irradiance required to produce purpura.

Contributing papers: Garden *et al.* 1986.

Table 3.1: A Summary of Pulsed Dye Laser Histology. (continued)

0.3 to 0.45 ms With normal or guinea pig skin, a 3 mm diameter spot, and 577 nm light damage was confined to the blood vessels. There was no rupture or haemorrhage but rather an agglutination of erythrocytes. The endothelium appeared degenerate. At suprathreshold fluences both the basal layer and the dermis near damaged blood vessels showed signs of necrosis. Tan *et al.* (1988) observed concentric rings of damage at these fluences. The inner ring had widely dilated empty blood vessels and edema between collagen bundles. Surrounding this area was a band of vessels filled with identifiable apparently well preserved erythrocytes. A second outer ring consisted of vessels with erythrocytes that formed large agglutinated masses. In this ring the erythrocytes and the endothelial cells appeared to be damaged. An additional aspect of this hitology was an investigation of the influence of spot diameter (1,3 and 5 mm). Larger spots were found to require a lower fluence for the onset of purpura and vascular damage extended deeper within the tissue.

With port wine stains, a 3 mm diameter spot, and 577 nm light intercellular edema was observed within the epidermis. Nevertheless, one month after illumination the epidermis appeared normal. The dermis exhibited some degeneration of collagen immediately adjacent damaged ectatic vessels. Once again there was an agglutination of erythrocytes and degeneration of vessel walls (apparently in proportion to the amount of agglutination). Some edema was apparent around the vessels. One month after illumination the lumen are smaller with thickened walls and more prominent endothelial cells. There is also some intercellular and extracellular haemosiderin.

Contributing papers: Tan *et al.* 1986, Morelli *et al.* 1986, Garden *et al.* 1986, and Tan *et al.* 1988.

Table 3.2: A Summary of Continuous Wave Laser Histology

Illumination time *Comments*

50 to 300 ms With skin from a pigs ear, a 1 mm diameter spot, 577 nm light damage to the epidermis was not apparent for an illumination time of 50 ms and the minimal fluence of 5.75 J/cm^2. However, at 300 ms the epidermis, dermis and blood vessels were all coagulated.

Contributing paper: Landthaler *et al.* 1986.

500 to 2000 ms With port wine stains, a 1 mm diameter spot , 577 nm light, and a fluence from 0 to 50 J/cm^2 there was virtual obliteration of the previous ectatic vessels. There was a tendency for "spongy" salmon-pink lesions to show some scarring.

Contributing paper: Cotterill 1986.

60 to 90 ms With port wine stains, a 1.3 mm diameter spot, and a fluence of 11 to 25 J/cm^2 the epidermis 24 hours after illumination showed some cellular necrosis and a subepidermal blister. Parts of the papillary and upper reticular dermis appeared degenerate, although all adnexal structures were normal. The ectatic vessels throughout the dermis had necrotic endothelial cells, some agglutinated and occasionally ruptured erythrocytes, but no ruptured vessels. There was greater coagulation on the top of the vessels than on the bottom. Three to six months after illumination the epidermis was normal, the dermis showed some increase in fibrous connective tissue but the collagen fibrils were normal. Within the deeper dermis the blood vessels exhibited marked subendothelial fibrosis with some complete occlusion of vessels. There was a slight increase in the number of normal sized capillaries. No haemosiderin was present.

Contributing paper: Walker *et al.* 1989 (included as appendix B).

3.2.2 Continuous wave dye

Cotterill (1986) and Landthaler *et al.* (1986) have performed histology on vascular skin after treatment with a continuous wave dye laser at 577 nm. Cotterill (1986) treated port wine stains using approximately 0.5 W with a 1 mm diameter spot and an illumination time of 500 to 2000 ms. The histology showed virtual obliteration of the previously present superficial ectatic vessels. Landather *et al.* (1986) took biopsies from the dorsal aspects of the ears of guinea pigs. They used a 1 mm diameter spot with 0.6 to 1.2 W and a 300 ms illumination time, or 0.9 W and a 50 ms illumination time. Only at the shorter illumination time was selective vascular coagulation observed, otherwise the coagulation included the epidermis and parts of the dermis.

3.2.3 Copper vapour

We have performed histology on four port wine stain patients. These patients were treated with a approximately 1.6 to 3.6 W of 578 nm light for 60 to 90 ms with a 1.3 mm diameter spot (Walker *et al.* 1989). Biopsies were taken pre-treatment and either 24 hours or 3 to 6 months post treatment.

The principal conclusions were that, as with the pulsed dye laser, selective vascular damage occurs with only minimal damage to dermal collagen and adnexal structures. Unlike the pulsed dye laser histology, there was no evidence of mechanical damage (vessel rupture and haemorrhage). The damage appears to be thermal and confined mainly to the endothelial cells. At 60 to 90 ms there is some epidermal necrosis 24 hours after illumination. Nevertheless, at 3 months the epidermis is completely normal. The results of the histology from this section and the previous are included in table 3.2.

The precise form of damage to cause necrosis of ectatic vessel with the minimum of damage to other cutaneous tissue has yet to be established. The histology presented here indicate that both mechanical and thermal damage will cause at least a temporary cessation of blood flow. However, the mechanical damage produced by the shortest of the pulsed dye lasers appears insufficient for long term therapeutic affects (Hulsbergen Henning *et al.* 1984). The clinical results have been improving as the pulse length of these lasers has increased, and thus, as the ratio of thermal to mechanical damage has increased. Similarly the clinical results of the continuous wave lasers have improved as the illumination time has decreased (Pickering *et al.* 1990b) and thus as the total cutaneous thermal damage has decreased. We expect for the optimum damage there is a specific thickness of endothelial cell that needs to be thermally denatured. However, we can not discount the possibility that some mechanical damage may be required.

3.3 Melanin Absorption

As we discussed in section 2.1, one of the principal reasons for using 577/578 nm light lasers is the low absorption by melanin at these wavelengths compared with the absorption at wavelengths produced by other dermatological lasers. Here again it is important to stress that the percentage of light penetrating through the melanin to the epidermis is dependent on the melanin concentration of the particular skin site being illuminated. When considering the effect of melanin absorption as well as the wavelength we must take into account the duration of illumination time, the irradiance, and the technique of illumination.

Melanin is produced by the melanocytes and deposited into small (0.3 by 1 μm) egg shaped structures called melanosomes. These melanosomes infiltrate the basal cells forming an even distribution of melanin.

Section 1.6 described the quasi-continuous nature of the light produced by the copper vapour laser. The length of each pulse (0.00005 ms) is much shorter than the characteristic time for the release of heat by melanosomes (a thermal relaxation time of approximately 0.001 ms, see appendix F). However, the interpulse time, 0.067 ms, allows for the heat generated within the melanosome to conduct away between pulses.

Histology by Murphy *et al.* (1983) after skin exposure to 0.00002 ms pulse from a XeF excimer laser at 351 nm indicated that a fluence of 0.12 J/cm^2 resulted in damage to melanosomes. A greater fluence resulted in damage to all melanosome containing cells. Similar results were obtained by Polla *et al.* (1987) with a 0.00004 ms pulse from a Ruby laser at 694 nm and a fluence greater than 0.3 J/cm^2. We postulate that with a similar fluence we would obtain similar histology to the ruby laser. However, the single pulse fluence of the copper laser is at most 0.04 J/cm^2 and hence we can expect not to have destruction of melanosomes and melanosome containing cells. At the melanosome damage threshold fluence with the Ruby laser and at the threshold fluence with a 0.00075 ms pulse at 560 nm (Margolis *et al.* 1989), there is separation of the epidermis from the dermis and bulla (blister) formation. This is a similar phenomenon to that which we observed with our histology of the copper vapour laser. Although there may not be direct damage to individual melanosomes, there may be heat build up within the cells which depends on the separation between melanosomes (that is the melanosomes are not thermally isolated from one another). Additionally, there may be a contribution to the heat of the epidermis due to heat conduction from ectatic vessels within the papillary dermis near the epidermal/dermal junction. The plasma leakage from any damaged vessels will also add to the bulla formation.

CHAPTER 4 TECHNIQUES AND RESULTS

For over three years we have used the copper vapour laser to treat a variety of cutaneous lesions. For each patient the treatment technique has been based on our previous techniques and the results of other clinicians' techniques. Additionally, we have utilised the results of our research into the physics of the treatment. This approach has been as an alternative to constructing an experiment for each new addition to our technique. Rather than subject some patients to an inferior technique just to prove the efficacy of a minor change in technique, we have attempted to provide the best possible treatment for all patients.
This strategy means that the scientific investigation of the clinical results and the influence of different techniques is unable to provide the definitive statistics that, say, a double blind experiment would. However, by taking objective measurements where possible (of area changes, power, illumination time or scan rate), attempting to quantify subjective measurements (initial colour, colour change, patient's feelings), and maintaining some consistency between treatments (minimal blanching) we are able to form (as opposed to prove) certain hypotheses regarding the treatment.

4.1 Clinical Technique

The first indication of the skin responding to the light from the copper vapour laser is whitening, or blanching, of the skin. We believe that this blanching is due to the protein surrounding the blood vessels becoming opaque (see chapter 8 for a discussion on protein denature). Although denature of epidermal tissue or vasodilation may also blanch the skin. The histological evidence (Walker *et al.* 1989) and the lack of an immediate return to normal skin colours (as is often the case with vasodilation) suggests endothelial cell denature is the most likely cause of blanching. The point at which blanching first appears has been called the minimal blanching end point. With some of our first treatments we noted an increase in the intensity of blanching with an increase in the power of the laser for the same rate of application of light. For consistency and because of the desire not to "overdo" the treatment (strong blanching as with the argon laser techniques is associated with a more frequent occurrence of scars) we decided to use minimal blanching as the end

point for all treatments, irrespective of the power delivered. This means that when the light is first applied to the skin the degree of blanching is immediately assessed (interactively by the surgeon) and the rate at which the fibre moves linearly across the skin is adjusted so as to produce minimal blanching.

The power available from the laser has increased over the three years as we have improved the hardware. However, there is often a fluctuation in power available due to the state of maintenance of the laser. These fluctuations are not normally more than 10% between each treatment session on any one day, but may vary more substantially over a longer period. Consequently, because of this and realising the consistency in end point we have analysed the results with respect to the power (or rate of scan as this correlates to the power).

The response of the patients to treatment may vary according to the lesion colour and the otherwise normal skin colour. For large lesions that occupy different areas of the body the melanin concentration may be different at different skin sites. This will result in a different quantity of light penetrating through to the dermis. Furthermore, the melanin concentration at any one site may differ over time depending on the current tan of the patient. As it is desirable to have as much light as possible reach the blood vessels, and not be absorbed by the melanin, we prescribe an ultraviolet sun block and melanin reducing creams to our patients. Further details of our treatment of vascular lesions are provided in Pickering *et al.* 1990b.

On occasions we have treated the brown pigmented lesions such as lentigo or naevus of Ota. Here we utilize both the green and yellow wavelengths of the laser in order to destroy the melanin. This technique usually involves a rapid scanning of the lesion resulting in partial vaporisation of the epidermis.

4.2 Clinical Results

After nearly 1500 treatment sessions we analysed in detail the results of those patients treated for port wine stains. In particular we analysed the results for the first treatment as a function of laser power and scan rate (the two of which are correlated, see figure 3 Pickering *et al.* 1990b). We measure the power using an integrating sphere that is regularly calibrated. The scan rate is measured by dividing the total time the laser was illuminating the lesion by the area of the lesion. Additionally, we attempted to categorise some patients as good or poor responders. The results are presented in detail in Pickering *et al.* 1990b. Table 4.1 is a brief indication of the treatments performed including the port wine stains.

It has been difficult to analyse the clinical results quantitatively. The measurement of colour has been made subjectively and the measurement of change in area of the treated lesion is often inaccurate. Thus, our analysis can only be taken as a guideline to the efficacy of the treatment rather than as proof.

In summary the port wine stain results were better at higher powers and correspondingly faster scan rates (shorter illumination times). The fluence did not vary

much between treatments. As with argon laser treatments (but not with pulsed dye laser treatments) the best results were from those with darker lesions. However, unlike the argon laser treatments we have been able to treat children and those with lighter lesions. The pulsed dye laser has also shown success with the treatment of children (Tan *et al.* 1989d).

The adverse effects were minimal, a $3.5 \pm 1.4\%$ (mean±sd) rate of scarring (where a scar is defined as any persistent atrophic or hypertrophic mark) and a $1.4 \pm 0.5\%$ rate of hypepigmentation and of hypopigmentation.

Of the 100 patients who had undergone four or more treatment sessions, only 10 had responded with a less than 30% reduction in lesion area and slight or no colour change. Conversely, 21 had a greater than 70% reduction in area. Additionally, 11% of those yet to undergo four treatment sessions had a greater than 70% reduction in area.

Table 4.1: The treatments performed with the copper vapour laser

Lesion	*Wavelength*	*Patient Nos.*	*Session Nos.*
Port wine stain	578	308	1068
Telangiectasia/Rosacea	578	106	154
Spider naevus	578	54	65
Cavernous haemangioma	578	18	28
Venous flares	578	17	32
Venous lake	578	8	9
Cherry angioma	578	3	3
Strawberry naevus	578	3	3
Campbell de Morgan	578	2	2
Ephilus/Lentigo	511 and 578	29	44
Tattoo	511 and 578	9	15
Naevus of Ota	511 and 578	2	5

4.3 Questionnaire

Any medical treatment designed to improve the quality of life rather than to save life must be subject to the scrutiny of the patients themselves. If the treatment either fails to produce a result that the patient is satisfied with or it traumatizes the patient to a degree that results in a further loss in quality of life then it must be deemed a failure.

To assess the treatment from the patient's perspective we decided to survey the patients. Brendan Ring as part of his Honours part three project designed a

suitable questionnaire (Ring 1988). This questionnaire was distributed to all past and present patients. It was based on a survey by John Dixon (Dixon *et al.* 1984a) of argon laser patients.

The only noteworthy results from patients with lesions other than those reported in Pickering *et al.* 1990a was from the small number of patients treated for venous flares on the legs. Half of these patients indicated they were not satisfied with the treatment. This was probably due to the frequent occurrence of hypopigmentation that occurred with these treatments. We have ceased to offer this treatment. This group of patients were the only exception to the positive response to the treatment.

For the paper we analysed the responses to the questionnaire of the patients who had been treated for either a port wine stain, for facial telangiectasia, or for a spider naevus. The questionnaire was sent to all patients, irrespective of the number of treatment sessions they had undergone. To summarise these results, 84% of port wine stain, 74% of telangiectasia, and 81% of spider naevus patients felt there had been an improvement in their appearance. Overall the impression of the treatment was very positive. Especially positive were the port wine stain patients; 91% said they would recommend the treatment to others, 84% would have the treatment again, and 60% indicated the overall effect the treatment on their lives was *very* good.

CHAPTER 5 AUTOMATIC SCANNING

As a method of applying the laser light to the lesion hand scanning of a fibre optic a few millimeters above the skin surface has two major problems. The first is the inaccuracy in the positioning of the light on the lesion. The second is the inaccuracy in the rate at which the light is applied to the lesion. Additionally, the maximum rate of application of light (minimum illumination time) is limited by the skill of the surgeon and the laser power available. With the technique we use, the minimum illumination time we are able to obtain is several times longer than the illumination time we have calculated to be optimal (see chapter 8 and Pickering *et al.* 1989a,b). Because of these limitations we have developed a robotic device to automatically scan the light across the lesion at a preset rate.

5.1 Why A Robot?

The minimal blanching technique described in section 4.1 and Pickering *et al.* 1990b requires the surgeon to manually scan a fibre optic back and forth approximately 2 mm above the skin and to interactively adjust the scan rate to achieve the desired end point (minimal blanching). To avoid over treatment of any one area the surgeon must allow a small gap between scan lines. With no light incident on these gaps there sometimes results a striped appearance after the initial one or two treatments. Fortunately with repeated treatments the striped appearance disappears. However, there is some redundancy in the number of treatments required. The surgeon also will not be treating each part of the lesion with exactly the same energy fluence (or illumination time) due to variation in the linear speed of the scanning fibre. This has been obvious near the periphery of the lesion where the scan rate slows down as the surgeon changes the direction of the scan. Latterly, the use of non transmitting gauze or cardboard placed immediately beyond the lesion periphery has allowed the surgeon to change the direction of scan on this material rather than on the lesion. Consequently the scan rate across the lesion is less variable. However, a constant scan rate can not be achieved manually.

The surgeon is limited to a maximum scan rate at which a reasonable degree of accuracy is able to be maintained. This rate depends on the individual surgeon's skill and may become quicker with practice. At present after several years of experience

our surgeon (Mr Peter Walker) is able to use a maximum scan rate of approximately 3 s/cm^2 (i.e. a linear speed of 2.7 cm/s). At this scan rate "minimal blanching" occurs with an irradiance of 500 to 600 W/cm^2. A greater irradiance at this scan rate results in excessive blanching. This rate corresponds to an illumination time of approximately 30 to 50 ms which is considerably longer than the optimal illumination time calculated as 1 to 10 ms. Thus, a robotic device ought to be designed to deliver a minimum blanching threshold irradiance at a rate that is at least three times faster than can presently be achieved by hand. Additionally, it should deliver the light considerably more accurately.

5.2 The Design

The initial design for this scanner originated from the Honours part three project and the masters thesis work of Chris N van Halewyn (van Halewyn 1985, van Halewyn 1987). Since I have only played a minor role in the design of this machine I shall restrict myself to only outlining the design.

Figure 5.1 is a schematic of the scanner. The light is directed onto the patient by the mirror attached to the two "x and y" stepping motors. The light is focussed to a small 1 to 5 mm (depending on laser beam divergence) diameter spot approximately 600 mm below the stepping mirror. This focussing is achieved by the 850 mm focal length lens which is also attached to a stepper motor ("z") to enable rapid focussing of the spot onto the patient. The video camera is focussed at the same position of the spot and looks down the same path length of the laser beam. This is enabled by a 45° angled mirror which reflects only 578 nm light and is transparent at other visible wavelengths. The image from the video camera is able to be displayed upon a computer screen with overlying text and graphics capabilities. Additionally, there are photodiodes capable of detecting the reflected light. Variations in the reflected light intensity may in future be used to regulate the treatment.

5.3 The Operation

The patient is placed under the scanning mirror and viewed by the video camera. The camera (and consequently the laser light, which is initially occluded by a shutter) is focussed onto the patient. The desired speed of movement of the focussed light is input into the computer (as an illumination time). Initially this speed depends on knowledge of the laser power and the minimal blanching threshold. Further development may allow the photodiode feedback mechanism to regulate the speed. Using the overlying graphics capabilities of the computer the image of the lesion is outlined on the screen, the computer calculates the commands to drive the stepping motors and prepares for execution. These commands are sent to the stepping motors once a start command is given. The light will only be incident on the lesion if a pneumatic footswitch is depressed. This footswitch allows a shutter in front of

the beam to be automatically opened by the computer. Thus the shutter will not automatically open unless the footswitch is depressed. After scanning the area the shutter is automatically closed. However if the footswitch is lifted then the shutter will close, thus preventing the light from reaching the patient.

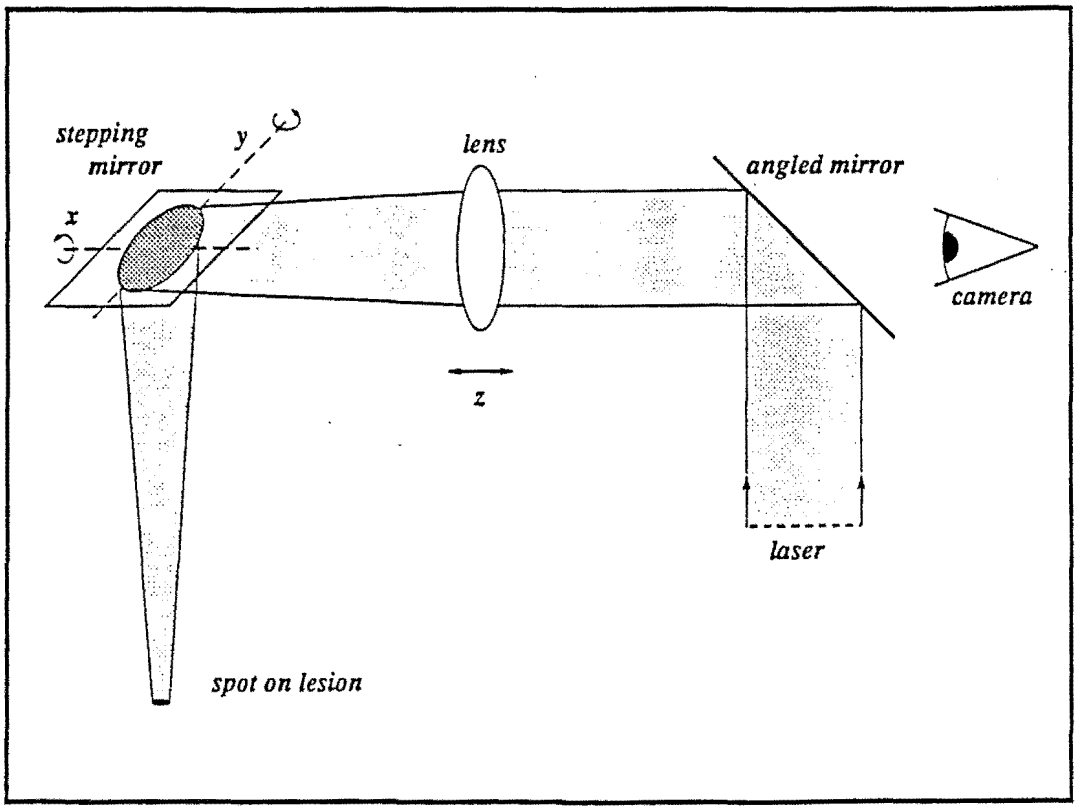

Figure 5.1: A schematic of the robot scanner device. The light is focused onto the patient by the 850 mm focal length lens and scaned across the lesion using the stepping mirror which is under the control of a computer. A video allows the operator to define the position of the lesion which is necessary for the computer to decide where the light needs to be scanned.

CHAPTER 6 RADIATIVE TRANSFER

The epidermis and dermis are both highly scattering media at the wavelengths of visible light. Light incident on either of these media, whether collimated or diffuse, undergoes numerous scattering events within the first few tens of micrometers. Additionally, chromophores within these media absorb light. This scattering and absorption combined with the angular distribution of the incident light determines the angular distribution and the total flux of light surrounding the blood vessels. Thus, calculation of the energy absorbed by the blood vessels depends on the knowledge of the optical characteristics of the epidermal and dermal tissue. A number of different models have been proposed to estimate the light distribution. The purpose of this chapter is to outline those models and to discuss their use within the modelling of laser treatment of vascular lesions.

6.1 The Nature of Scattering

Chandrasekhar (1949), Ishimaru (1978), and Bohren and Huffman (1983) are the texts from which are drawn much of the material for this chapter. They each describe the scattering of light from small particles in a different way.

An electromagnetic wave incident upon a single particle (such as a molecule or an aggregation of molecules) will set into oscillatory motion some of the charges within the particle. The accelerated particles radiate electromagnetic energy. It is this radiation that we think of as the *scattered* radiation. Meanwhile some of the incident radiation may be *absorbed* by the particle. For example it may be transfered to vibratory modes of the particle which we note as thermal energy. A detailed electromagnetic theory of scattering from a single particle may give us details of the amplitudes and phases of the scattered radiation. When a number of particles are close enough to each other such that there is significant interaction between their scattered electromagnetic fields, we have to consider multiple scattering theories. Analytical multiple scattering theories start with either Maxwell's equations or wave equations, and together with the absorbing and scattering characteristics of the particles, can yield the distribution of energy within the system. In principle these theories can include all diffraction, interference, and multiple scattering effects.

For our purposes we are interested in obtaining the power flux density ($I(\mathbf{r}, \hat{\mathbf{s}})$)

within a unit solid angle in a frequence range $(\nu, \nu + d\nu)$ at any point $\mathbf{r}$ within the medium in the direction of unit vector $\hat{\mathbf{s}}$. $I(\mathbf{r}, \hat{\mathbf{s}})$ is normally referred to as the radiance or specific intensity (within this document normally referred to, simply, as the intensity). We consider only monochromatic light and elastic scattering, therefore we may ignore the frequency dependent part of $I(\mathbf{r}, \hat{\mathbf{s}})$ (therefore the units of $I(\mathbf{r}, \hat{\mathbf{s}})$ are $\mathrm{W/m^2sr}$). The flux of power within a solid angle $d\omega$ through an area da (figure 6.1) is expressed in terms of the intensity:

$$dP = I(\mathbf{r}, \hat{\mathbf{s}}) \cos\theta da d\omega \tag{6.1}$$

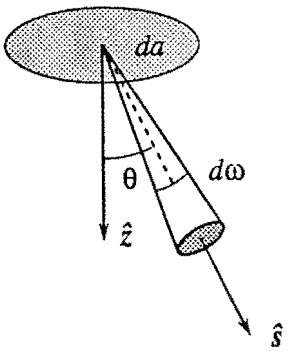

Figure 6.1: The power flux within a unit solid angle $d\omega$ through an area da at a point $\mathbf{r}$. $\hat{\mathbf{s}}$ is a vector at an angle θ with respect to the unit normal $\hat{\mathbf{z}}$. The intensity is in direction $\hat{\mathbf{s}}$ and the power dP is given by equation 6.1.

By integrating the intensity over all solid angles we obtain the radiant energy fluence rate, or space irradiance, $\Phi(\mathbf{r})$ ($\mathrm{W/cm^2}$);

$$\Phi(\mathbf{r}) = \int_{4\pi} I(\mathbf{r}, \hat{\mathbf{s}}) d\omega \tag{6.2}$$

which, when multiplied by the absorption coefficient σ_a (/cm), yields the power absorbed by the tissue at that point (in $\mathrm{W/m^3}$)). This volumetric absorbed power is a term of the bio-heat equation (equation 7.1). This equation determines the time dependent temperature variations within the tissue as a function of the incident power and of the illumination time. We can obtain the irradiance and consequentially the volumetric absorbed power by assuming there is no correlation between the electromagnetic fields from different particles, thus the addition of powers rather than fields holds. This is the basis of transport theory which does not deal with interference and diffraction effects but rather with the transport of energy through the medium. Transport theory and analytic theory can be shown to be linked through the specific intensity which is the statistical average of the randomly varying Poynting vector ($\mathbf{S}(\mathbf{r}, t) = \mathbf{E}(\mathbf{r}, t) \times \mathbf{H}(\mathbf{r}, t)$, see Ishimaru section 7-8).

6.2 The Transport Equation

The angular dependence of this scattering may be represented by a transport equation (Ishimaru 1978):

$$\hat{\mathbf{s}}\cdot\nabla I_d(\mathbf{r},\hat{\mathbf{s}}) = -\sigma_t(\mathbf{r})I_d(\mathbf{r},\hat{\mathbf{s}}) + \sigma_t(\mathbf{r})\int_{4\pi} I_d(\mathbf{r},\hat{\mathbf{s}}')p(\hat{\mathbf{s}}',\hat{\mathbf{s}})d\omega' + S(\mathbf{r},\hat{\mathbf{s}}) \tag{6.3}$$

where

$I_d(\mathbf{r},\hat{\mathbf{s}})$ is the intensity as defined above, but for diffuse light only,

$S(\mathbf{r},\hat{\mathbf{s}})$ is the source function, and

$p(\hat{\mathbf{s}}',\hat{\mathbf{s}})$, the phase function[1], is the relative probability of a photon scattering from direction $\hat{\mathbf{s}}'$ into direction $\hat{\mathbf{s}}$ and is defined such that

$$\int_{4\pi} p(\hat{\mathbf{s}}',\hat{\mathbf{s}})d\omega' = \frac{\sigma_s}{\sigma_t} \tag{6.4}$$

where

ω' is the solid angle, and

$\sigma_t(\mathbf{r})$ is the total attenuation coefficient such that $\sigma_t(\mathbf{r}) = \sigma_s(\mathbf{r}) + \sigma_a(\mathbf{r})$ and $\sigma_s(\mathbf{r})$ and $\sigma_a(\mathbf{r})$ are the scattering and absorption coefficients.

The first term on the right hand side of equation 6.3 is the intensity decrease (in the direction $\hat{\mathbf{s}}$) due to the absorption or scattering of scattered light that was originally travelling in direction $\hat{\mathbf{s}}$. The second term is the gain in intensity due scattering into direction $\hat{\mathbf{s}}$ from all other directions $\hat{\mathbf{s}}'$. As we are interested in collimated light incident on the surface of the scattering medium as the only source, the source term becomes

$$S(\mathbf{r},\hat{\mathbf{s}}) = \frac{\sigma_t}{4\pi}p(\hat{\mathbf{s}}',z)I_c(\mathbf{r},z) \tag{6.5}$$

where z is parallel to the angle of incidence of the collimated beam and $I_c(\mathbf{r},z)$ satisfies

$$\frac{dI_c(\mathbf{r},z)}{dz} = -\sigma_t I_c(\mathbf{r},z). \tag{6.6}$$

Equation 6.3 is not normally analytically solvable and has been inhibitively difficult to solve by numerical means. For us to apply the bio-heat equation we wish to calculate the radiant fluence rate ($\Phi(\mathbf{r})$) within the blood vessels. We shall discuss six approximate solutions to equation 6.3 and how applicable they may be.

[1]The term phase function is an historical accident in this context. It originated in astronomy where it referred to lunar phases. However, in this context the phase function represents the angular distribution of the scattered power and has no relation to either lunar phases or the phase of a wave.

6.3 Solutions to the Transport Equation

If we consider each of the three structures (or media), the epidermis, the dermis, and the blood vessels, to be comprised of a distribution of scattering particles in an otherwise homogeneous medium, then the solution to the transport equation would require the calculation of the radiant flux rate (irradiance) throughout each of these media. As each medium has different absorption and scattering characteristics the solution would require the solution of (at least) three transport equations! By considering only three media we have already limited the accuracy of the solution. For instance in section 2.1 we examined four distinct layers within the epidermis. Each of these layers may respond differently to incident light.

Prior to considering solutions to the transport equation we must consider a collimated beam of light incident upon the skin surface. That is, we consider the light as it travels from a medium of low refractive index (air, $n_a \approx 1$) to one of higher refractive index (stratum corneum, $n_s = 1.55$). At the interface of the two media there occurs a certain amount of reflection known as Fresnel's reflection. The magnitude of the reflection is for collimated unpolarised light incident perpendicular to the skin surface:

$$R = \frac{(n_a - n_s)^2}{(n_a + n_s)^2} \approx 0.05 \tag{6.7}$$

That is, approximately 5% of the light that is incident at the skin surface is reflected. However, the skin surface is not perfectly flat, therefore there is likely to be a greater percentage of light reflected than this. We shall now summarise solutions to the transport equation which deal with the non-reflected incident light.

6.3.1 Beer's law

This is the most straightforward of the solutions and states that the incident light is exponentially attenuated as it passes through tissue. The light lost from the collimated beam is assumed to be absorbed or scattered out of the beam and hence the intensity at depth z is:

$$I(\mathbf{r}, z) = I(\mathbf{r}, 0) \exp[-\sigma_t z] \tag{6.8}$$

In a medium where scattering is significant in comparison to absorption (such as the epidermis and dermis) this approximation will underestimate the intensity because scattered light adds considerably to the total flux. Equation 6.8 then becomes the equation for the collimated intensity $I_c(\mathbf{r}, z)$. However, where absorption dominates scattering equation 6.8 is a good approximation. This is the case within blood at 577/578 nm where the absorption coefficient is nearly eighty times the scattering coefficient (van Gemert *et al.* 1986). Because of the collimated nature of the light the intensity and irradiance are identical. Often irradiance is used as a synonym for the specific intensity of a collimated beam as it is incident on the skin surface.

Beer's law has been used as an estimate of the irradiance within a port wine stain in the model of van Gemert *et al.* (1986).

6.3.2 Kubelka-Munk

This two-flux one-dimensional model is based on illumination by a perfectly diffuse source and considers a diffuse inward moving flux (F_+) and a diffuse outward moving flux (F_-) such that:

$$\frac{dF_+(z)}{dz} = -(S+K)F_+(z) + SF_-(z) \tag{6.9}$$

$$-\frac{dF_-(z)}{dz} = -(S+K)F_-(z) + SF_+(z) \tag{6.10}$$

where z is in the inward direction and S and K are the Kubelka-Munk scattering and absorption coefficients. Sdz represents the fractional contribution to the flux due to scattered light from the oppositely directed flux within the differential distance dz. Kdz represents the fractional loss of light due to absorption within the differential distance dz. S and K may be related to the transport equation scattering and absorption coefficients σ_s and σ_a (see for example Star *et al.* 1988). Hence, the contribution of scattered light to the inward and outward fluxes increases the irradiance above that which is determined by Beer's law. This model has been extended to include collimated light (van Gemert *et al.* 1987b), but it still lacks the capability of producing the intensity as a function of direction. Wan *et al.* (1981) used the Kubelka-Munk model to calculate the expected transmission and reflectance of human epidermis and found the results compared favourably with experimental measurements. Lahaye and van Gemert (1985) used this model to calculate the light distribution within port wine stain for a Gaussian incident beam by calculating $I(z)$ and multiplying by the shape of the beam.

6.3.3 The diffusion approximation

This approximation assumes that light is scattered almost uniformly after numerous scattering events. However there is some anisotropy in the intensity such that the inward transport of energy is retained (figure 6.2).

Mathematically we have

$$\begin{aligned} I_d(\mathbf{r},\hat{\mathbf{s}}) &= I_{isotropic} + I_{forward\ peak\ compensation} \\ &= \frac{1}{4\pi}\int_{4\pi} I_d(\mathbf{r},\hat{\mathbf{s}})d\omega + \frac{3}{4\pi}\int_{4\pi} I_d(\mathbf{r},\hat{\mathbf{s}})\hat{\mathbf{s}}\cdot\hat{\mathbf{z}}d\omega \\ &= U_d(\mathbf{r}) + \frac{3}{4\pi}\mathbf{F}_d(\mathbf{r})\cdot\hat{\mathbf{s}} \end{aligned} \tag{6.11}$$

where $U_d(\mathbf{r})$ is the average diffuse intensity and $\mathbf{F}_d(\mathbf{r})$ is the net diffuse flux vector.

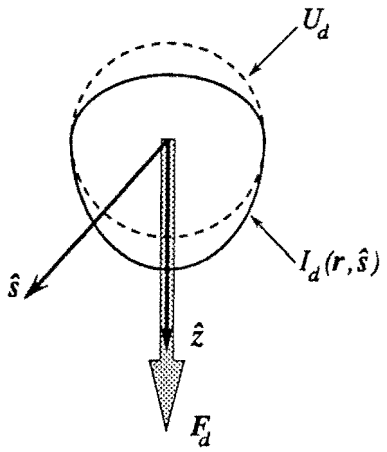

Figure 6.2: The diffuse intensity $I_d(\mathbf{r},\hat{\mathbf{s}})$ is the sum of the isotropic irradiance $U_d(\mathbf{r})$ and a peak flux $\mathbf{F}_d$ in the forward or downward direction $\hat{\mathbf{z}}$.

For a slab of infinite thickness and without sources (that is considering the solution only at a great depth) the solution to 6.11 is (Star *et al.* 1988, page 445)

$$I_d(z,\mu) = I_d(0,\mu)\exp[-\sigma_{eff}z]D(\mu) \tag{6.12}$$

where

z is the depth of the skin,

$I_d(0,\mu)$ is the incident intensity,

μ is the cosine of the angle between $\hat{\mathbf{s}}$ and the positive z axis (i.e. $\mu = \cos(\theta)$ of figure 6.2), and

$D(\mu)$ is given by

$$D(\mu) = \frac{[1+3g(1-a)\mu/k]}{1-k\mu} \tag{6.13}$$

where

the albedo $a = \frac{\sigma_s}{\sigma_t}$,

g is the anisotropy factor defined as the average cosine of the scattering angle ($g = \int_{4\pi} p(\hat{\mathbf{s}}',\hat{\mathbf{s}})\cos\theta\, d\omega'$), and

$k = \frac{\sigma_{eff}}{\sigma_t}$,

where σ_{eff} is the solution to

$$1 = \frac{a}{2k}[1 + \frac{3g(1-a)}{k^2}]\ln(\frac{1+k}{1-k}) - \frac{3g(1-a)}{k^2}. \qquad (6.14)$$

For example if we use the optical constants of human dermis at 577 nm (from van Gemert *et al.* 1989b we have $g = 0.787$, $\sigma_s = 210\,/\text{cm}$, $\sigma_a = 2.2\,/\text{cm}$ and therefore from equation 6.14 we have $\sigma_{eff} = 17.1\,/\text{cm}$). $D(\mu)$ is then the shape of figure 6.3 which represents the relative intensity with respect to direction. The exact magnitude of the intensity depends on the depth within the tissue. For any given depth in any given direction the intensity will be proportional to the intensity in figure 6.3 in that direction. From equation 6.12 we see that the magnitude of intensity decreases exponentially with depth.

The basic assumption of this approximation is that the angular flux is linear anisotropic which holds far from boundaries and if scattering dominates absorption. Van Gemert *et al.* (1987b) has shown that even with dominant scattering the diffusion approximation is not valid if the scattering is strongly forward orientated. Unfortunately this is the case within the skin. Jacques *et al.* (1987) illustrated the strong forward nature for scattering within the dermis at 633 nm.

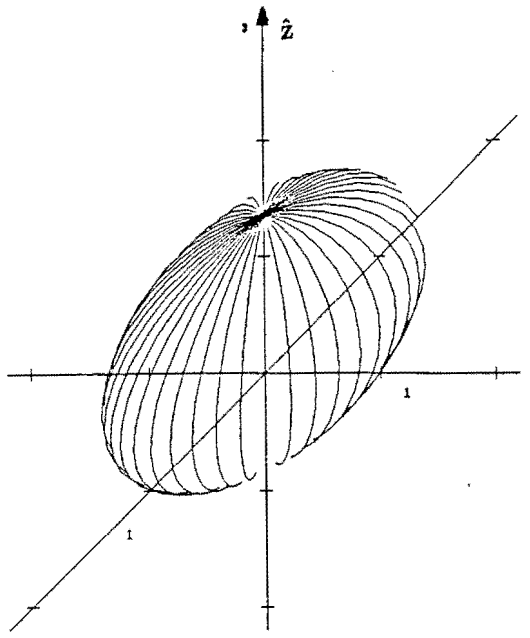

Figure 6.3: The three dimensional distribution of light represented by $D(\mu)$ of the diffusion approximation varies only in total irradiance with depth. It is symmetrical around the $\hat{z}$ (inward direction) with a greater intensity in the positive $\hat{z}$ direction. This diagram illustrates the distribution for 577 nm with $g = 0.787$, $\sigma_s = 210\,/\text{cm}$. $\sigma_a = 2.2\,/\text{cm}$. Note the intensity in the $\hat{z}$ direction is 1.3 units, but is only 0.7 units in the $-\hat{z}$ direction.

6.3.4 Seven flux model

Simply stated, this model considers contibutions to the total flux from six orthogonal directions due to scattered light and one contribution due to collimated light (figure 6.4). The collimated light undergoes exponential attenuation according to Beer's law. We have six linear coupled differential equations of the form (Yoon *et al.* 1987)

$$\begin{aligned}\frac{\partial F_{+y}(x,y,z)}{\partial y} + \sigma_t F_{+y} &= \sigma_t[\{w_{y,x}F_{+x} + w_{y,-x}F_{-x} \\ &\quad + w_{y,y}F_{+y} + w_{y,-y}F_{-y} \\ &\quad + w_{y,z}F_{+z} + w_{y,-z}F_{-z}\} \\ &\quad + w_{y,z}F_c(x,y,z)] \end{aligned} \tag{6.15}$$

and similarly for F_{+x}, F_{+z}, F_{-x}, F_{-y} and F_{-z}. If i and j can be any of x, y, or z then $w_{i,j}$ is the portion of the flux from the i direction being scattered into the j direction. The $w_{i,j}$ are weights which describe the phase function $p(\hat{\mathbf{s}}', \hat{\mathbf{s}})$ of equation 6.3.

The collimated flux F_c obeys

$$\frac{\partial F_c(x,y,z)}{\partial z} = -\sigma_t F_c(x,y,z). \tag{6.16}$$

For a given (measured, see next subsection) phase function it is possible to deduce the irradiance as a function of the fluxes from the seven directions.

6.3.5 The modified Henyey-Greenstein phase function

The Henyey-Greenstein phase function describes scattering from a single particle (Henyey and Greenstein 1941). It is a function produced to fit experimental data and normally takes the form:

$$p_{hg}(\hat{\mathbf{s}}', \hat{\mathbf{s}}) = \frac{\sigma_s}{\sigma_t} \frac{1 - g_{hg}^2}{(1 + g_{hg}^2 - 2g_{hg}\mathbf{s}\cdot\hat{\mathbf{s}})^{\frac{3}{2}}} \tag{6.17}$$

where

$\hat{\mathbf{s}}'\cdot\hat{\mathbf{s}} = \cos\theta$ and θ is the angle between the $\hat{\mathbf{z}}$ axis and the vector $\hat{\mathbf{s}}$ as in figure 6.2,

g_{hg} varies from 1, totally forward orientated scattering, to 0, isotropic scattering, and to -1, totally backward orientated scattering.

Jacques *et al.* (1987) used this single scatterer phase function as a basis for describing the experimental results of HeNe (633 nm) laser light scattering within thin samples

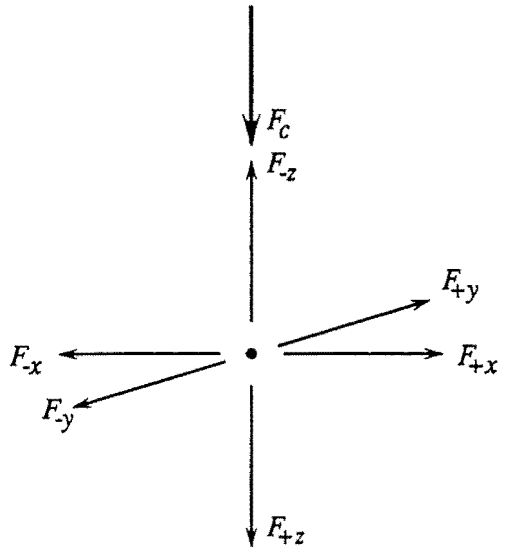

Figure 6.4: The seven flux model incorporates six scattered fluxes, the intensities of which are determined by some phase function, and one collimated flux F_c which attenuates according to Beer's law.

of human dermis. Their modified phase function (p_{mhg}) now consists of an isotropic part and an anisotropic Henyey-Greenstein part

$$p_{mhg}(z, \cos\theta) = b(z) + (1 - b(z)) \frac{1 - g_{mhg}^2(z)}{(1 + g_{mhg}^2(z) - 2g_{mhg}(z)\cos\theta)^{\frac{3}{2}}} \tag{6.18}$$

where z is the depth and $b(z)$ is the fractional component of isotropic scattering. The intensity may be calculated as a function of θ:

$$I(z, \cos\theta) = \mathsf{SCALE}\, p_{mhg}(z, \cos\theta) \tag{6.19}$$

where SCALE is a function of optical depth $\sigma_t z$ and the albedo σ_s/σ_t (Jacques *et al.* (1987) did not specify the function any further). The anisotropy factor g (defined as the average cosine of the scattering angle, see section 6.3.3) is related to the modified phase function anisotropy factor by $g = (1 - b(0))g_{mhg}(0)$. Once again this approach may be used to find the intensity as a function of angle. However, measurements must first be made at the wavelength of interest to determine the optical characteristics of the tissue. The difference in irradiance and relative spatial distribution of the intensity with depth is illustrated by figure 6.5 which is a two dimensional representation of the intensity as a function of angle at depths of 100 and 500 μm.

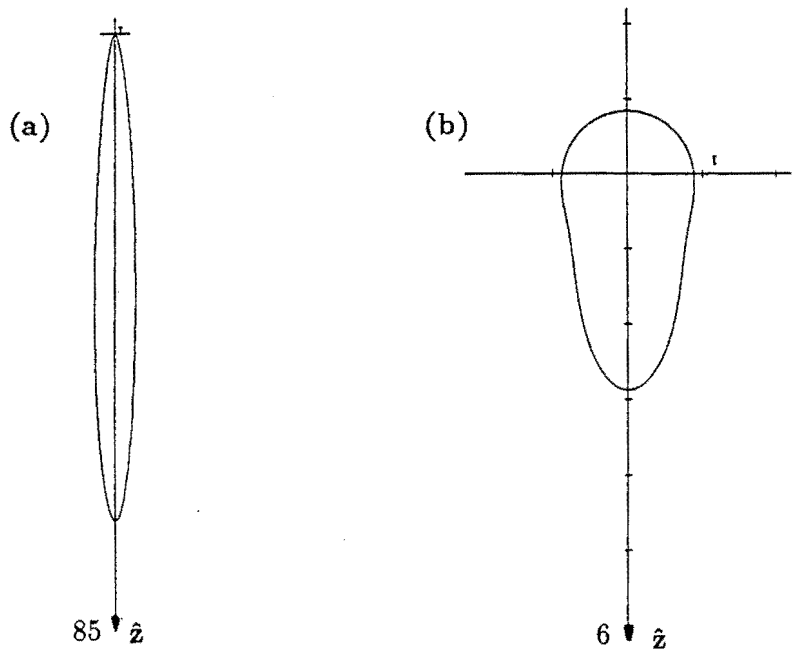

Figure 6.5: The two dimensional light distribution at depths of 100 μm (a) and 500 μm (b) within the dermis as calculated with Jacques *et al.* (1987) modified Henyey-Greenstein phase function. Near the surface most of the light is scattered forward in the positive z direction while deeper within the dermis the light has undergone numerous scattering events and become more isotropic.

6.3.6 Monte Carlo calculations

A photon travelling through a scattering media will be likely to encounter a number of particles from which it will scatter before encountering a particle that absorbs it. The average length of path between scattering events depends on the density of the media and the cross sectional area of the scatterers. The scattering angle of each event depends on the nature of the scattering particle as does the probability of absorption. For any media these properties are described by the optical constants σ_a, σ_s, and g. The Monte Carlo method described by Cashwell and Everett (1959) considers variables such as the path length and the change in direction as random variables. Each of the variables is characterised by a probability density function ($P(x)$) which is defined as

$$\int_a^b P(x)dx = 1 \tag{6.20}$$

where x ($a \leq x \leq b$) is a random variable. Thus, the distribution of random events, x_{rnd}, for variable x can be simulated by choosing a random number, RND, with a distribution between 0 and 1 such that:

$$\int_a^{x_{rnd}} P(x)dx = RND \tag{6.21}$$

If we take as an example the path length between each scattering event, then the

average distance a photon travels between scattering events (the mean free path) is given by

$$\lambda = \frac{1}{\sigma_t} \tag{6.22}$$

and the probability density function is

$$P(l) = \frac{1}{\lambda} \exp[-\frac{l}{\lambda}] \tag{6.23}$$

where l is the length between scattering events.

Thus 6.23 into 6.20 yields

$$l_{rnd} = -\ln(1 - RND)\lambda \tag{6.24}$$

which is calculated between each scattering event. Similarly a function for the angle scattered may be produced that calculates θ_{rnd} for each scattering event.

The direction of the scattering angle has a probability distribution which is described by functions such as the modified Henyey-Greenstein phase function p_{mhg} or the diffusion approximation's $D(\mu)$. At any scattering event there is a probability σ_a/σ_t that the photon will be absorbed.

Rather than follow the path of each individual photon the Monte Carlo calculation utilises a weighted sum of photons, or a photon packet, such that at each scattering event the weighted sum is reduced by a factor $1-\sigma_a/\sigma_t$ due to absorption at that point.

This method allows the absorbed light within any unit volume of skin and the remitted light to be calculated as a function of the distribution and number of photons incident upon the skin. Keijzer (1989) and Wilson and Adam (1983) are two examples of the use of this method for a single medium.

6.3.7 Summary of solutions to the transport equation

Most of the transport models have been used to calculate the space irradiance through a one dimensional model of the epidermis or a bloodless dermis. Some of these results are illustrated in figure 6.6 for a $1\,\mathrm{W/cm^2}$ beam incident upon a bloodless dermis.

However, we are most interested in the light absorbed within the skin by the melanin and haemoglobin. Any model we use must take into account these two factors. This implies that we must consider separately the optical characteristics of the epidermis, dermis, and blood. Further, we need to consider the three dimensional nature of the blood vessels. For most of the models above this means solving the transport equation for collimated light incident upon the epidermis, scattered light with a calculated intensity distribution incident on the dermis and scattered light of another intensity distribution (dependent on depth) incident on each part of a blood vessel. This appears to be best achieved by employing different optical

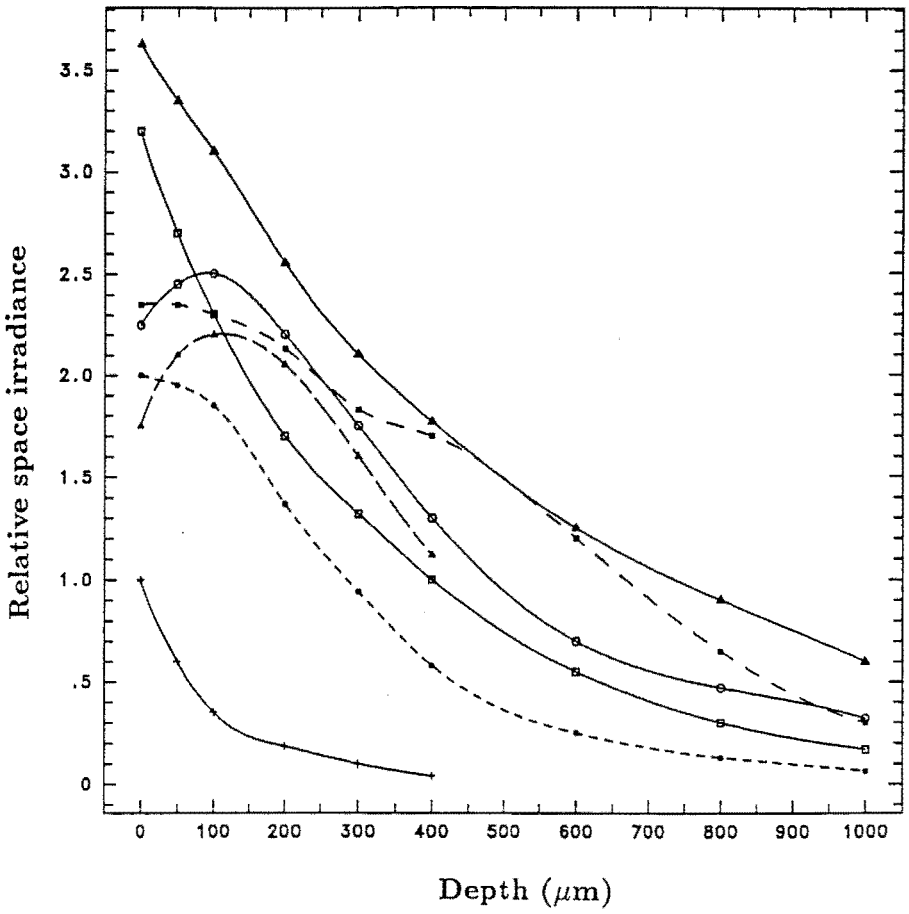

Figure 6.6: The space irradiance for a 1 W/cm^2 collimated infinite diameter beam incident upon a bloodless dermis. The solid lines are from figure 7a of Welch *et al.* (1987) and represent Beer's law (crosses), Seven flux (open squares), Diffusion (open circles), and Kubelka-Munk (open triangles) for a medium that is highly scattering dominated ($\sigma_a = 1$, $\sigma_s = 100$, $S = 75$, $K = 2$ all arbitrary units). The diffusion approximation is not strictly as described in this chapter but takes into account the effect of the boundary at the skin surface. The closed circle dotted line represents a Monte Carlo calculation from van Gemert *et al.* (1989a). Here the optical characteristics are $\sigma_a = 6$ /cm, $\sigma_s = 414$ /cm, $g = 0.91$, and a phase function that is isotropic except for a delta function in the positive $\hat{z}$ direction. The closed square dashed line is a Kubelka-Munk model with the addition of a collimated beam. The light is assumed incident on a 65 μm thick epidermis, under which is 300 μm of dermis, then an 80 μm thick blood plexus. The closed triangle dashed line is the Henyey-Greenstein phase function calculation of Star *et al.* (1988) using the optical characteristics of dermis at a wavelength of 633 nm as measured by Jacques *et al.* (1987) ($\sigma_a = 2.7$ /cm, $\sigma_s = 187.3$ /cm, $g = 0.81$).

characteristics g, σ_s, σ_a for each of the three media and utilising the Monte Carlo model to calculate the heat deposited throughout the skin (Smithies 1989). In this case the transition from one medium to another must be taken into account. We must be aware that even the choice of only three distinct media is an assumption and that the calculations depend on the determination of the three optical characteristics for each media. As we shall illustrate in the next chapter there shall be a number of further simplifying approximations.

CHAPTER 7 THE MODEL

Different treatment modalities produce different clinical responses from the skin. The various treatment modalities can differ significantly in respect to wavelength, irradiance, and illumination time. For any one modality not all lesions respond identically. To understand the reasons for these differences in response and to attempt to define some "optimal" treatment parameters, we have undertaken to numerically model the laser light interaction with the skin. As with any model, various approximations and assumptions have been made. In this chapter we describe the model and the assumptions.

7.1 Yellow Light

The choice of yellow 577/578 nm light as the optimal wavelength for the treatment of vascular lesions was based on the absorption spectra of human skin chromophores (figures 2.2 and 2.4, chapter 2). To damage the ectatic vessels we presume it is desirable to coagulate their surrounding endothelial cells. Also, it is desirable to avoid coagulation of any other cutaneous structures that may result in scar formation. 577/578 nm light provides for both these conditions. First, it is not well absorbed by melanin (especially in comparison to the 488 to 514.5 nm wavelengths of the argon laser), and second it is absorbed sufficiently well by haemoglobin to allow for rapid heating of the blood vessels before an excess of heat can be released to the surrounding tissue. This process depends on the length of illumination and the irradiance of the incident light. These are the two treatment parameters which we wish to optimise. As we have discussed, the melanin concentration can have a significant effect on the quantity of light entering the dermis. However, this concentration plays no part in our model of the optimal illumination times and the optimal irradiance incident upon the vessel. It is only when we consider the optimal irradiance incident on the skin surface that knowledge of the melanin concentration is important.

Recently, 585 nm has been suggested as the preferred wavelength. We shall discuss the reasons for this suggestion in chapter 9. However, throughout this chapter we shall concentrate on 577/578 nm light.

7.2 Treatment Modalities

Treatment modalities employ one of two distinct endpoints, namely blanching or purpura. Clinically, blanching is the whitening of the skin seen immediately on application of the laser light. Normally there is an incident irradiance below which no blanching occurs. This irradiance depends on the pigmentation of the skin, the wavelength, and the illumination time. Argon, continuous wave dye, and copper vapour laser techniques have all utilized blanching as the clinical endpoint (most blanching techniques now utilise minimal blanching). Purpura is the blue/grey appearance of the skin some 5 to 15 minutes after application of 577 nm light from a pulsed dye laser. The threshold irradiance is defined as that which only just produces purpura within this time scale, this is normally the clinical endpoint.

The principal difference between the two techniques is the length of illumination time (considering yellow light lasers only). The pulsed dye laser produces short single pulses of 0.0003 ms to 0.45 ms in duration. The other lasers employ much longer illumination times of 30 ms to several hundred milliseconds.

Blanching techniques have employed a variety of irradiances and illumination times. We have already described our own technique in chapter 4 and Pickering *et al.* 1990b . Briefly, it is a manual scanning technique with a 1.3 mm diameter spot, an irradiance of 50 to 600 W/cm^2, and corresponding illumination times of 500 to 30 ms. The shorter illumination times (higher irradiances) produce the best clinical results. Lanigan and Cotterill (1989) have used a continuous wave dye laser with a 2 mm diameter spot, an irradiance of 10 to 20 W/cm^2, and illumination times of 200 to 2000 ms. Rather than a scanning technique they employ mechanical shutters to control the illumination time. Another blanching technique uses a very small diameter spot, 0.1 mm, high irradiance, 1200 to 10000 W/cm^2, and a very slow tracing technique. The tracing technique, with either a continuous wave dye or low powered copper vapour laser, is to trace the light along individual blood vessels (observed under magnification) at a sufficiently slow rate to blanch them (Schiebner 1989, van Hassalt and Liu 1989). Unfortunately illumination times can not be accurately determined from the data available but they appear to be in the order of several tens to several hundreds of milliseconds.

The purpura techniques produce their best clinical results with their longest pulse length (0.45 ms). On the other hand we have shown that the minimal blanching techniques produce their best results at their shortest illumination time (30 ms). This suggests that the optimal treatment may result with an illumination time somewhere between 0.45 ms and 30 ms.

Recently, sub-marginal blanching (some slight erythema) has been suggested as a sufficient and desirable endpoint with a frequency doubled Nd:YAG laser at 532 nm (Laffitte *et al.* 1989).

7.3 The Numerical Calculations

Details of the model have been published in Pickering *et al.* 1989a,b. This section is a summary of the important components of the model here. It is a finite difference model based on the bio-heat equation:

$$\rho C_v \frac{\partial T(x,y,z,t)}{\partial t} = \sigma_a \Phi(x,y,z) + \eta \nabla^2 T(x,y,z,t) \tag{7.1}$$

where $\sigma_a \Phi(x,y,z)$ is the power absorbed at coordinate (x,y,z) as defined in section 6.1. The second term on the right hand side of the equation represents the energy change per unit time from coordinate (x,y,z) due to the heat conduction. ρ, C_v, and η are the tissue density, heat capacity, and conductivity respectively (see table 2 of Pickering *et al.* 1989a).

The numerical calculation uses a grid of 81 by 81 points spaced 3 μm apart. The vessel is assumed to be positioned at the centre of this grid. The grid points that lie within the circumference of the vessel may absorb light ($\sigma_a \Phi > 0$) elsewere no light is absorbed ($\sigma_a \Phi = 0$). The interval between successive calculations of temperature rise due to light absorption and temperature change due to conduction was 1/3000th of the total calculation time (usually 10 to 35 ms). Heat conduction was calculated at each grid point using a second order two dimensional method of finite differences (Carslaw and Jaeger 1967)(note - no heat conducts parallel to the vessel's longitudinal axis). Mathematically for each grid point (n,m) after each time interval the new temperature due to conduction is:

$$T_{n,m}^{new} = \frac{\eta}{\rho C_v} \frac{1}{(grid\,spacing)^2} [T_{n+1,m}^{old} + T_{n,m+1}^{old} + T_{n-1,m}^{old} + T_{n,m-1}^{old} - 4T_{n,m}^{old}] \tag{7.2}$$

The calculations for the two published papers were made on a VAX 8350 computer whilst subsequent calculations have been made on a SUN 3/60 workstation.

This model was originally designed to determine the optimal treatment parameters of illumination time and irradiance. We are able to obtain the temperature profile of the vessel at any time during or after illumination.

7.3.1 Previous models

The first attempt at describing the physics of laser treatment of port wine stains was made by Anderson and Parrish of the Harvard Medical School(Anderson and Parrish 1981a,b, 1983). Their model discussed the light flux at different depths as a function of wavelength based on the Kubelka-Munk model (section 6.3.2), the absorption spectra of the chromophores within the skin, and the possibility of selectively coagulating blood vessels with a sufficiently short pulse of 577 nm light. The basis for this model was that:

> "Coagulation necrosis is useful for causing haemostasis due to the denaturation of plasma proteins and the closing of vessels." (Anderson and Parrish 1983 page 524).

On this basis they assumed the target was blood and the target temperature was approximately 70 °C. Furthermore, they estimated that excess conduction of heat to the surrounding tissue could be avoided by an illumination time shorter than the thermal relaxation time of the vessel. Their thermal relaxation time is based on a Gaussian temperature profile across the width of the vessel and defined as:

> *The time it takes for the central temperature to fall to half way between its peak temperature and the temperature of the vessel surroundings.*

The criterion *the illumination time must be shorter than the thermal relaxation time of the vessels* has become a stumbling block in the literature. Often this is claimed to be a physical requirement. In essence this criterion is only a rule of thumb. As an expression for the rate of conduction of heat it obviously allows for some heating of the immediate surroundings of the vessel lumen. But, the criterion is based on an arbitrary choice of the maximum temperature falling by 50%. Thus, this criterion does not indicate whether there is sufficient heat conducted to coagulate the vessels. This is contrary to the use of this criterion as a requirement for optimally damaging the vessels. For example

> "...pulse width is significantly lower than the thermal relaxation time of the irradiated vessel (...), allowing sufficient time for a transient local temperature rise to destroy the vessel..." (Glassberg *et al.* 1988 page 1201),

> "For enhanced specifity, the pulse duration should be equal to or less than the thermal relaxation time for that target." (Tan *et al.* 1989 page 868).

A four layer skin model was developed by van Gemert *et al.* (1982) to estimate the temperatures within port wine stains due to argon laser treatment. The epidermis, superficial dermis, blood plexus, and deeper dermis were the four parallel layers. The epidermis was approximately 60 μm thick and the blood plexus a further 300 μm below the epidermal/dermal junction. Fluences within the skin were based on the Kubelka Munk approximation. Their conclusion was: at 500 nm, with a pulse longer than 0.1 s, and an irradiance sufficient to coagulate the blood plexus, the epidermis and superficial dermis also underwent coagulation. They calculated, at this wavelength, to avoid heat conduction effects that result in coagulation of the superficial dermis, the illumination time must be less than 0.05 ms. They determined a criterion for the applied power ($P(0)$) such that temperature rise within

the epidermis must be less than within the blood plexus. By applying this criterion with such a short illumination time we have

$$\frac{A_b}{A_e} \cdot \frac{P(b)}{P(0)} \gg 1 \tag{7.3}$$

where

A_b and A_e are the Kubelka-Munk absorption coefficients for blood and the epidermis respectively,

$P(b)$ and $P(0)$ are the power at the depth of the blood plexus and on the skin surface respectively.

Lahaye and van Gemert (1985) extended this model to include an individual rectangular blood vessel as an alternative to a layer of blood. They applied this model with a variety of wavelengths, spot sizes and illumination times. The optimal treatment parameters were found to be a 1 to 10 ms illumination time, a minimum beam radius of 0.1 mm, and a wavelength of 415, 577 or 540 nm. Later (van Gemert *et al.* 1986) the model was again extended with a 80 μm diameter cylindrical blood vessel situated 300 to 600 μm below the epidermis. Once more they concluded that the optimal parameters were a 1 to 10 ms illumination time at 577 nm (now considering the benefits of avoiding melanin absorption).

Equation 7.3 was formulated when the optimal illumination time was thought to be less than 0.05 ms and consequently conduction effects were negligible. Later models took into account conduction and suggest much longer illumination times. Thus equation 7.3 is not suitable as it stands as an estimate of the optimal incident irradiance.

Neither of these models looked at where exactly the coagulation temperature should be reached. They assumed a blood temperature of 70 °C at the top of the vessel was sufficient for coagulation. However, this does not guarantee coagulation of the vessel. The inaccuracies of these models prompted us to develop our numerical model.

7.3.2 Assumptions

With any model there are a number of assumptions made, often to assist the ease of computation. In this section we list the assumptions we have made and discuss their influence on the model.

(i) We, like van Gemert and co-workers, have assumed that the cutaneous tissue characteristics of density, heat capacity, and conductivity may be approximated by the corresponding characteristics of water (see table 2 Pickering *et al.* 1989a). We also assume that these characteristics are invariant with temperature over the 30 to 100 °C range.

(ii) The blood vessels are represented by perfect cylinders parallel to the skin surface. Histology shows capillaries often do not to have circular cross sections but rather elliptical cross sections. However, the concept of capilliry plexus running parallel to the surface has been well established by histology (Ryan 1973).

(iii) There is no heat loss due to blood flow. Welch *et al.* (1980) calculated that blood flow within normal skin does not significantly (less than 10% error) effect the temperature rise at the end of laser illumination for illumination times shorter than 50 seconds. For the large 150 μm diameter vessels of deeply located port wine stains, we can estimate a volume flow rate of approximately 50 times normal capillaries and hence a 10% error for illumination times longer than 1 second. As we are considering much shorter illumination times any error due to blood flow is negligible.

(iv) The haemoglobin is homogeneously distributed throughout the vessel. In reality the haemoglobin is concentrated within the erythrocytes which contribute 45% of the blood by volume. However, these erythrocytes are donut shaped structures (disk-like with a depression in the centre) of approximately 7 μm diameter which is relatively small on the scale of most ectatic vessels (from 30 to 150 μm diameter) So, they are distributed reasonably evenly throughout the vessel. For very small vessels (normal capillary size) the erythrocytes may be in single file along the vessel and separated by plasma, by no means a homogeneous distribution of haemoglobin and thus our model is not very suitable for modelling the response of normal skin. For very large vessels the erythrocytes may tend to conglomerate along the central axis of the vessel. This inhomogeneous distribution may be a potential source of error in our model.

An erythrocyte density of 45% of the blood by volume and donut shape erythrocytes suggest that they are almost continually in contact with one another. Therefore, unless the illumination time is very short (say much shorter than the thermal relaxation time of the erythrocytes, 0.006 ms – see appendix F) and the irradiance low, the erythrocytes will not be thermally isolated from each other.

(v) The vessel under investigation is thermally isolated from other vessels and from the epidermis. Van Gemert *et al.* (1986) suggested that for any time shorter than 10 ms the vessel would be isolated from the epidermis at a depth of greater than 300 μm. Furthermore, for a density of vessels such as measured by Barsky *et al.* (1980) and an illumination time below 30 ms the vessels are, on average, thermally isolated (Appendix F).

(vi) The beam is infinitely wide, collimated, and perpendicular to the skin surface. This allows us to neglect heat flow along the longitudinal axis of the vessel. This assumption is applicable to a beam diameter that is large in comparison to the vessel diameter (beam diameters greater than 0.5 mm).

(vii) Absorption within the blood dominates over scattering at 577/578 nm because the blood absorption coefficient is some forty to fifty times greater than the scattering coefficient. However for some other wavelengths this may not be an applicable assumption.

(viii) We have used an absorption coefficient of blood of 430 /cm (van Gemert *et al.* 1986). More recently there has been experimental work to quantify the optical characteristics of epidermis, dermis, and blood with greater accuracy. A summary of these optical characteristics is presented in table 7.1. The variation in the optical properties diminishes somewhat the accuracy of the numeric answers, but does not diminish the relative effects observed due to differences in wavelength, irradiance, vessel diameter, or illumination time. We have assumed that the absorption is invariant with temperature up to 100 °C. However, recent experiments by Tan *et al.* (1989b,c) suggest that this may not be a valid assumption.We discuss this further in section 8.3.

(ix) Neither experiment nor theory has quantified the damage required to necrose the ectatic vessels. Some coagulative thermal damage (as opposed to mechanical damage due to vaporisation of blood) has been shown to be necessary. Because of this the model assumes a temperature and a distance (thickness) from the vessel lumen at which the damage occurs. Both of these assumptions have been investigated for their influnce on the treatment parameters. By introducing a damage integral that estimates the extent of protein denature as a function of time and temperature we have been able to quantify the coagulation temperature with a greater degree of certainty. Additionally, it is not known how haemoglobin reacts to high temperatures caused by rapid local heating. Haemoglobin may denature in the same way as other proteins and having denatured may cease to absorb light. We have modelled this possibility and we discuss its plausibility and its possible ramifications on the treatment.

(x) The spatial distribution of light within a scattering medium such as the skin is difficult to quantify. There has been no experimental investigation into the angular spatial distribution of light within port wine stains. The experiments on normal skin show the total irradiance to be considerably higher than that which is calculated by Beer's law of exponential decay of incident light. Additionally, near the skin surface the angular distribution of scattered incident light is predominantly in the forward direction. We have investigated the changes in the optimal treatment parameters under the influence of changes in the spatial distribution of light around the blood vessels.

Table 7.1: Radiative transport equation absorption and scattering characteristics of epidermis, dermis, and blood.

Wavelength	*Epidermis*			*Dermis*			*Blood*			*Source*
nm	σ_{a_e}	σ_{s_e}	g_e	σ_{a_d}	σ_{s_d}	g_d	σ_{a_b}	σ_{s_b}	g_b	
500	22.2	57.7		6.14	130.0		140	10.4		1
577	18.3	48.6		4.18	91.6		376	9.6		
500							107			2
577	37	480	0.787	2.2	210	0.787	354			
585	36	470	0.79	2.2	205	0.79	191			
590							70			
633				2.7	187.3	0.807				3

Kubelka-Munk absorption and scattering characteristics of epidermis, dermis, and blood.

Wavelength	*Epidermis*		*Dermis*		*Blood*		*Source*
nm	K_e	S_e	K_d	S_d	K_b	S_b	
500	70	70					4
500	65	29	12	15	125		5
500	36.7	36.7	11.3	90.8	115	12.5	2,6
577	30	30	7.5	69	430	9.8	

Sources

1 Welch *et al.* 1989
2 van Gemert *et al.* 1989b
3 Jacques and Prahl 1987
4 Wan *et al.* 1981
5 Lahaye and van Gemert 1985
6 van Gemert *et al.* 1986

CHAPTER 8 THE OPTIMAL TREATMENT

The optimal treatment must be that which consistently produces the best clinical result. Some of the mechanisms for damaging the ecatatic vessels (thermal and mechanical) have been observed through histology (chapter 3). We have assumed that the optimal damage is due to the thermal denaturation of the endothelial cells. Theoretically denaturation may be described as resulting from heating to a coagulation temperature and maintaining that temperature for some period of time. The damage criterion is denaturation at a pre-determined distance (coagulation thickness) above the vessel lumen. The optimal treatment parameters would be those that meet this damage criterion without inducing mechanical damage through the vaporisation of blood. At 577/578 nm we have investigated the treatment parameters of irradiance and illumination time, and several definitions of the optimal damage coagulation temperature and thickness.

8.1 The Damage Criteria

Bearing in mind the assumptions discussed in the previous chapter we have defined the optimal damage criterion as:

> Irreversible damage to the ectatic blood vessels without damage to other cutaneous tissue.

In terms of our numerical model this statement reads:

> A temperature sufficient for denaturation of protein at a point a specified distance above (towards the skin surface) the vessel lumen.

We consider only "above the vessel lumen" because the endothelial cells tend to be wound in a helical fashion along the length of the vessel. Consequently each cell at some stage will be "above the vessel lumen". To determine the appropriate distance above the lumen (which we call the coagulation thickness) requires knowledge of the thickness of the endothelial cells and the threshold heating level for necrosis of these cells. Initially we suggested (as have others - Anderson and Parrish 1981b, van Gemert *et al.* 1982) that coagulation occurred at a maximum temperature of 70 °C. Although it was postulated that protein denatured within 1 ms at 70 °C (Priebe

and Welch 1978), it was not clear that this temperature was maintained for a long enough period within the endothelial cells or instead that this temperature may have been greater than required. We first investigated this assumption by modelling the optimal treatment parameters for 60 °C as well as 70 °C and used later the damage integral to calculate coagulation.

The methodology was to vary the illumination time to obtain the correct ratio of: an increase in temperature at the coagulation point, to an increase in temperature within the lumen (such that the maximum blood temperature would be 100 °C and the temperature at the coagulation point would be that defined as the coagulation temperature, usually 60 °C or 70 °C). Once this correct ratio was obtained we used the linear relationship between the temperature increase and the fluence at a constant illumination time to obtain the optimal fluence (and therefore irradiance) incident upon the vessel.

8.2 Individual Vessels

8.2.1 Vessel size

Our first theoretical paper (Pickering *et al.* 1989a) calculated, for a coagulation temperature of 70 °C and coagulation thickness of 6 μm, the variation in optimal irradiances and illumination times with vessel diameters.

Despite the large variation in vessel diameters the optimal illumination time showed very little variation (Table 3, Pickering *et al.* 1989a). But for the largest vessel (100 μm diameter) the optimal incident irradiance was approximately half of the optimal irradiance for the smallest vessels (30 μm diameter).

A large vessel absorbs a greater percentage of the light incident upon it than a smaller vessel because of the magnitude of the absorption at 577/578 nm (50% of the light is absorbed within 16 μm of blood). As the coagulation thickness is the same for all vessel sizes a larger vessel is likely to require a smaller irradiance. A smaller vessel releases heat generated within it more quickly than a larger vessel and therefore to generate sufficient heat for coagulation the illumination time needs to be longer.

Normal capillaries are approximately 7 μm in diameter. Therefore they will absorb much less than 25% of the light incident upon them and will release the heat generated to the surroundings 20 times as quickly as a 30 μm ectatic capillary. This implies that these capillaries are unlikely to be damaged with the treatment parameters we have defined as ideal for the ectatic vessels.

8.2.2 Coagulation temperature and endothelial cell thickness

We calculated the optimal treatment parameters for a coagulation temperature of 60 °C and several different coagulation thicknesses (0, 3, 6, 9 μm). The results are

summarised in table 3 of Pickering *et al.* 1989b.

Compared to the variation in illumination times due to different vessel diameters the variation due to different coagulation temperatures or thicknesses is large. As an example we shall discuss the difference between the treatment parameters at a coagulation thickness of 0 μm and 3 μm (at 0 μm the endothelial cell protein is unlikely to denature whilst at 3 μm, we surmise, most endothelial cells, average thickness 4 to 6 μm Barsky *et al.* 1980, would coagulate). Compared with using 0 μm as a coagulation thickness, 3 μm requires an illumination time that is, on average, four times longer and an irradiance two and a half times less (an overall 60% increase in incident energy). Previous models (section 7.3.1) had assumed that heating of the haemoglobin within the lumen to a pre-defined coagulation temperature was the requirement to necrose the vessels. Here we see that this assumption does not necessarily allow coagulation of endothelial cells.

8.3 Damage Integral

8.3.1 The integral

It is not sufficient to state that an ectatic blood vessel will be irradicated just by raising its endothelial cells temperatures to 60 or 70 °C. The probability of coagulative necrosis of these cells at these temperatures must be established. We may define cell necrosis as the denaturation of protein within the cells. For example this is readily observed when the "white" of an egg turns opaque in a frying pan. We also assume that the blanching of the skin under laser illumination is indicative of protein denature. However, we must emphasise that the optimal damage in terms of the ratio of thermal to mechanical and the healing process has not been established.

Living tissue contains many different proteins with a variety of structures and sizes. We would expect each protein to denature with a different rate function of temperature. The difference in the energy of the initial and final states of a single protein reaction, ΔH, vary greatly between protein types . However, there is a correlation between the energy involved in the reaction and the change in entropy, ΔS, of the system. This correlation is such that the rates of reaction are approximately the same for all protein reactions (within a factor of 2, see Johnson *et al.* 1974, page 253). This is because of the relationship between the rate of reaction and the free energy (ΔG):

$$\textit{reaction rate} \propto \exp(-\frac{\Delta G}{RT}) = \exp(-\frac{\Delta H}{RT}) \exp(-\frac{\Delta S}{R})$$

Thus, Henriques (1947) was able to quantitate the thermal damage of whole tissue by the damage integral:

$$\Omega = P \int_0^t \exp(-\frac{\Delta E}{RT}) dt \tag{8.1}$$

where

Ω is an arbitrary function describing tissue injury,

T is the (time dependent) temperature (in K),

R is the universal gas constant (8.314 J mol^{-1} K^{-1}),

P and ΔE are the experimentally determined pre-exponential constant and experimental activation energy constant respectively.

By measuring the time taken for a reaction to take place (judged by histological examination), at a steady state temperature, Henriques was able to calculate the activation energy ΔE. The pre-exponential constant P then depends on the arbitrary choice of $\Omega = 1$ to indicate thermal necrosis. For a single protein media this corresponds to denaturation of $1 - e^{-1}$ or 63% of the molecules (Welch 1984). The damage integral calculations are usually placed into one of three categories (Erez and Shitzer 1980):

1	$\Omega \leq 0.53$	Tissue damage is reversible (that is healing takes place),
2	$0.53 < \Omega < 1.0$	Tissue damage may be irreversible,
3	$\Omega \geq 1.0$	Tissue damage is completely irreversible (that is coagulative necrosis transforms the cells into a homogeneous mass of proteins).

Henriques and Moritz (Henriques 1947, Henriques and Moritz 1947) experiments to determine P and ΔE were based on studies of the epidermis of pig skin. Other workers have also experimentally determined values for P and ΔE. These are summarised in table 8.1. We have used the values of Henriques (1947) below 44 °C and Welch (1984) above 44 °C.

Table 8.1: Experimentally determined damage integral constants

Authors	P (s^{-1})	ΔE $(kJ\,M^{-1})$	*Temperature range* (°C)	*Comments*
Henriques 1947	3.1×10^{98}	630		used pig skin
Stoll and Greene 1959	3×10^{98}	630	52 to 63	experimental and predicted results differed by as much as a factor of 6
Welch 1984	4.3×10^{64}	420	44 to 50	
	9.4×10^{104}	670	> 50	
Welch and Polhamus 1984	1.3×10^{99}	630	45 to 63	monkey retina

A simple calculation ($\Delta t \approx \Omega / P \exp(-\Delta E/RT)$) shows that for a steady state temperature of 70 °C, and using the damage integral constants of Welch (1984), that Ω will exceed 1 in 0.21 ms. For all except the shorter pulse lengths of the pulsed dye lasers this is a short time in comparison to the illumination time. However, the treatment is not in a steady state, therefore we calculate Ω numerically in conjunction with our finite difference model.

Figure 8.1 shows the temperature contours of a 50 μm diameter vessel immediately after it has been illuminated for 5.5 ms with an irradiance of 520 W/cm^2 on the top surface of the vessel. Figure 8.2 is of the same vessel but illustrates the damage contours for $\Omega = 1$ (solid line) and $\Omega = 0.53$ (broken line) after the effect of heat conduction for a further 29.5 ms has been accounted for (by this stage the maximum temperature is below 40 °C). We find that for the illumination times between 0.45 and 30 ms that irreversible necrosis occurs where the maximum temperature is in the range of 68 to 72 °C.

8.3.2 Haemoglobin as a protein

Haemoglobin is also a protein and therefore we must ask the question; what effect can denaturation of haemoglobin have on the treatment? Hu *et al.* (1970) established a time dependent steady state coagulation temperature for haemoglobin, once more around 65 to 70 °C.

As a comparison to erythrocyte response to illumination by pulsed dye laser, Tan *et al.* (1989b) microscopically examined erythrocytes after they had been heated (to between 32 and 100 °C). The procedure was to place a vial of erythrocytes in a bath of boiling water and to remove the vial when the erythrocytes reached the predetermined temperature. The erythrocytes were then microscopically examined and their absorption spectrum observed. The results of the spectral analysis are shown in figure 8.3. The sharp decrease in absorption after heating to greater than 70 °C is expected, due to the denaturation of the haemoglobin protein. However, the sharp increase in absorption (a factor of 14) between 32 °C and 70 °C has not previously been reported. If this change in absorption were to occur on the laser illumination timescales, the heating of the vessels is likely to be more rapid than we have assumed, resulting in the maximum temperature occuring closer to the top of the lumen. However, the experiment did not measure the absorption at these temperatures but rather some considerable time after they had been reached. Furthermore, the method of heating used much longer timescales than laser illumination and was due conduction of heat into the erythrocytes, not the direct absorption of laser illumination and consequent heat generation within the erythrocytes.

To investigate the influence of no absorption immediately after denaturation of protein, we ran our finite difference model with the condition that where $\Omega \geq 1.0$ no light is absorbed. This has a dramatic effect on our temperature contours as can be seen by comparing figure 8.1 with figures 8.4 and 8.5. Figure 8.4 has the

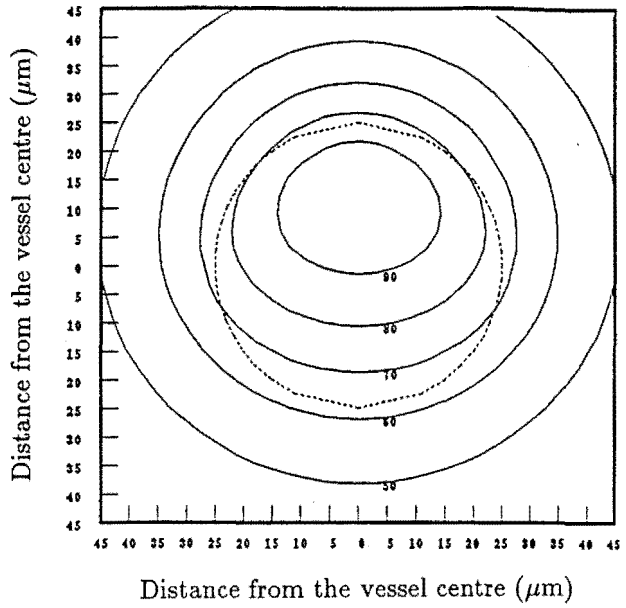

Figure 8.1: The temperature contours of a 50 μm diameter vessel after it has been heated for 5.5 ms with an irradiance on the top surface of the vessel of 520 W/cm^2. The dotted circle defines the vessel lumen.

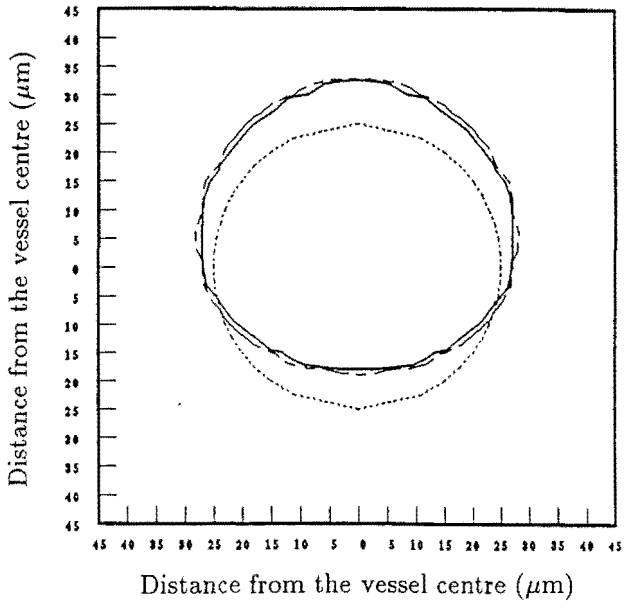

Figure 8.2: The damage contours of a 50 μm diameter vessel after it has been heated for 5.5 ms with an irradiance on the top surface of the vessel of 520 W/cm^2. The solid line indicates that all protein within it has undergone irreversible damage. The dashed line indicates that all protein between it and the solid line may have undergone irreversible damage and all protein outside of it will at most be reversibly damaged. The dotted circle defines the vessel lumen.

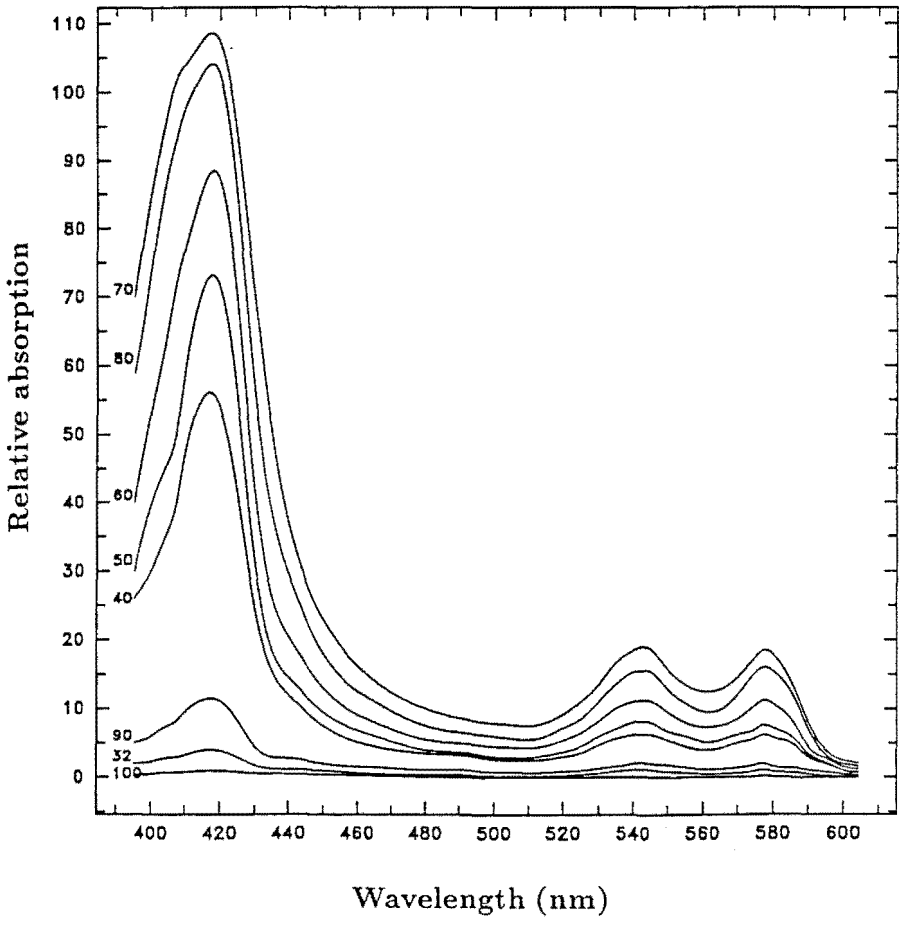

Figure 8.3: The erythrocytes absorb a greater fraction of light as their peak temperature increases until they reach the protein denaturation temperature of 70 °C. Based on figure 5 of Tan *et al.* 1989b.

identical input parameters to figure 8.1 whereas figure 8.5 has an illumination time 0.0003 ms of and an irradiance of 3 300 000 W/cm^2. This results in the coagulation of the endothelial cells to, at most, 2 μm above the top of the vessel lumen. There is some evidence that denaturation of haemoglobin does not take place under the influence of laser illumination as just described. Assuming zero light absorption at haemoglobin temperatures above 70 °C suggests that an endothelial cell coagulation temperature of 70 °C can not be achieved further than 2 μm from the vessel lumen (for all illumination times longer than 0.0003 ms the coagulation thickness was even less than 2 μm). The histological evidence of longer time scale illumination suggests that coagulation occurs at much greater distances from the lumen than 2 μm.

The early pulsed dye laser results showed evidence of vessel and erythrocyte ruptures that were indicative of steam formation and temperatures well in excess of 70 °C. Recently, Tan *et al.* (1989b) investigated the effect of a 0.36 ms pulsed laser on red blood cells in solution and compared the damage to heat damage as a result of imersion in a water bath (the absorption spectra of these water bath heated cell is seen in figure 8.3). The results were ultrastructurally quite different. In particular, laser induced damage showed electron lucent vacuoles (cavities) within the erythrocytes. The diameter of these vacuoles increased with increasing irradiance. A subsequent study (Tan *et al.* 1989c) shows the morphology to be independent of the oxygen status of the blood and therefore the vacuoles are most likely to be indicators of steam formation.

We have yet to determine that endothelial cell necrosis is the only condition necessary for the removal of ectatic vessels. It may be necessary to induce collagen formation to decrease the size of the vessel lumen. This may require thermal damage further out from the lumen than just the endothelial cells.

8.4 Scattered Light

Prior to this section we have considered only isolated vessels with collimated incident light. As discussed in chapter 6 this is gross simplification. We know that light undergoes numerous scattering events within the tissue. Therefore, the light is incident upon the vessel from all sides (not just from the top) and from all directions. Jacques *et al.* (1987) illustrated that within cutaneous tissue light is scattered primarily in the forward direction. This implies that near the skin surface, where on average each photon has undergone relatively few scattering events, the majority of the light will be incident on the top surface of the vessel with an angle of incidence near to vertical. Deeper within the skin the photons have undergone numerous scattering events and the light distribution has become much more isotropic (figure 8.6). Here the total irradiance is less, due to the previous absorption of light nearer the skin surface. As there is an inward transport of energy the photons must have on average a net inward direction. We can approximate these two extremes by for vessels near the surface, collimated incident light, which has been the subject of the preceding

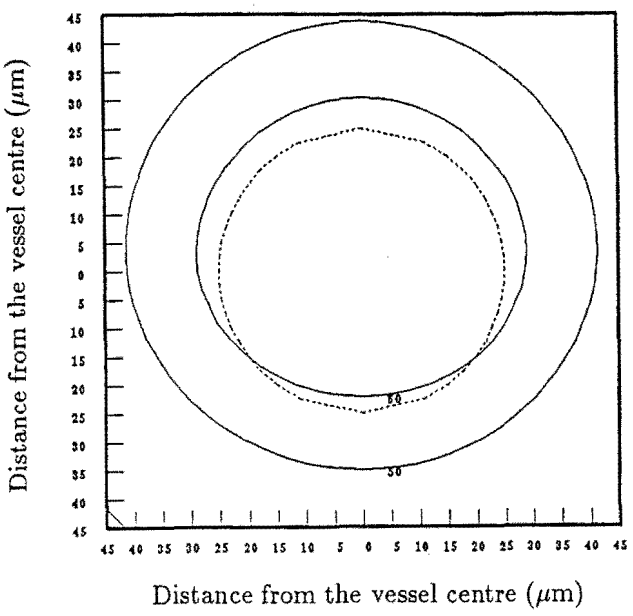

Figure 8.4: The temperature contours of a 50 μm diameter vessel after it has been heated for 5.5 ms with an irradiance on the top surface of the vessel of 520 W/cm^2. When the haemoglobin is calculated to have denatured it has been assumed that light has ceased to be absorbed. The dotted circle defines the vessel lumen.

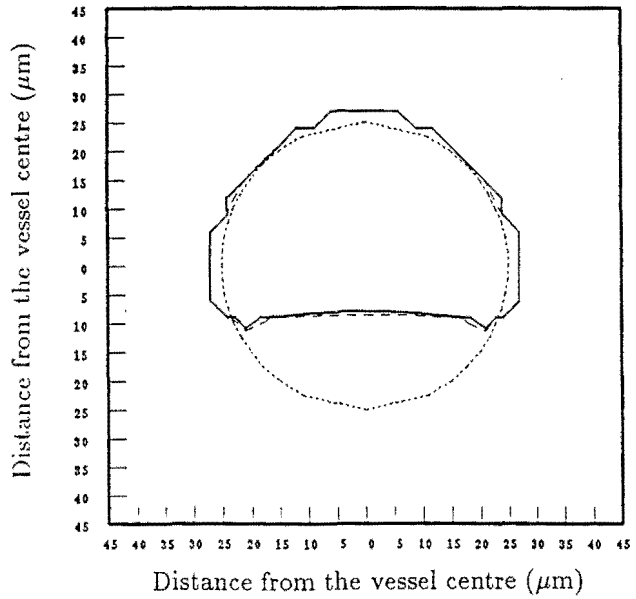

Figure 8.5: The damage contours of a 50 μm diameter vessel after it has been heated for 0.0003 ms with an irradiance on the top surface of the vessel of 3 300 000 W/cm^2. When the haemoglobin is calculated to have denatured it has been assumed that light has ceased to be absorbed. Note the point 2 μm above the vessel lumen has coagulated. The dotted circle defines the vessel lumen.

sections and Pickering *et al.* 1989a,b, and for vessels deeper within the skin, diffuse incident light which may be approximated by the diffusion approximation (see section 6.3.3).

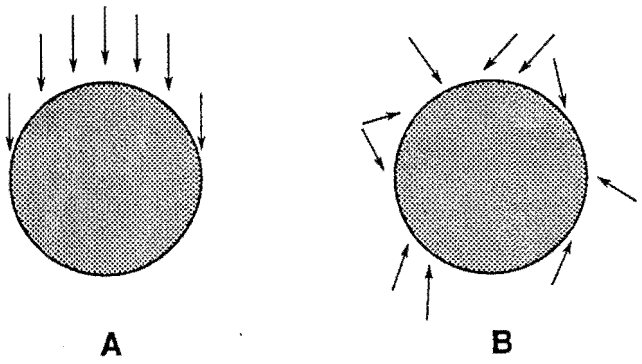

Figure 8.6: For vessels near the top of the dermis the incident light is on the top of the vessel and approximately collimated (A). Deeper within the dermis the light has undergone numerous scattering events and is incident on the vessel from all directions (B).

The diffusion approximation has a diffusion pattern (geometry) that, at sufficient depths (approximately 200 μm or greater), is independent of depth within the tissue. At these depths only the intensity varies with depth (exponentially). If we assume that the intensity change with depth between the extreme top and extreme bottom of the vessel is not large, the irradiance at any point within the vessel may be approximated as the sum of the intensity over all solid angles, as given by the diffusion pattern, multiplied by an exponentially decreasing function of intensity (Beer's Law) due to the absorption of light as it travels through the blood. The path length through blood depends on the direction of incidence (see figure 8.7).

The magnitude of the irradiance incident on the skin surface necessary to necrose the vessel will depend, in part, on the vessel depth. As we saw in chapter 6 the calculation of irradiance with depth depends on the scattering model used. Therefore, in this section we shall concentrate on the differences in optimal illumination time given by the two models of incident light (the collimated and the diffusion patterns).

Figures 8.8 and 8.9 are respectively collimated and diffusion approximation temperature profiles of a 50 μm diameter vessel illuminated for 5.5 ms with an incident irradiance sufficient to raise the maximum blood temperature to 100 °C. The col-

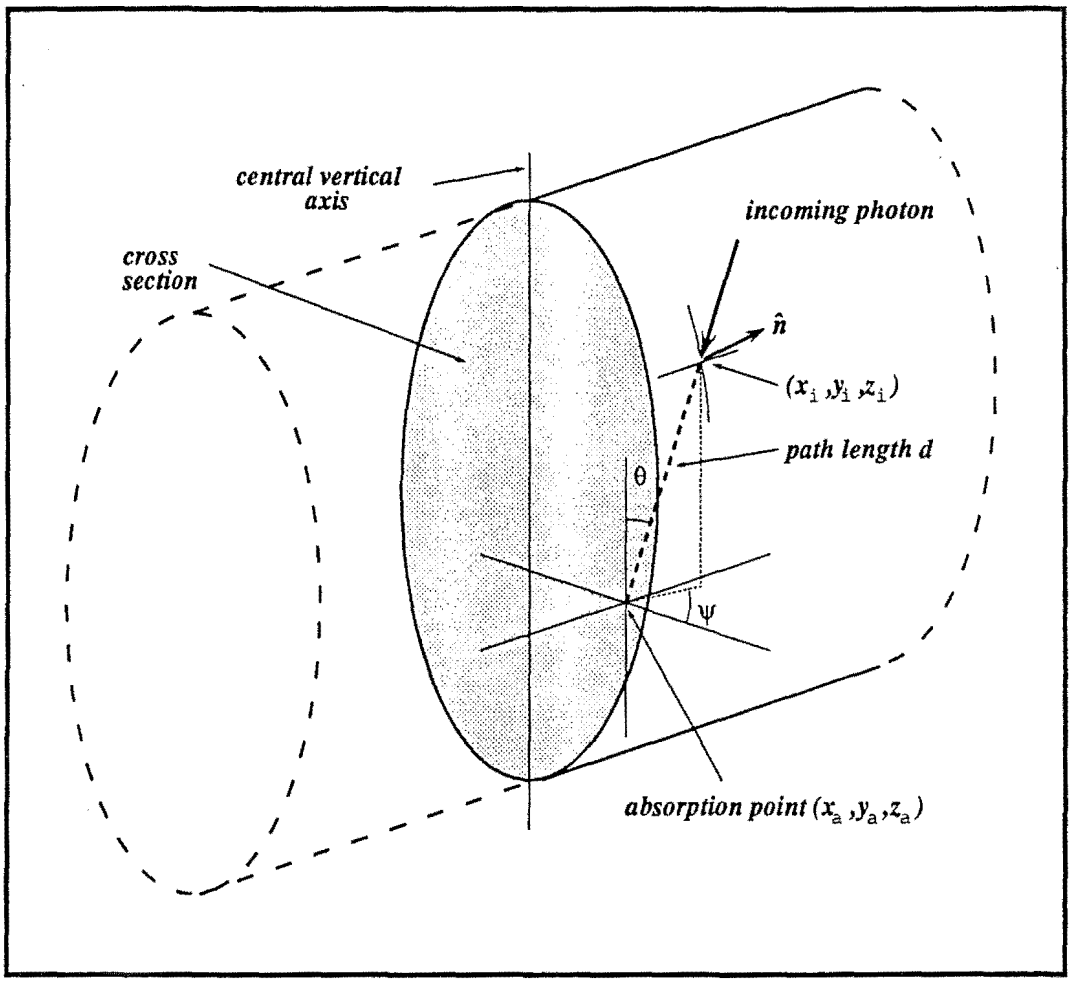

Figure 8.7: Light incident on the blood vessel at point (x_i, y_i, z_i), from direction (ϕ, ψ), has a relative intensity according to the diffusion approximation proportional to $D(\cos(\theta)) = \frac{1+3g(1-a)\cos(\theta)/k}{1-k\cos(\theta)}$ where g, a, k have been described in 6.3.3. This light is further attenuated by a factor $\exp(-\sigma_a d)$ where d is the path length through which the light passes before the remaining light is absorbed at point (x_a, y_a, z_a)

limated case (figure 8.8) has a coagulation thickness of 6 μm and coagulation temperature of 70 °C. The diffuse case (figure 8.9) illustrates an overall greater heating throughout the vessel with the higher temperature contours extending deeper within the vessel than they do in the collimated case. However, if we consider only the vertical cross section of the two temperature profiles (figure 8.10) we observe that, at this illumination time, the diffusion approximation also results in producing our (defined) coagulation condition. We have modelled the diffusion approximation using the optimal illumination times (for collimated incidence light) from Table 3 Pickering *et al.* 1989b for 30, 50, and 100 μm diameter vessels, a 70 °C coagulation temperature, and 3 and 6 μm coagulation thicknesses. In all six cases the coagulation temperature was reached at a thickness within 1 μm from the collimated coagulation thickness of 3 or 6 μm. Thus, according to our damage criteria, both collimated incidence and diffusion approximation models produce the same optimal illumination times.

The diffusion approximation shows a greater overall damage because of the higher temperatures obtained on each side of the central vertical axis (this axis is shown in figure 8.7). The "true" temperature profiles will be somewhere between these two. Near the skin surface (within the papillary dermis) the profile will more closely resemble that of collimated incidence whilst at greater depths the light has undergone many more scattering events and the temperature profiles will more closely resemble those given by the diffusion approximation.

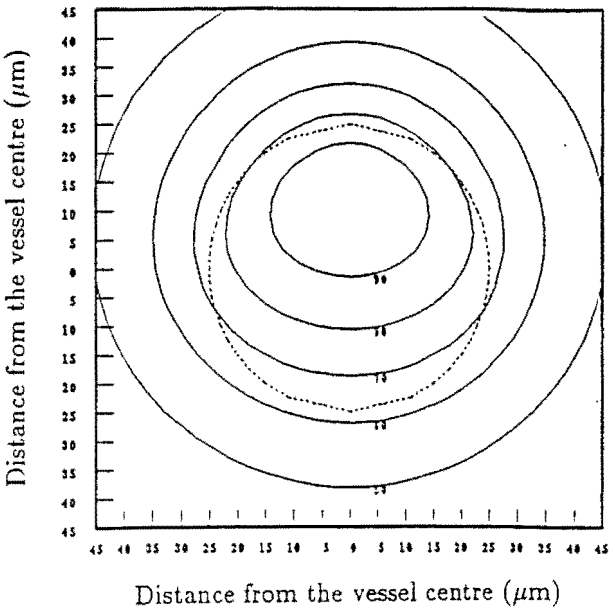

Figure 8.8: A 50 μm diameter vessel illuminated for 5.5 ms with collimated incident light and an irradiance sufficient to raise the maximum blood temperature to 100 °C. This produces the optimal coagulation conditions of 70 °C at a point 6 μm above the vessel lumen. Note this is identical to figure 8.1

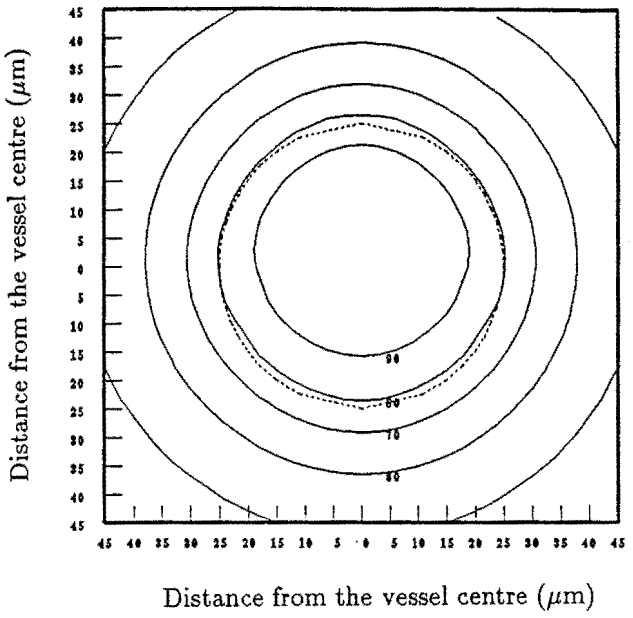

Figure 8.9: A 50 μm diameter vessel illuminated for 5.5 ms with diffuse incident light, calculated with the diffusion pattern, and an irradiance sufficient to raise the maximum blood temperature to 100 °C. Note 70 °C is attained at a point 5.5 μm above the vessel lumen.

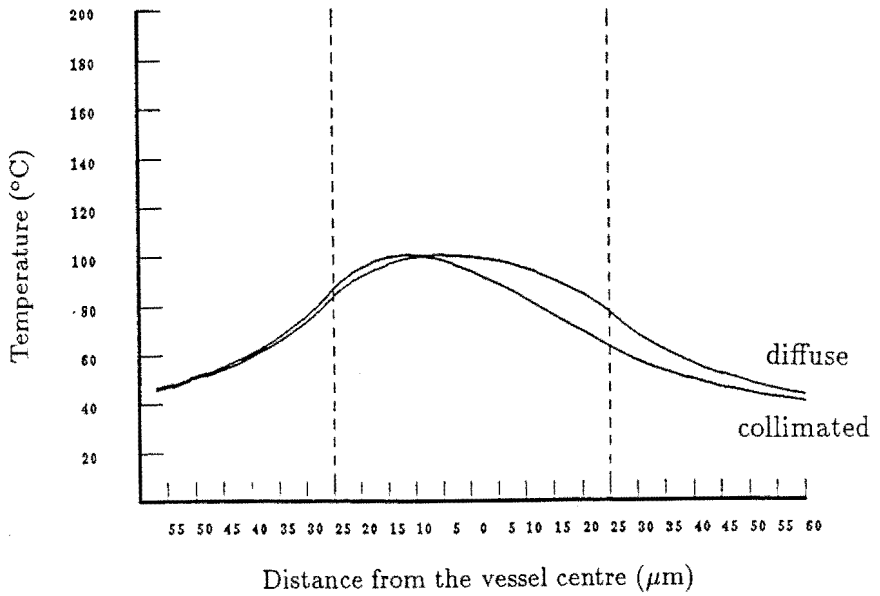

Figure 8.10: The central vertical cross sections of figures 8.8 and 8.9. At the top of the vessel both cross sections show the optimal coagulation condition.

8.5 Vessel Depth

As we have established an apparent invariance with depth of the optimal illumination time, we must now attempt to attain the variation in optimal irradiance with depth. With one exception, the models to attain irradiance as a function of depth discussed in chapter 6 do not take into account the influence of an absorbing three dimensional object such as the blood vessels. Although the Kubelka-Munk models of van Gemert and co-workers (van Gemert *et al.* 1982, 1986, and Lahaye and van Gemert 1985) include a blood vessel, the vessel is two dimensional and the incident light is just a convolution of collimated light and the beam profile. The exception is the Monte Carlo model. Mr Derek Smithies (1989) has developed a Monte Carlo model to calculate the energy absorbed within a cylindrical blood vessel at any depth within the dermis. This model accounts for the influence of an overlying epidermis and the scattering properties of the dermis. The light is assumed to be collimated when incident on the epidermis, but does not have infinite extent. The beam size and shape are two of the input parameters to the program.

To attempt to remain close to our original assumption of an infinitely wide beam we have used a beam of 1 mm diameter (large in comparison to the vessel sizes) and with a rectangular shaped profile (i.e. the radiance is constant across the beam). There has been some experimental work as to the optimal beam size for treatment (Tan *et al.* 1988). The conclusion for pulsed lasers was that the beam diameter should be at least 1 mm in diameter and preferably larger. This was based on the histological results of illumination of guinea pig skin (which has non-ectatic vessels). The larger beam diameters were found to cause vessel damage at greater depths. A 5 mm beam diameter is now used with the pulsed dye lasers. The main concern with small beam diameters is that a substantial amount of the incident light is very rapidly scattered out of the original beam. Therefore light flux upon the vessels is reduced and the treatment becomes less effective because the deeper vessels are often insufficiently damaged.

To calculate the light absorbed within the vessel we used the optical constants for epidermis, dermis and blood as given in table 8.2. These are the most recent optical characteristics for the epidermis and dermis (see table 7.1) except for the absorption coefficient for blood which is the same as we have used previously.

We ran the model for three depths (150, 300, and 500 μm) and two vessel sizes (50 and 100 μm diameter). The results of these models (the calculated absorption within the vessel) were input into our bio-heat equation model with the optimal illumination times previously calculated. The irradiances at the surface of the skin giving the optimal coagulation are presented in table 8.3. Figures 8.11 and 8.12 illustrate the differences in the temperature profiles for a 50 μm diameter vessel, illuminated for 5.5 ms with sufficient irradiance to attain the coagulation conditions of coagulation thickness of 6 μm and coagulation temperature of 70 °C at vessel depths of 300 and 500 μm respectively. As expected the deeper vessels' profiles

more closely resemble the diffusion approximation profile and the shallower vessels' profiles the collimated profile. At 150 μm depth the vessels were very close to the epidermis and as a result the profiles were affected by this (figure 8.13). As with our collimated case the larger vessel required a smaller incident irradiance. However, we note the coagulation thicknesses are not within the ± 1 μm of the expected 6 μm. This suggests an alteration in the illumination times may be necessary. We also note that in the case of the 50 μm diameter vessel the optimal irradiance at a depth of 300 μm is less than that at 150 μm.

Table 8.2: The optical parameters used in the Monte Carlo calculations

Tissue	g	σ_a (cm^{-1})	σ_s (cm^{-1})
Epidermis	0.787	37	480
Dermis	0.787	2.2	210
Blood	1	4300	0

Beam diameter	-	1 mm
Beam profile	-	rectangular
No. photon packets	-	784349
Photons per packet	-	10000
Wavelength	-	578 nm
Epidermal depth	-	100 μm

Table 8.3: The irradiance at the skin surface as a function of the depth of the vessels using Monte Carlo calculations

Vessel diameter (μm)	*Vessel depth (μm)*	*Illumination time (ms)*	*Irradiance (W/cm^2)*	*Coagulation thickness (μm)*
50	150	5.5	940	5
50	300	5.5	780	4
50	500	5.5	1660	7
100	150	5.0	610	5
100	300	5.0	810	2
100	500	5.0	1530	3

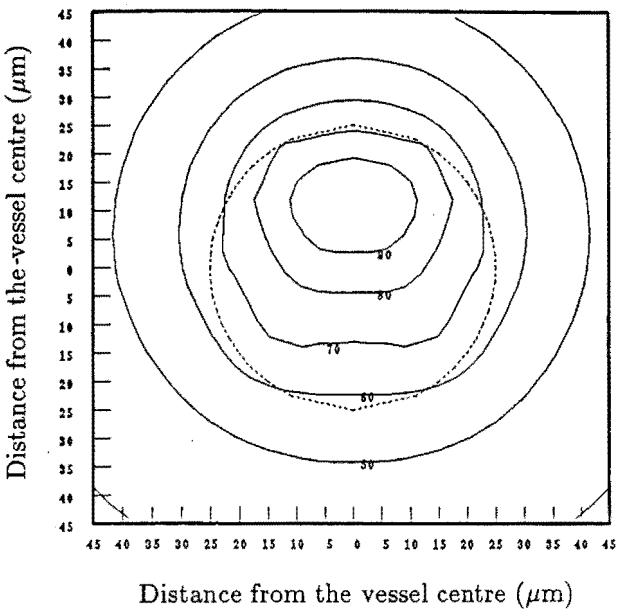

Figure 8.11: A 50 μm diameter vessel illuminated for 5.5 ms and 780 W/cm^2 at a depth of 300 μm, calculated using a Monte Carlo algorithim.

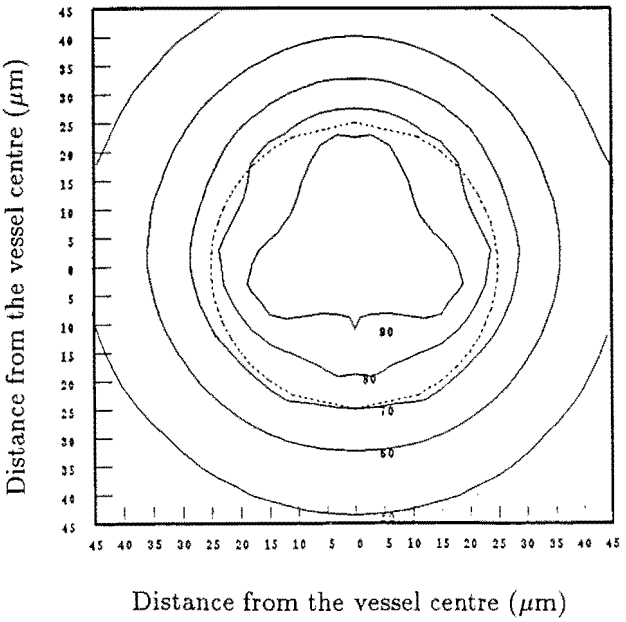

Figure 8.12: A 50 μm diameter vessel illuminated for 5.5 ms and 1660 W/cm^2 at a depth of 500 μm, calculated using a Monte Carlo algorithim.

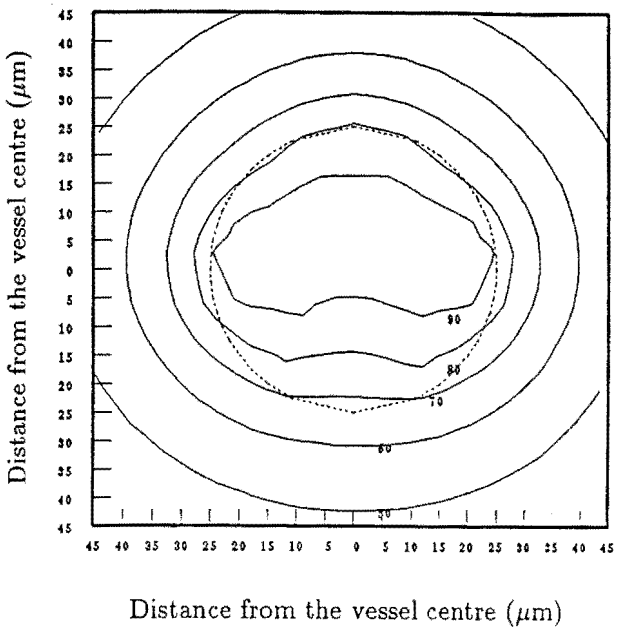

Figure 8.13: A 50 μm diameter vessel illuminated for 5.5 ms and 940 W/cm^2 at a depth of 150 μm. calculated using a Monte Carlo algorithim. The vessel is very close to the epidermal/dermal junction (at a depth of 100 μm) and the absorption has been influenced by this. It appears that on top of the vessel the incident light is almost collimated, whilst there is also light incident on the sides of the vessel. This light is probably less collimated. This profile does not take into account any heat conduction from the epidermis.

CHAPTER 9 THE CLINICAL TREATMENT

To date, the range of illumination times used clinically has been from 0.0003 ms to 0.45 ms and from 30 ms to several hundred milliseconds. In this chapter we apply our numerical model to these clinical illumination times. The two illumination time ranges has a different clinical and histological reactions. Our model provides an explanation for this difference. We also investigate a recent suggestion that 585 nm is the optimal wavelength with the pulsed dye lasers.

9.1 Illumination Times

To our knowledge the optimal treatment parameters discussed in this thesis have yet to be applied clinically. Illumination times used have been both shorter and longer than the theoretical optimal. The short illumination times are from the pulsed dye lasers and have ranged from 0.0003 ms to 0.45 ms. These short illumination times are characterised by the purpuric end point (the blue/grey discolouration of the skin some 5 to 15 minutes after illumination). The longer illumination times are from the continuous wave or quasi-continuous wave lasers. They range from several seconds down to our shortest illumination time of 30 ms. These treatments utilise the blanching (whitening) or minimal blanching end point. We shall consider each of these illumination time regimes in detail.

9.1.1 Long illumination times (Blanching)

The closest that a long illumination times have come to the optimal has been 30 ms (Pickering *et al.* 1990b). This was with approximately 500 to 600 W/cm^2 of light incident on the skin surface. With lower power densities much longer illumination times have been used (Lanigan and Cotterill 1989, Pickering *et al.* 1990b).

Once more we use a 50 μm diameter vessel as an example. In this case the vessel was illuminated with collimated light for 30 ms and an irradiance of 330 W/cm^2 (figure 9.1). The irradiance was such as to obtain a maximum blood temperature of 100 °C. This results in protein denature at a thickness much greater than is necessary to coagulate the endothelial cells (figure 9.2). A lower irradiance may result in immediate coagulation only at the desired coagulation thickness. For example for a coagulation temperature of 70 °C and a coagulation thickness of 6 μm this irradiance

would be 246 W/cm^2. Even with this irradiance there will still be excessive heat conducted from the vessels.

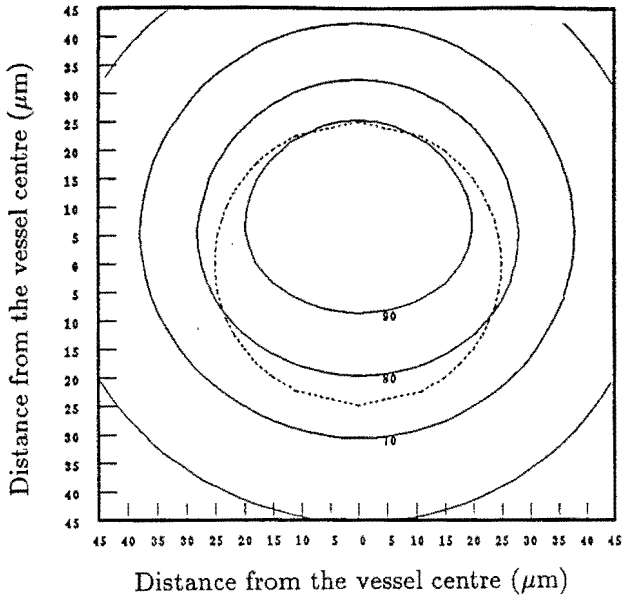

Figure 9.1: A 50 μm diameter vessel illuminated with collimated light for 30 ms and an incident irradiance on the vessel of 330 W/cm^2.

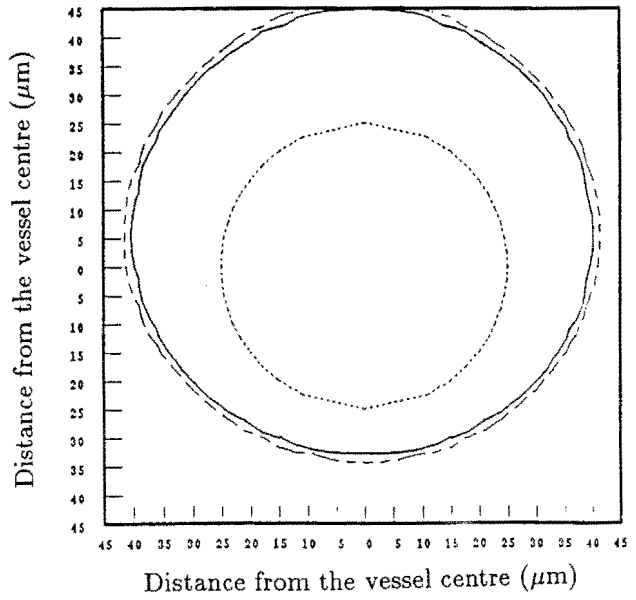

Figure 9.2: The damage contour for a 50 μm diameter vessel illuminated with collimated light for 30 ms and an incident irradiance on the vessel of 330 W/cm^2.

9.1.2 Short illumination times (Purpura)

Clinically these shorter than optimal illumination times have been produced by the flash lamp pumped pulsed dye lasers. The first of these lasers to be trialed used a 0.0003 ms pulse (Anderson and Parrish 1981b, Greenwald *et al.* 1981). Later developments lengthened the pulse to 0.45 ms (Glassberg *et al.* 1988). The energy per pulse is regulated to produce purpura some 5 to 15 minutes after illumination. Purpura is defined as the extravasation of blood, however this appears in contradiction to the histological findings after exposure with the longer single pulses. Rather than haemorrhage, apparently as a result of mechanical damage to vessel walls caused by vaporisation of red blood cells (seen with the shortest pulses – Anderson and Parrish 1981b, Greenwald *et al.* 1981, Garden *et al.* 1988), there is no haemorrhage but only the thrombosis of red blood cells (Garden *et al.* 1986, 1988).

With this apparent anomaly in mind we first modelled the 0.36 ms illumination time (the then longest pulsed dye laser pulse length) with a fluence incident on the vessel top surface of 2.1 J/cm^2 – 30% of the fluence incident on the skin surface. We used a value of 30% as we had assumed the irradiance will have been attenuated by melanin absorption and by scattering from the beam. As we have discussed in section 6.3.7 the total irradiance may not be as drastically reduced as this except deep within the dermis. Again we must note that the attenuation depends on the melanin concentration of the illuminated site. Although 30% of the incident fluence is arbitrary, it is likely to underestimate the real fluence and will therefore serve our purpose of illustrating the high temperatures produced by the pulsed dye lasers. Figure 4 of Pickering *et al.* 1989b is of a 50 μm diameter vessel with the treatment parameters of 0.45 ms and 4660 W/cm^2 (i.e. 2.1 J/cm^2). We note that the isotherms indicate a temperature well in excess of 100 °C. This is still the case with the 0.45 ms pulse with a similar fluence (figure 9.3). These temperature profiles have not taken into account the phase change at 100 °C and thus the higher temperatures are misleading. Some time before the completion of the pulse the blood temperature will have reached 100 °C, and any additional energy will be used to vaporise the haemoglobin. For the treatment parameters of figure 9.3 this additional energy will vaporise approximately 5% of the haemoglobin. Given the 1000 times expansion on vaporisation there is the possibility for disruption due to steam formation and pressure waves (see section 8.3.2 for a discussion on the histology of erythrocytes after short pulse illumination). To approximate more closely the real thermal effects, we ignore vaporisation, but restrict the maximum blood temperature to 100 °C. By forbidding any additional input of energy at any point that has reached 100 °C, we obtain a thermal profile which suggests a greater degree of thermal damage to the endothelial cells (figures 9.4 and 9.5).

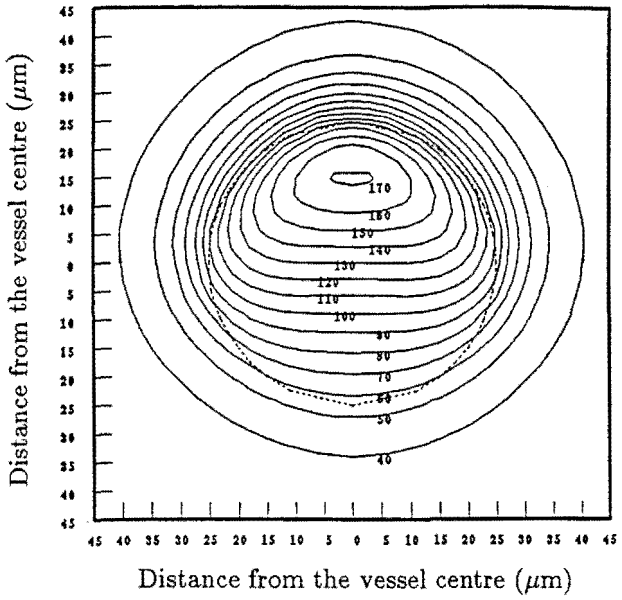

Figure 9.3: A 50 μm diameter vessel illuminated for 0.45 ms with 4660 W/cm^2 (2.1 J/cm^2). The temperatures exceed 100 °C because no phase change has been taken into account.

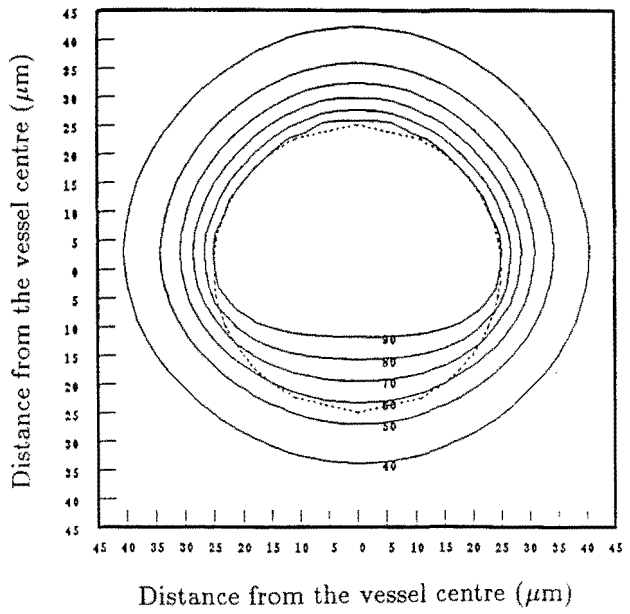

Figure 9.4: A 50 μm diameter vessel illuminated for 0.45 ms with 4660 W/cm^2 (2.1 J/cm^2). The temperatures have been limited to 100 °C because of the phase change. The resulting conduction suggests the possible coagulation of endothelial cells.

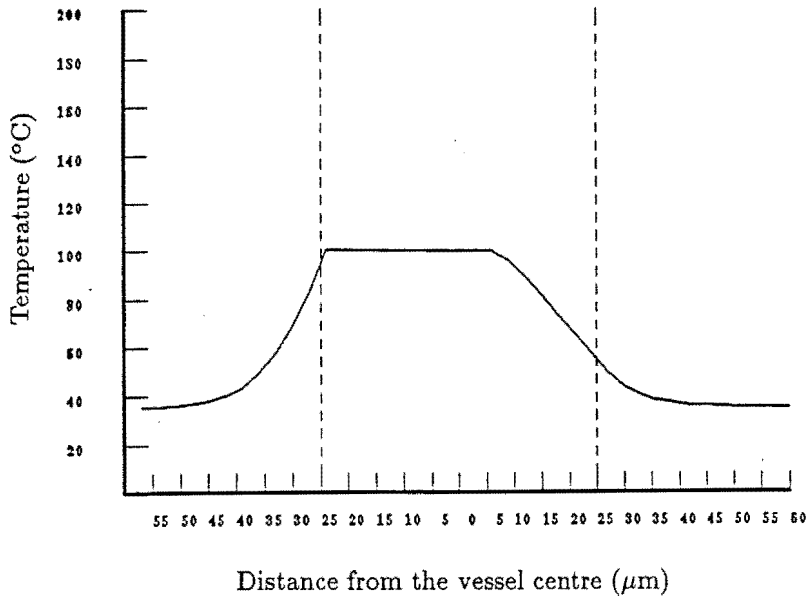

Figure 9.5: A central vertical cross section of 9.4. The coagulation temperature of 70 °C is attained at a thickness of 5 μm.

9.1.3 Comparison between illumination times

We may compare the thermal profiles of the previous two subsections with those of the optimal illumination time in section 8. Figure 9.6 compares the central vertical cross section for a 50 μm diameter vessel illuminated for 0.45 ms, 5.5 ms, and 30 ms with the constraint that the central temperature is not allowed to exceed 100 °C. We see that the longest illumination times result in coagulation to a thickness in excess of what is presumed necessary for necrosis of the vessel, but the shorter illumination time results in less coagulation than necessary. In figure 9.7 we compare the optimal illumination time with 0.45 ms and an irradiance of 30% of that incident on the skin surface. In this case we have forbidden any input of energy where the temperature reached 100 °C, as a result we observe coagulation that is closer to optimal.

9.2 A New Optimal Wavelength?

Early laser treatments used the untuned argon laser at wavelengths between 488 and 514.5 nm (Soloman *et al.* 1968, Goldman *et al.* 1976, Cosmon *et al.* 1980). Later the laser was tuned to 514.5 nm (Tan *et al.* 1986, Walker 1986 unpublished). The reasons for the preferential use of 577/578 nm were discussed in chapter 2. Other wavelengths to be trialed for selective photothermolysis have been 532 (Apfelberg 1986, Laffitte *et al.* 1989) and 540 nm (Hulsbergen Henning and van Gemert 1983). A recent development has been the suggestion that 585 nm will provide a better

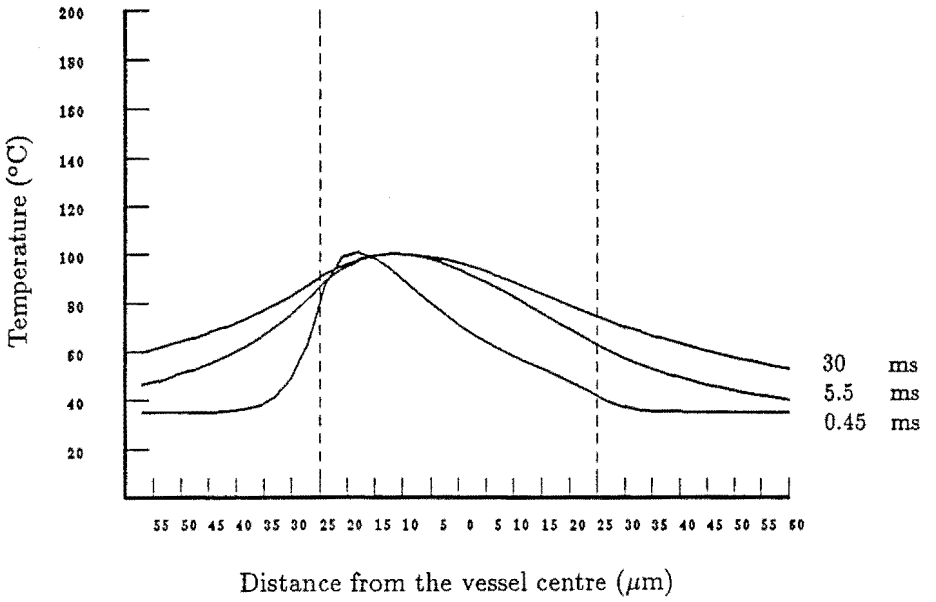

Figure 9.6: A central vertical cross section of a 50 μm diameter vessel illuminated for 0.45 ms, 5.5 ms, and 30 ms with the constraint that the central temperature is not allowed to exceed 100 °C.

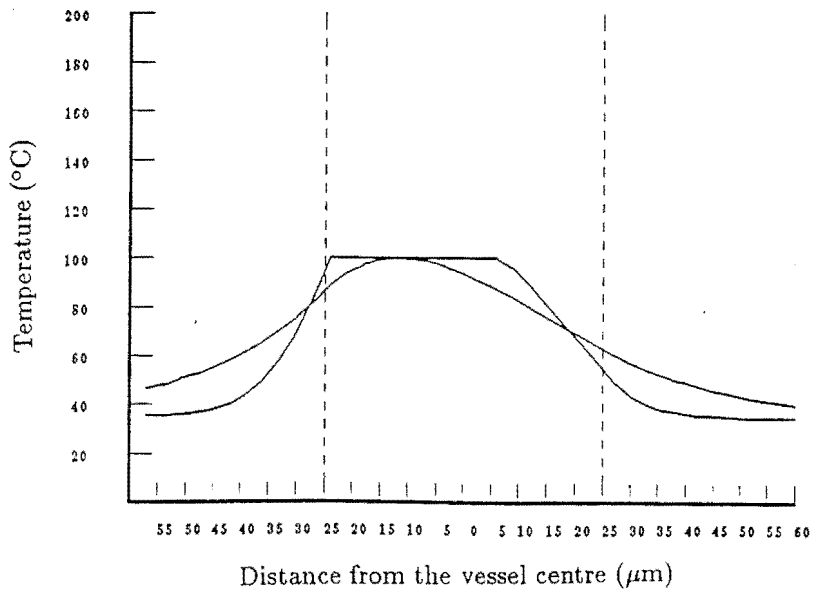

Figure 9.7: A central vertical cross section of a 50 μm diameter vessel illuminated for 0.45 ms with 4660 W/cm^2 (2.1 J/cm^2) in comparison to the optimal cross section.

treatment. We shall discuss this in some detail here.

9.2.1 585 and 590 nm with short illumination times

On the basis of histology it has been suggested that 585 nm be used in preference to 577 nm with the pulsed dye lasers (Tan *et al.* 1989a). The histology suggest that at 585 nm there was greater damage deeper within the dermis. Two albino pigs were illuminated with a pulsed dye laser (0.45 ms) at wavelengths between 572 and 590 nm. The optical characteristics of cutaneous tissue do not vary appreciably over this wavelength range, however the absorption characteristics of blood do vary over this range. The absorption coefficient of blood at 585 nm is approximately half that at 577 nm (closer to the absorption at 514.5 nm). At 590 nm the absorption coefficient is one fifth of that at 577 nm, and only a factor of two greater than the absorption coefficient of other dermal tissue. The most recently determined absorption and scattering characteristics for cutaneous chromophores for 575, 585, and 590 nm have been given in tabel 7.1.

The other phenomenon associated with 585 nm was the apparent greater damage at larger depths. This was accompanied by a photomicrograph which illustrated one vessel shadowing another. Because of the stronger absorption at 577 nm, this shadowing effect is likely to be greater and is likely to occur with smaller vessels. Van Gemert *et al.* (1989b) in investigating this phenomena has also suggested that different wavelengths may produce the greatest damage for different vessel sizes. This suggestion is based on the criterion of a greater temperature rise within the vessel than within the epidermis. We discussed this criteria in section 7.3.1. A summary of their findings are presented in figure 9.8.

We may use the bio-heat equation model to compare the wavelengths at an illumination time of 0.45 ms. First we constrain the irradiance so as to avoid any vaporisation (figures 9.9, 9.10, and 9.11). Second we remove the constraint and illuminate the vessels with the same irradiance of 4660 W/cm^2 (figures 9.12, 9.13, and 9.14).

The isotherms at 585 nm more closely resemble those of the optimal treatment, they are more rounded and the higher temperatures are not just confined to the top of the vessel. However, if we consider only the central vertical cross sections for each wavelength there appears to be only a slight difference in temperatures near the top of the vessel (figures 9.15, and 9.16). It may well be that the difference in the treatments is partly a result of greater overall damage around the circumference of the vessel rather than just at the topmost point.

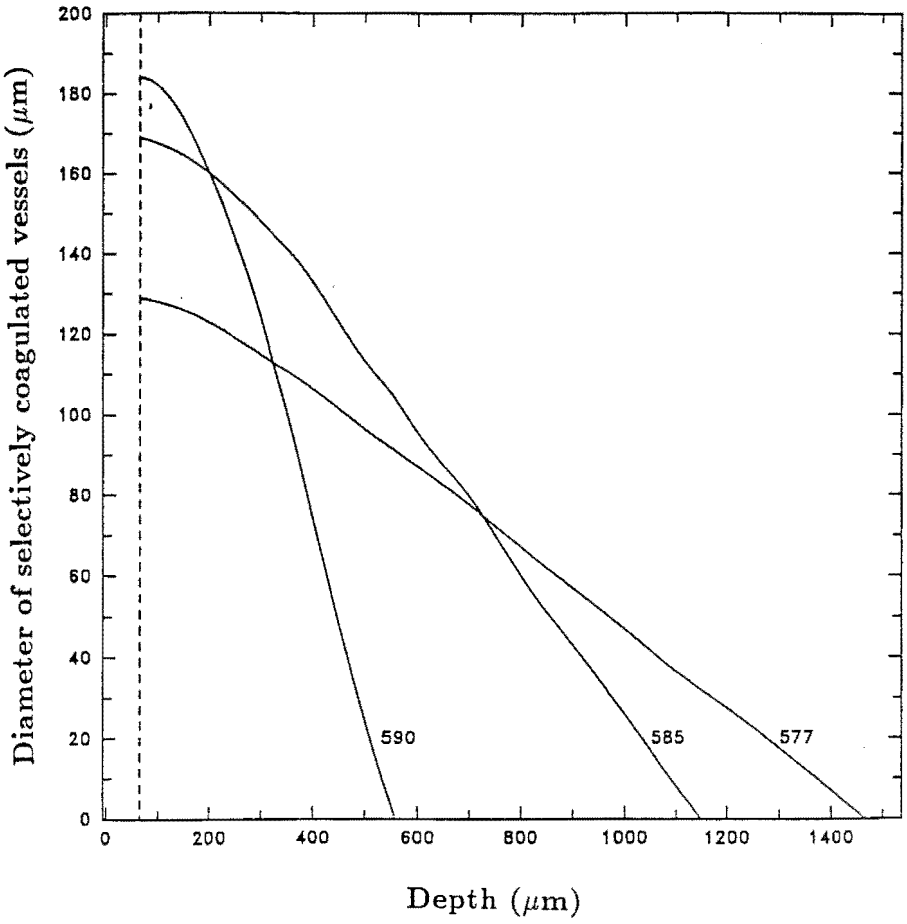

Figure 9.8: The damage depends on the combination of vessel depth, vessel diameter, and wavelength, with different wavelengths being more effective for different vessel sizes and depths.

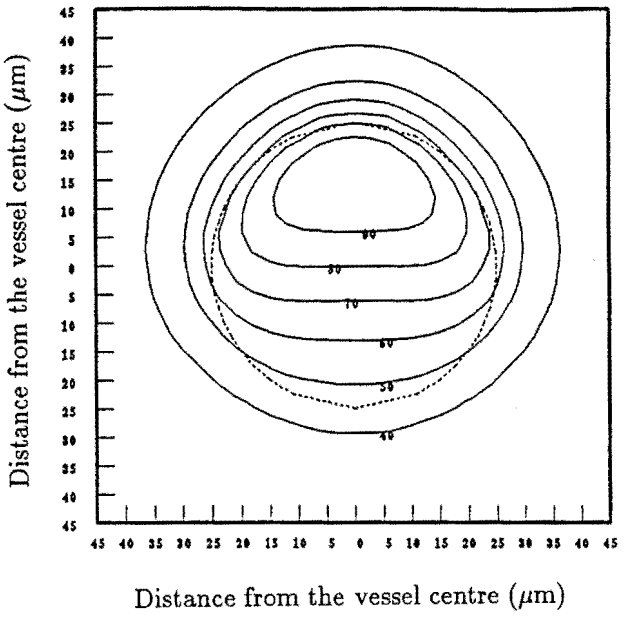

Figure 9.9: A 50 μm diameter vessel illuminated for 0.45 ms at 577 nm and a fluence sufficient only to reach a maximum vessel temperature of 100 °C.

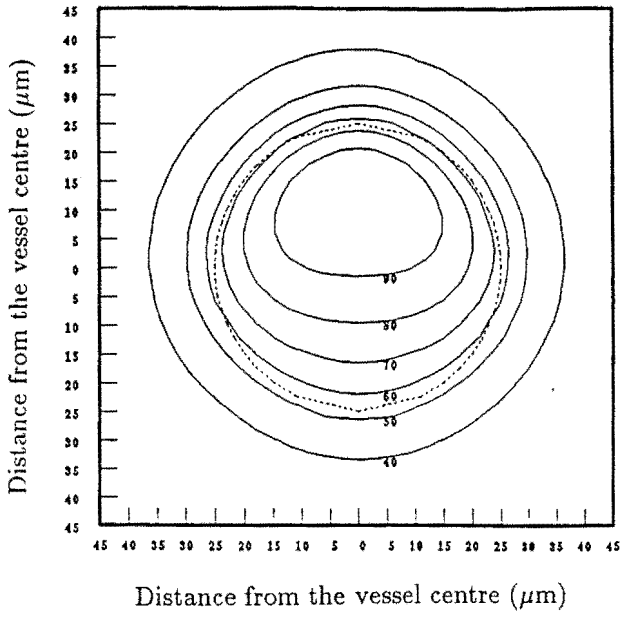

Figure 9.10: A 50 μm diameter vessel illuminated for 0.45 ms at 585 nm and a fluence sufficient only to reach a maximum vessel temperature of 100 °C.

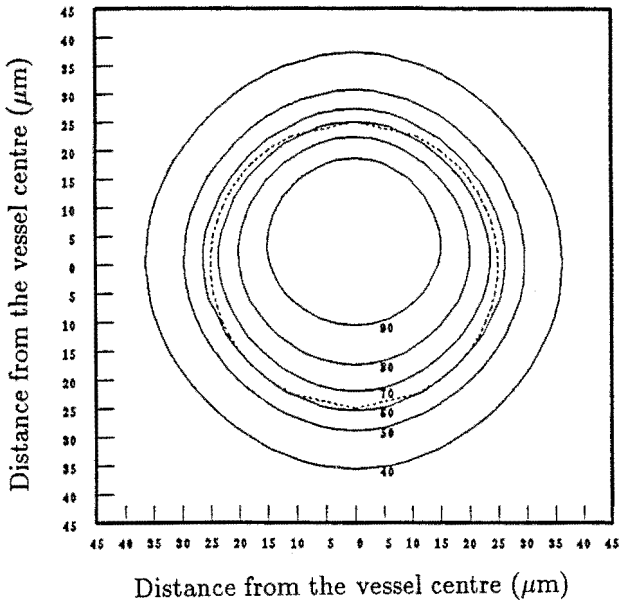

Figure 9.11: A 50 μm diameter vessel illuminated for 0.45 ms at 590 nm and a fluence sufficient only to reach a maximum vessel temperature of 100 °C.

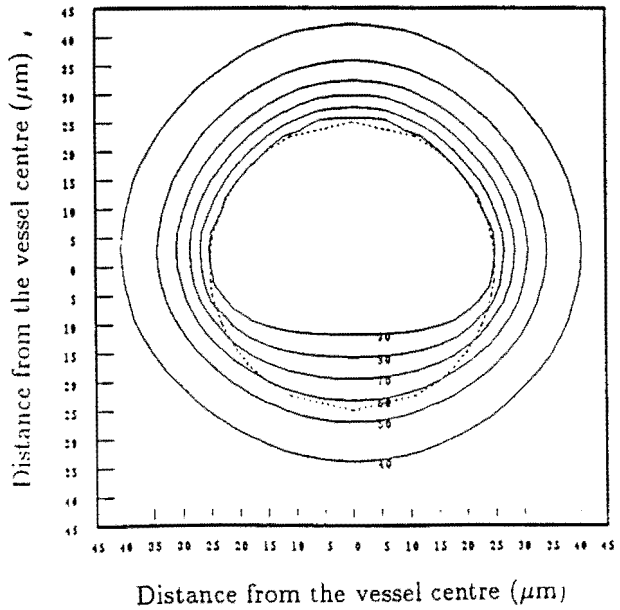

Figure 9.12: A 50 μm diameter vessel illuminated for 0.45 ms at 577 nm and 4660 W/cm^2 (2.1 J/cm^2). Vaporisation may be taking place with energy input where the temperature has reached 100 °C. Note this profile is identical to figure 9.4.

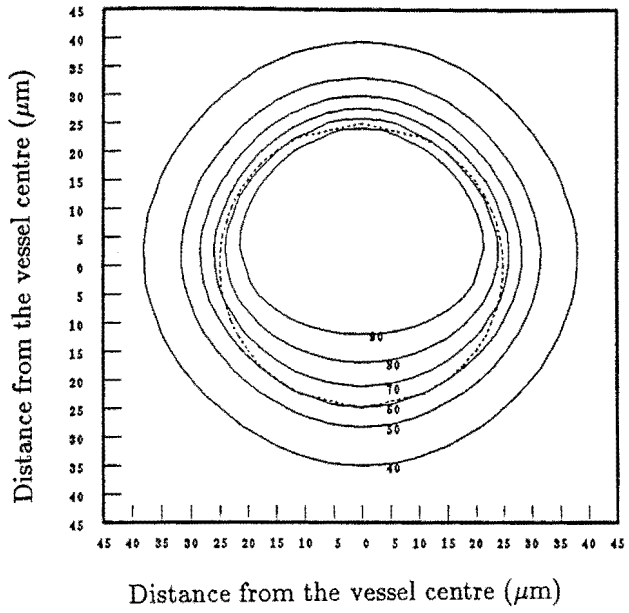

Figure 9.13: A 50 μm diameter vessel illuminated for 0.45 ms at 585 nm and 4660 W/cm^2 (2.1 J/cm^2). Vaporisation may be taking place with energy input where the temperature has reached 100 °C.

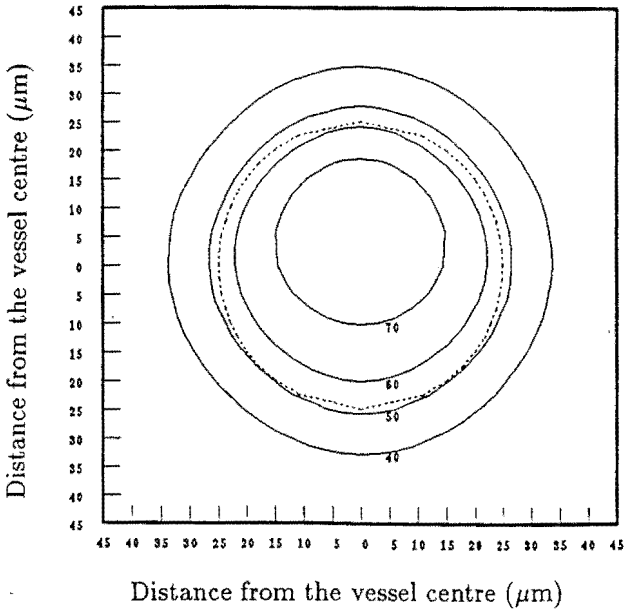

Figure 9.14: A 50 μm diameter vessel illuminated for 0.45 ms at 590 nm and 4660 W/cm^2 (2.1 J/cm^2). Vaporisation may be taking place with energy input where the temperature has reached 100 °C.

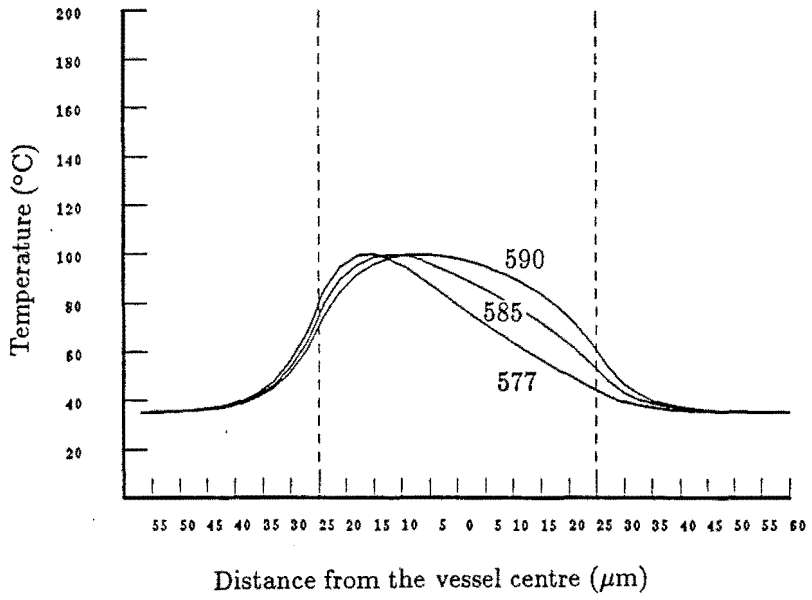

Figure 9.15: The central vertical cross section of figures 9.9, 9.10, and 9.11. The irradiance is constrained so that the central temperature does not exceed 100 °C.

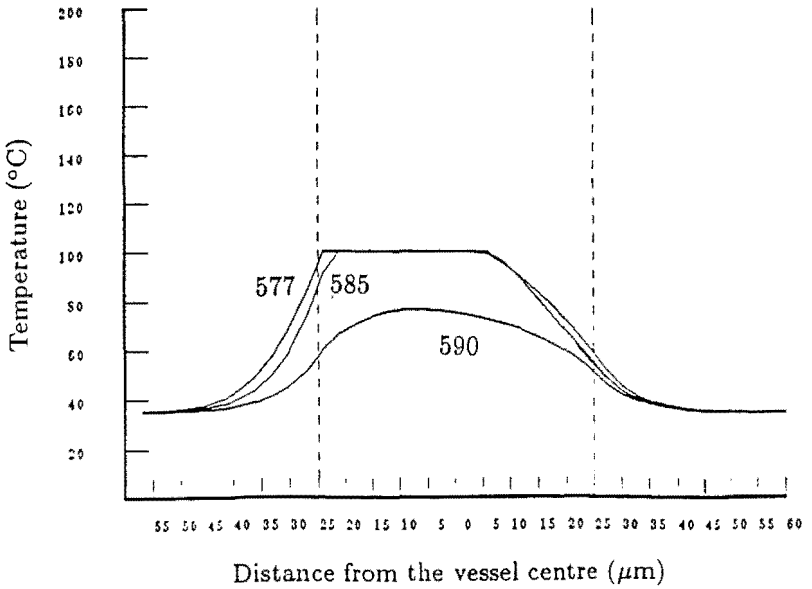

Figure 9.16: The central vertical cross section of figures 9.12, 9.13, and 9.14. Vaporisation may be taking place with energy input where the temperature has reached 100 °C. The illumination time is 0.45 ms and the irradiance is 4660 W/cm^2.

CHAPTER 10 DISCUSSION

From this thesis we have reached four conclusions. First, the 578 nm wavelength from a 20 W copper vapour laser provides a method of removal of vascular lesions. Second, the necrosis of ectatic vessels requires, at a minimum, some denaturation of their endothelial cells. The extent of the denaturation is yet to be determined. Third, the optimal treatment parameters are a wavelength of 577/578 nm, an irradiance of 400 to 3000 W/cm^2, and an illumination time of 1 to 10 ms. Fourth, illumination times shorter than the optimal will vapourise the haemoglobin and those longer than the optimal will denature protein beyond the endothelial cells.

10.1 Conclusion 1: The 20 Watt Copper Vapour Laser

Port wine stain patients and other vascular lesion patients have shown a positive response to copper vapour laser treatment. Their clinical response has been on a par with results from other treatment techniques (Pickering *et al.* 1990b). They have exhibited a very positive psychological response (Pickering *et al.* 1990a). Histology has shown selective damage to the blood vessels without damage to other cutaneous tissue (Walker *et al.* 1989). Additionally, the extent of lightening and removal of the birthmark has improved as the illumination time has progressively become shorter.

10.2 Conclusion 2: The Optimal Damage

Histology has shown that mechanical damage alone, caused by vaporisation of haemoglobin, expansion, and consequential rupture of the vessels is insufficient to cause permanent damage to these vessels. There is a requirement for some thermal damage of the endothelial cells of these vessels. Our histology (Walker *et al.* 1989) indicates that for a 60 to 90 ms illumination time and irradiance of 160 to 360 W/cm^2 that the extent of the thermal damage extends to slightly beyond the endothelial cells. The pulsed dye laser histologies at 0.45 ms and 13000 W/cm^2 indicate minimum coagulation of endothelial cells, but rather thrombosis of erythrocytes and some microvaporisation. My observation of these two treatment modalities, obtained from the literature and the recent 8th Congress of the International Society for Laser Surgery and Medicine, are that the clinical results are very similar. I con-

clude that the optimum damage is somewhere between that indicated by the two sets of histology.

10.3 Conclusion 3: The Model of the Physics

The development of a numerical model to describe the treatment has led to the establishment of theoretical optimal treatment parameters. The treatment parameters being the illumination time, the irradiance, and the wavelength of light. The optimal wavelength had been established by Anderson and Parrish and others as 577 nm because of the absorption characteristics of melanin and haemoglobin at this wavelength in comparison to other wavelengths. The optimal illumination time for 577/578 nm light varies (slowly) according to vessel size (Pickering *et al.* 1989a), more substantially according to coagulation temperature and thickness (Pickering *et al.* 1989b), and negligibly according to vessel depth (chapter 8). The optimal irradiance must be sufficient to raise the vessel's endothelial cells to the requisite coagulation temperature at the requisite coagulation thickness. This depends on the depth of the vessel.

Given the assumptions made, the uncertainties in some of the tissue's optical characteristics, and the variation in vessel sizes, our numerical model gives an optimal illumination time range of 1 to 10 ms. By extrapolating from the Monte Carlo results and the optimal collimated light irradiances, we can suggest that for most ectatic vessels the optimal irradiance will be between 400 and 3000 W/cm^2. Note that this range is between the clinically used 60 ms irradiance of 360 W/cm^2 and the 0.45 ms irradiance of 13000 W/cm^2.

This optimal illumination time estimation is partially supported by the clinical evidence. The treatment results have been shown to improve with the pulsed dye laser treatments as the pulse length has been increased from 0.0003 ms to 0.45 ms and also improve as the copper vapour laser illumination times have decreased from several hundred milliseconds to 30 ms (Pickering *et al.* 1990b). Thus, the clinical evidence suggests an optimal illumination time between 0.45 and 30 ms.

10.4 Conclusion 4: Understanding the Treatment Protocols

We have modelled the two extremes of 577/578 nm light treatment. The blanching (whitening) technique heats the endothelial cells beyond the coagulation thickness and thus does some unwanted damage. The purpura (blue/grey) technique damages the erythrocytes while apparently not allowing for heat conduction. Yet, both these techniques have produced similar clinical results.

The model predicts temperatures sufficient to coagulate the dermal collagen occur at a distance well beyond the vessel lumen with the long illumination times. At an illumination time of 300 ms Landthaler *et al.* (1986) observed this non specific damage. Although not pronounced we also noted some dermal damage with our

histology and illumination times of 60 to 90 ms (Walker *et al.* 1989, included as appendix B).

For the shorter than optimal illumination times the model predicts that the blood will reach a temperature of 100 °C and that any additional input of energy will result in vaporisation of the blood. This phenomenon was apparent with the shortest illumination times (0.0003 to 0.0015 ms) which resulted in rupture of erythrocytes and vessels due to the rapid expansion caused by vaporisation. However, the longer pulsed dye lasers (0.3 to 0.45 ms) did not reveal ruptured erythrocytes or vessels. It was not until Tan *et al.* (1989b,c) illustrated that the laser light produced vacuoles within the erythrocytes that some vaporisation was apparent.

10.5 Summary

During the course of this thesis it has been pleasing to note the improvement in treatment results as we have applied the knowledge gained from our theoretical considerations. The automatic scanner is the next step towards the optimal treatment. This scanner will be able to provide evidence of the effect of illumination times within our theoretical optimal range of 1 to 10 ms. As the optimal treatment parameters depend on the size and depth of the ectatic vessels a method is required to enable the tailoring of the treatment to the individual. Possible methods include spectral analysis of the lesion colour (Feather *et al.* 1988), transcutaneous microscopy (Shakespeare and Carruth 1986), or interactve assessment of the damage during treatment by a method such as measuring the degree of blanching. Further modelling, especially with the Monte Carlo algorithim, and study of the optimal damage criteria, will define the optimal treatment parameters even more accurately.

REFERENCES

Anderson RR and Parrish JA, (1981a); *The optics of human skin.*, J Invest Dermatol, **77**, 13-19.

Anderson RR and Parrish JA, (1981b); *Microvasculature can be selectively damaged using dye lasers.*, Lasers Surg Med, **1**, 263-276.

Anderson RR and Parrish JA, 1983; *Selective photothermolysis: Precise microsurgery by selective absorption of pulsed radiation.*, Science, **220**, 524-527.

Apfelberg DB, Morton MR, and Lash H, (1976); *Argon laser management of cutaneous vascular deformities.*, West J Med, **124**, 99-101.

Apfelberg DB, Kosek J, Morton MR, and Lash H, (1979); *Histology of port wine stains following argon laser treatment.*, Br J Pl Surg, **32**, 232-237.

Apfelberg DB, Bailin P, and Rosenberg H, (1986); *Preliminary investigation of KTP/532 laser light in the treatment of hemangiomas and tattoos.*, Lasers Surg Med, **6**, 38-42.

Apfelberg DB, Smith T, Morton MR, Lash H, and White DN, (1987); *Dot or pointillistic method for improvement in results of hypertrophic scarring in the argon laser treratment of portwine hemangiomnas.*, Lasers Surg Med, **6**, 552-558.

Arndt KA, (1984); *Treatment technics in argon laser therapy.*, J Am Acd Dermatol, **11**, 90-97.

Barsky SH, Rosen S, Geer DE, and Noe JM, (1980); *The nature and evolution of port wine stains: A computer assisted study.*, J Invest Dermatol, **74**, 154-157.

Bohren CF and Huffman DR, (1983); *Absorption and scattering of light by small particles.*, John Wiley and Sons, New York.

Buecker JW, Ratz JL, and Richfield DF, (1984); *Histology of port-wine stain treated with carbon dioxide laser.*, J Am Acad Dermatol, **10**, 1014-1019.

Butler PH, van Halewyn CN, and Walker EP, (1987); *Optimizing the laser treatment of port wine stains.*, unpublished.

Carruth JAS and McKenzie AL, (1986); *Medical Lasers: Science and clinical practice.*, Adam Hilger Ltd., Bristol and Boston.

Carslaw HS and Jaeger JC, 1967; *Conduction of heat in solids. Ch 18*, Clarendon Press, Oxford.

Cashwell ED and Everett CJ, (1959); *Monte Carlo method for random walk problems.*, Pergamon Press, New York.

Chandrasekhar S, (1950); *Radiative transfer.*, Clarendon Press, Oxford.

Cosman B, (1980); *Experience in the argon laser therapy of port wine stains.*, Pl Recon Surg, **65**, 119-129.

Cotterill JA, (1986); *Preliminary results following treatment of the skin using a continuous wave tunable dye laser which emits at 577 nm.*, Clin Exp Dermatol, **11**, 628-635.

Craig RDP, Purser JM, Lessells AM, and Hufton AP, (1985); *Argon laser therapy for cutaneous lesions.*, Br J Pl Surg, **38**, 148-155.

Dixon JA, Rotering RH, and Huether SE, (1984a); *Patient's evaluation of argon laser therapy of port wine stain, decorative tattoo, and essential telangiectasia.*, Lasers Surg Med, **4**, 181-190.

Dixon JA, Huether SE, and Rotering RH, (1984b); *Hypertrophic scarring in argon laser treatment of port-wine stains.*, Pl Recon Surg, **73**, 771-779.

Erez A and Shitzer A, (1980); *Controlled destruction of temperature distributions in biological tissues subjected to monoactive electrocoagulation.*, Trans ASME J Biomech Eng, **102**, 42-49.

Feather JW, Ellis DJ, and Leslie G, (1988); *A portable reflectometer for the rapid quantification of cutaneous haemoglobin and melanin.*, Phys Med Biol, **33**, 711-722.

Finlay JL, Arndt KA, Noe JL, and Rosen S, (1984); *Argon laser-port-wine stain interaction.*, Arch Dermatol, **120**, 613-617.

Garden JM, Tan OT, Kerschmann R, Boll J, Furumoto H, Anderson RR, and Parrish JA, (1986); *Effect of dye laser pulse duration on selective cutaneous vascular injury.*, J Invest Dermatol, **87**, 653-657.

Garden JM, Polla LL, and Tan OT, (1988); *The treatment of port-wine stains by the pulsed dye laser.*, Arch Dermatol, **124**, 889-896.

Gaylarde PM, Dodd HJ, and Sarkeny I, (1987); *Port-wine stains (letter).*, Arch Dermatol, **123**, 861-862.

van Gemert MJC, de Kleijn WJA, and Hulsbergen Henning JP, (1982); *Temperature behaviour of a model port-wine stain during argon laser coagulation.*, Phys Med Biol, **9**, 1089-1104.

van Gemert MJC, Welch AJ, and Amin AP, (1986); *Is there an optimal laser treatment for port wine stains ?*, Lasers Surg Med, **6**, 76-83.

van Gemert MJC, Welch AJ, and Tan OT, (1987a); *Limitation of carbon dioxide lasers for treatment of port wine stains.*, Arch Dermatol, **123**, 71-73.

van Gemert MJC, Welch AJ, Star WM, Motamedi M, and Cheong W-F, (1987b); *Tissue optics for a slab geometry in the diffusion approximation.*, Lasers Med Sci, **2**, 295-302.

van Gemert MJC, Schetts GACM, Bishop MS, Cheong W-F, and Welch AJ, (1988); *Optics of tissue in multi-layer slab geometry.*, Lasers Life Sci, **2**, 1-18.

van Gemert MJC, and Welch AJ, (1989a); *Time constants in thermal laser medicine.*, Lasers Surg Med, **9**, 405-421.

van Gemert MJC, Welch AJ, Miller ID, and Tan OT, (1989b); *Can physical modelling lead to an optimal laser treatment strategy for portwine stains ?*, concept for a chapter in *Laser applications in medicine and biology. Vol 5.* ed. ML Wolbarsht, Plenum Publishers, New York.

Glassberg E, Lask GP, Tan EML, and Uitto J, (1988); *The flashlamp-pumped 577-nm pulsed tunable dye laser: Clincal efficacy and in vitro studies.*, J Dermatol Surg Oncol, **14**, 1200-1208.

Goldman L, Dreffer R, Cockwell RJ, and Perry E, (1976); *Treatment of portwine marks by an argon laser.*, J Dermatol Surg, **2**, 385-388.

Greenwald J, Rosen S, Anderson RR, Harrist T, MacFarland F, Noe JL, and Parrish JA, (1981); *Comparitive histological studies of the tunable dye (at 577 nm) laser and argon laser: The specific vascular effects of the dye laser.*, J Invest Dermatol, **77**, 305-310.

van Halewyn CN, (1985); *Argon laser treatment of port wine stains.*, Undergraduate project report, Physics Department, University of Canterbury, Christchurch, New Zealand.

van Halewyn CN, (1987); *Laser treatment of port wine stains.*, MSc thesis, Physics Department, University of Canterbury, Christchurch, New Zealand.

van Hassalt CA and Liu KC, (1989); *Copper vapour laser treatment of superficial vascular lesions (including PWS) in the asian skin.*, 8th Congress of the International Society for Laser Surgery and Medicine, Nov 4-7 1989, Taipei, ROC.

Henriques FC Jr., (1947); *Studies of thermal injury. 5. The predictability and significance of thermally induced rate processes leading to irreversible epidermal injury.*, Arch Path, **43**, 489-502.

Henriques FC Jr. and Moritz AR, (1947); *Studies of thermal injury. 1. The conduction of heat to and through skin and the temperatures attained therin. A theoretical and an experimental investigation.*, Am J Path, **23**, 531-549.

Henyey LG and Greenstein JL, (1941); *Diffuse radiation in the galaxy.*, Astroph J, **93**, 70-83.

Hu C-L and Barnes FS, (1970); *The thermal-chemical damage in biological material under laser irradiation.*, IEEE trans Biomed Eng, **BME-17**, 220-229.

Hulsbergen Henning JP and van Gemert MJC, (1983); *Port wine stain coagulation experiments with a 540-nm continuous wave dye laser.*, Lasers Surg Med, **2**, 205-210.

Hulsbergen Henning JP, van Gemert MJC, and Lahaye CTW, (1984); *Clinical and histological evaluation of portwine stain treatment with a microsecond-pulsed dye-laser at 577 nm.*, Lasers Surg Med, **4**, 375-380.

Ishimaru A, (1978); *Wave propagation in random media. Vol 1.*, Academic Press, New York.

Jacobs AH and Walton RG, (1976); *The incidence of birthmarks in the neonate.*, Pediatrics, **58**, 2, 218-222.

Jacques SL, Alter CA, and Prahl SA, (1987); *Angular dependence of HeNe laser light scattering by human dermis.*, Lasers Life Sci, **1**, 309-333.

Johnson FH, Eyring H, Jones Stover B, (1974); *The theory of rate processes in biology and medicine.*, John Wiley and Sons, New York.

Keijzer M, Jacques SL, Prahl SA, and Welch AJ, (1989); *Light distributions in artery tissue: Monte Carlo simulations for finite-diameter laser beams.*, Lasers Surg Med, **9**, 148-154.

Laffitte F, Guillet H, Chavoin JP, Rouge D, and costagliola M, (1989); *Automatic scanning of large PWS, and preliminary report on the use of 532 nm wavelength.*, 8th Congress of the International Society for Laser Surgery and Medicine, Nov 4-7 1989, Taipei, ROC.

Lahaye CTW and van Gemert MJC, (1985); *Optimal laser parameters for port wine stain therapy: a theoretical approach.*, Phys Med Biol, **30**, 573-587.

Landthaler M, Haina D, Brunner R, Waidelich W, and Braun-Falco O, (1986); *Effects of argon, dye, and Nd: YAG lasers on epidermis, dermis, and venous vessels.*, Lasers Surg Med, **6**, 87-93.

Lanigan SW and Cotterill JA, (1989); *Psychological disabilities amongst patients with port wine stains.*, Br J Dermatol, **121**, 209-215.

Lanigan SW, Cartwright P, and Cotterill JA, (1989); *Continuous wave dye laser therapy of port wine stains.*, Br J Dermatol, **121**, 345-352.

Margolis RJ, Dover JS, Polla LL, Watanabe S, Shea CR, Hruza GJ, Parrish JA, and Anderson RR, (1989); *Visible action spectrum for melanin-specific selective photothermolysis.*, Lasers Surg Med, **9**, 389-397.

Miller BF and Keane CB, (1987); *Encyclopedia and dictionary of medicine, nursing, and allied health.*, WB Saunders Company, Philadelphia.

Morelli JG, Tan OT, Garden J, Margolis R, Seki Y, Boll J, Carney JM, Anderson RR, Furumoto H, and Parrish JA, (1986); *Tunable dye laser (577 nm) treatment of port wine stain.*, Lasers Surg Med, **6**, 94-99.

Murphy GF, Shepard RS, Paul BS, Menkes A, Anderson RR, and Parrish JA, (1983); *Organelle-specific injury to melanin-containing cells in human skin by pulsed laser irradiation.*, Lab Invest, **49**, 680-685.

Nakagawa H, Tan OT, and Parrish JA, (1985); *Ultrastuctural changes in human skin after exposure to a pulsed laser.*, J Invest Dermatol, **84**, 396-400.

Noe JM, Barsky SH, Geer DE, and Rosen S, (1980); *Port wine stains and the response to argon laser therapy: Successful treatment and the predicative role of color, age, and biopsy.*, Pl Recon Surg, **65**, 130-136.

Ohmori S and Huang C-K, (1981); *Recent progress in the treatment of port wine staining by argon laser: Some observations on the prognostic value of relative spectro-reflectance (RSR) and the histological classification of the lesions.*, Br J Pl Surg, **34**, 249-257.

Olbricht SM, Stern RS, Tang SV, Noe JM, and Arndt KA, (1987); *Complications of cutaneous laser surgery.*, Arch Dermatol, **123**, 345-349.

Paul BS, Anderson RR, Jarve J, and Parrish JA, (1983); *The effect of temperature and other factors on selective microvasculature damage caused by pulsed dye laser.*, J Invest Dermatol, **81**, 333-336.

Pickering JW, Butler PH, Ring BJ, and Walker EP, (1989a); *Thermal profiles of a blood vessel heated by a laser.*, Austral Physical Eng Sci Med, **12**, 11-15.

Pickering JW, Butler PH, Ring BJ, and Walker EP, (1989b); *Computed temperature distributions around ectatic capillaries exposed to yellow (578 nm) laser light.*, Phys Med Biol, **34**, 1247-1258.

Pickering JW, Butler PH, Ring BJ, and Walker EP, (1990a); *Copper vapour laser treatment of port wine stains: a patient questionnaire.*, Lasers Med Sci, accepted October 1989.

Pickering JW, Walker E,P Butler PH, and van Halewyn CN, (1990b); *Copper vapour laser treatment of port wine stains and other vascular malformations.*, Br J Plast Surg, accepted November 1989.

Polla LL, Margolis RJ, Dover JS, Whitaker D, Murphy GF, Jacques SL, and Anderson RR, (1987); *Melanosomes are a primary target of Q-switched ruby laser irradiation in guinea pig skin.*, J Invest Dermatol, **89**, 281-286.

Pratt AG, (1953); *Birtmarks in infants.*, Arch Dermatol and Syphil, **67**, 302-305.

Priebe LA and Welch AJ, (1978); *Asymptotic rate process calculations of thermal injury to the retina following laser irradiation.*, Trans ASME J Biomech Eng, **100**, 49-54.

Ratz JL and Bailin PL, (1987); *The case for use of the carbon dioxide laser in the treatment of port-wine stains.*, Arch Dermatol, **123**, 74-75.

Ring BJ, (1988); *The treatment of port wine stains by copper vapour laser: Theoretical derivation of ideal treatment parameters and patient evaluation of existing treatment.*, Undergraduate project report, Physics Department, University of Canterbury, Christchurch, New Zealand.

Ryan TJ, (1973); *The blood vessels of the skin. Part B, vol 2, The physiology and pathophysiology of the skin.* Ed A Jarrett., Academic press, London.

Scheibner A and Wheeland RG, (1989); *Argon-pumped tunable dye laser therapy for facial port wine stain hemangiomas in adults–A new technique using small spot size and minimal power.*, J Dermatol Surg Oncol, **15**, 277-282.

Shakespeare PG and Carruth JAS, (1986); *Investigating the structure of the port-wine stain by transcutaneous microscopy.*, Laser Med Sci, **1**, 107-110.

Smithies DJ, (1989); Private communication.

Smoller BR and Rosen S, (1986); *port-wine stains: A disease of altered neural modulation of blood vessels ?.*, Arch Dermatol, **122**, 177-179.

Soloman H, Goldman L, Henderson B, Richfield D, and Franzen M, (1968); *Histopathology of the laser treatment of port-wine lesions.*, J Invest Dermatol, **50**, 141-146.

Stoll AM and Greene LC, (1958); *Relationship between pain and tissue damage due to thermal radiation.*, J Appl Physiol, **14**, 373-382.

Stone MP, (1989); Private communication.

Star WM, Marijnissen JPA, and van Gemert MJC, (1988); *Light dosimetry in optical phantoms in tissues: I Multiple flux and transport theory.*, Phys Med Biol, **33**, 417-434.

Tan OT, Kerschmann R, and Parrish JA, (1984); *The effect of epidermal pigmentation on selective vascular effects of pulsed lasers.*, Lasers Surg Med, **4**, 365-374.

Tan OT, Carney JM, Margolis R, Seki Y, Boll J, Anderson RR, and Parrish JA, (1986); *Histologic responses of port-wine stains treated by argon, carbon dioxide, and tunable dye lasers.*, Arch Dermatol, **122**, 1016-1022.

Tan OT, Motemedi M, Welch AJ, and Kurban AK, (1988); *Spotsize effects on guinea pig skin following pulsed irradiation.*, J Invest Dermatol, **90**, 877-881.

Tan OT, Murray S, and Kurban AK, (1989a); *Action spectrum of vascular specific injury using pulsed irradiation.*, J Invest Dermatol, **92**, 868-871.

Tan OT, Morelli JG, Whitaker D, Boll J, and Murphy G, (1989b); *Ultrastructural changes in red blood cells following pulsed irradiation in vitro.*, J Invest Dermatol, **92**, 100-104.

Tan OT, Morrison P, Murray S, and MacNicholl Jr. EF, (1989c); *Red blood cell responses to pulsed laser irradiation.*, SPIE Laser Surgery, **1066** , 154-164.

Tan OT, Sherwood K, and Gilchrest BA, (1989d); *Treatment of children with port-wine stains using the flashlamp-pulsed tunable dye laser.*, New Eng J Med, **320**, 416-421.

Tong AKF, Tan OT, Boll J, Parrish JA, and Murphy GF, (1987); *Ultrastructure: Effects of melanin pigment on target specificity using a pulsed dye laser (577nm).*, J Invest Dermatol, **88**, 7474-752.

Touquet VLR and Carruth JAS, (1984); *Review of the treatment of port wine stains with the argon laser.*, Lasers Surg Med, **4**, 191-199.

Walker EP, (1986); unpublished.

Walker EP, Butler PH, Pickering JW, Day W, Fraser R, and van Halewyn CN, (1989); *Histology of port wine stains after copper vapour laser treatment.* Br J Dermatol, **121**, 217-223.

Wan S, Anderson RR, and Parrish JA, (1981); *Analytical modelling for the optical properties of the skin with in vitro and in vivo applications.*, Photochem Photobiol, **34**, 493-499.

Welch AJ, Wissler EH, and Priebe LA, (1980); *Significance of blood flow in calculations of temperature in laser irradiated tisssue.*, IEEE Trans Biomed Eng, **BME-27**, 164-166.

Welch AJ, (1984); *The thermal response of laser irradiated tissue.*, IEEE J Quant Elec, **QE-20**, 1471-1481.

Welch AJ and Polhamus GD, (1984); *Measurement and prediction of thermal injury in the retina of the rhesus monkey.*, IEEE Trans Biomed Eng, **BME-31**, 633-643.

Welch AJ, Yoon G, and van Gemert, (1987); *Practical models for light distribution in laser irradiated tissue.*, Lasers Surg Med, **6**, 488-493.

Welch AJ, Pearce JA, Diller KA, Yoon G, and Cheong W-F, (1989); *Heat generation in laser irradiated tissue.*, Trans ASME J Biomech Eng, **111**, 62-68.

Wilson BC and Adam G, (1983); *A Monte Carlo model for the absorption and flux distributions of light in tissue.*, Med Phys, **10**, 824-830.

Yoon G, Welch Aj, Motamedi M, and van Gemert MJC, (1987); *Development and application of three dimensional light distribution model for laser irradiated tissue.*, IEEE J Quant Elec, **QE-23**, 1721-1733.

Appendix A PICKERING ET AL. 1989A

Pickering JW, Butler PH, Ring BJ, and Walker EP, (1989a); *Thermal profiles of a blood vessel heated by a laser.*, Australasian Physical and Engineering Sciences in Medicine, **12**, 11-15.

Australasian Physical & Engineering
Sciences in Medicine (1989) Vol. 12 No. 1

THERMAL PROFILES OF BLOOD VESSELS HEATED BY A LASER*

John W. Pickering[1], Philip H. Butler[1], Brendan J. Ring[1], E. Peter Walker[2]

[1] *Physics Department, University of Canterbury, Christchurch, New Zealand*
[2] *Milford Chamber, 249 Papanui Road, Christchurch, New Zealand*

Abstract

Thermal profiles of ectatic capillaries, modelled on those found in port wine stain birthmarks, are calculated by a method of finite differences. Yellow 578nm light is assumed to illuminate these vessels. The coagulation of endothelial cells is assumed to occur when the cells are heated to at least 70°C. We model this by asking that a point 6μm above the top of the vessel lumen attains a temperature of 70°C. We constrain the parameters to prevent heating of blood above 100°C, so as to avoid vapourisation. The treatment parameters of dose and illumination time are varied until they produce thermal profiles that show the model's coagulation conditions.

These ideal treatment parameters are found to be dependent on the size of vessel being treated and are rather longer than the thermal relaxation time of the vessel and also much longer than the pulses of pulsed dye lasers.

Keywords

Laser, Port wine stains, modelling.

Introduction

The preferred treatment for port wine stains and other conditions involving the ectatic capillaries is laser therapy[1]. Lasers that produce light that is selectively absorbed by haemoglobin and minimally absorbed by other cutaneous pigments are most ideal. This is because the desire is to thermally damage the ectatic capillaries whilst minimising damage to any other part of the skin. Yellow light from 570 to 585nm is considered the best candidate as it both corresponds to an absorption peak of haemoglobin and also is not sufficiently absorbed by the melanin in the epidermis to cause excessive heating within the epidermis and the papillary dermis. Lasers that produce yellow light are dye lasers tuned to 577nm and the copper vapour laser at 578nm.

* *Presented at Engineering and Physical Sciences in Medicine 1988, Brisbane, September 1988.*

In order to provide the "ideal treatment" we need to know details of the thermal state of the blood vessels during treatment. Here we define the ideal treatment as that which serves to produce coagulation of the endothelial cells of blood vessels whilst minimising any temperature rise further away from the vessel. The ideal treatment parameters are those of dose (in J/cm^2) and illumination time (in ms) that result in the ideal treatment[2]. The classification of port wine stains in terms of blood vessel diameter is shown in Table 1.

Previous models have been either analytical[3] or numerical[2,4]. The analytical model is based on attempting to heat the vessel within the thermal relaxation time of the vessel. The numerical models produce treatment parameters that are based on preventing excessive heat conduction from the epidermis to the dermis. These models do not calculate the heat conducted to the endothelial cells and any resultant temperature rise, rather they assume vessel coagulation when the blood reaches the desired coagulation temperature. In this paper we numerically model the heating of individual blood vessels and attempt to define the treatment parameters that lead to the coagulation of the endothelial cells.

TABLE 1

Port Wine Stain Classification

Type[1]	Description[1]	% in population[1]	Vessel diameter[1]
Constricted	Vessels only slightly larger than normal & in subpapillary layer.	41	≤45μm
Intermediate	Vessels larger than normal & in sub-papillary layer.	29	45-45μm
Dilated	Vessels considerably larger than normal.	25	≥55μm
Deep located	As with dilated but spread throughout dermis.	5	≥55μm

[1] Ohmori and Huang 1981 [2] Noe et al 1980

TABLE 2

Tissue Parameters

Density	ρ	=	10^3 Kg/m3
Heat Capacity	C_v	=	3.5 x 10^3 J/kg °C
Thermal Conductivity	η	=	0.62 W/m °C
Absorption Coefficient of blood at 577nm	α	=	430/cm
Ambient skin & blood temperature	T_0	=	35°C

Method

The tissue parameters (Table 2) we use are constants of our model. They are the same parameters as for other models[2-4] and assume only that the heat capacity, density and conductivity are approximately equal for blood and other cutaneous tissue. The absorption coefficient of blood, α, is given by van Gemert et al[6] for 577nm light and the light intensity, I, is attenuated as

$$I = I_0 e^{-\alpha x}$$

where x is the depth of blood. Hence we are ignoring the small contribution of scattering towards attenuation.

Absorption of light by haemoglobin will result in heating of the blood and thermal conduction of heat from the blood to surrounding tissue. With heating occurring on the sub-second time scales there is negligible heat loss due to blood flow[5]. As a consequence we can reduce any model of a single blood vessel to a model of two spatial dimensions by looking only at a transverse cross section of the vessel. We consider only the case where the intensity of incident light is constant across the vessel. This is the case when the beam diameter is much greater than the vessel diameter.

Endothelial cells are 4 to 6μm thick[6]. We use the 6μm figure to ensure coagulation of all endothelial cells.

Coagulation of blood vessels is assumed to occur when the endothelial cells at the top of the vessel reach 70°C. This value is based on the measurements of Barnes et al[7] and Jacques and Prahl[8] where 70°C is shown to produce irreversible tissue damage. Furthermore this value has been the standard value used in other models[2-4]. However we assume that only the top of the vessel needs to reach this temperature because of the tendency for endothelial cells to wind themselves in a helical fashion along the length of the blood vessel. Further away from the vessel the temperature must be kept to a minimum in order to avoid unnecessary damage.

We ask that the temperature within the vessel does not exceed the vapourisation point of blood (approximately 100°C). Any vapourisation tends to result in reversible mechanical damage to the vessel wall, and subsequent haemorrhaging[2,9]. For the purposes of simplicity we have assumed a homogeneous distribution of haemoglobin throughout the vessel, a reasonable assumption given the small volume of an erythrocyte compared with the volume of the ectatic vessel. The basis for the model as described is illustrated by figure 1.

The temperature, T, for any point (x,y) within the bounds of the model will vary with time, t, depending on the light absorbed and heat conducted at that point according to the heat transfer equation[10]:

$$\rho C_v \frac{\partial T(x,y,t)}{\partial t} = \alpha I_0 e^{-\alpha d(x,y)} + \eta \nabla^2 T(x,y,t)$$

where (absorption term)

$$\alpha I_0 e^{-\alpha d(x,y)} = 0 \quad t<0 \text{ and } t > t_{illumination}$$

$$\text{or } d(x,y) \rightarrow \infty$$

and where d(x,y) is the depth below the top surface of the vessel.

This equation was solved by a finite difference method using a FORTRAN program run on a VAX 8350 computer. Simple, first order differences in a square grid were used for the derivatives. The size of the grid was chosen so that increasing the distance of the square boundary from the blood vessel by a factor of ten caused less than a 1% change in the resultant temperature values.

This program allowed us to compute a temperature profile for a vessel cross section at any time during or after illumination with a given dose of light. We computed profiles for a variety of vessel diameters

and for each diameter varied the illumination time and the energy dose. We thus established the parameters that give a temperature profile with 70°C at the top surface of the endothelial cells and not more than 100°C within the vessel.

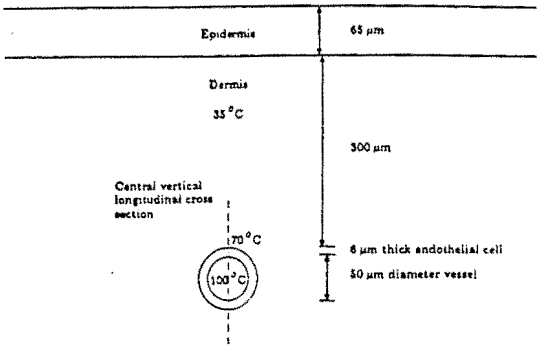

Figure 1. The port wine stain model. The situation shown is that of coagulation of the endothelial cells at 70°C whilst allowing the vessel lumen to attain as a maximum 100°C. 300nm is the average depth for ectatic vessels below the epidermal – dermal junction.[4]

Results

The coagulation temperature for the endothelial cells is reached about 0.2ms after the end of the illumination period.

Figure 2 shows the isotherms for a cross section of a 5mm diameter vessel when the coagulation conditions apply. That is immediately after the end of a 5.5ms illumination period with 2.87 J/cm². Because of the near circular symmetry we are able to represent the key elements of this plot by a vertical cross section. We next plot (Figure 3) the temperature along this central vertical longitudinal cross section (see figure 1) as a function of time. These treatment parameters just produce the coagulation temperature of 70°C at the top surface of the endothelial cells. The blood temperature is maintained below the vapourisation point throughout the thermal process. The temperature at a greater distance from the blood vessel is kept as low as possible. Hence, according to our assumptions these treatment parameters are the ideal for this vessel size.

Table 3 gives the ideal treatment parameters for a range of vessel sizes each of which was determined in the manner just described. Estimates for the necessary energy dose upon the skin surface were made assuming an intensity loss between the surface and vessel of 30 to 50% due to melanin absorption and scattering.

Discussion

Previous modelling[9,11] has suggested that the illumination time must be shorter than the thermal relaxation time of the vessel. The thermal relaxation time is defined as the time required for the vessel to fall to a temperature half way between those of its initial and elevated temperatures. The choice of 50% of the temperature difference is somewhat arbitrary and hence it is not valid to use the thermal relaxation time as an upperbound for the ideal illumination time. Our model shows that the illumination times to produce coagulation without varpourization are rather longer than the thermal relaxation time of the vessel. For example the thermal relaxation time for a 50μm diameter vessel is approximately 1ms compared to our ideal time of 5.5ms.

Table 3 also illustrates the vessel size dependence of the ideal treatment. In practice it may be that vessel size can be determined by the correlation between vessel size and colour, shown to exist by Barsky and co-workers[4,12-15].

For treatment parameters for vessels of 30 to 100μm diameter are remarkedly similar. For most port wine stains the vessel diameter is in the range 45 to 55μm[12-17] and the "ideal" treatment parameters are an illumination time of 5.5mns and dose incident upon the skin surface of 4 to 6 J/cm².

TABLE 3

The Ideal Treatment Parameters

Vessel diameter	Energy flux incident upon vessel	Energy flux required at skin's surface*	Heating time
μm	J/cm²	J/cm²	ms
30	4.38	6.3 – 8.8	5.9
50	2.87	4.1 – 5.7	5.5
80	2.06	2.9 – 4.1	5.0
100	1.94	2.8 – 3.9	5.0

* assuming 30–50% of light incident upon the skin surface is absorbed before reaching the vessel.

References

1. Carruth, J.A.S. and McKenzie, A.L., *Medical Lasers, 1986* Adam Hilger Ltd., Bristol.

2. Gemert van, M.J.C., Welch, A.J., Amin, A.P., *Is there an optimal laser treatment for port wine stains?*, Lasers Surg Med (1986), 6:76-83.

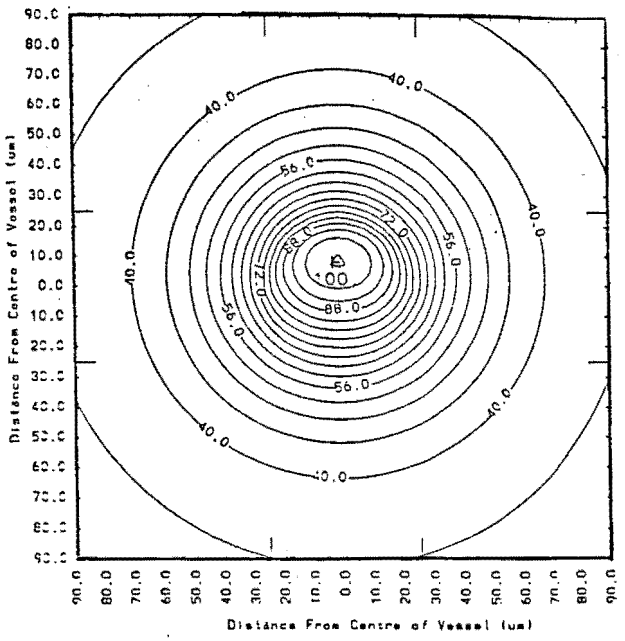

Figure 2. A cross section of a 50mm diameter (indicated by the extended graduations) vessel immediately after the end of 5.5ms illumination with 2.9 J/cm² of 578nm light. The vessel is illuminated from the top. The contours are isotherms. The temperature of the endothelial cell 6um from the top of the vessel lumen (at 31um on the upper vertical scale) just reaches 70°C.

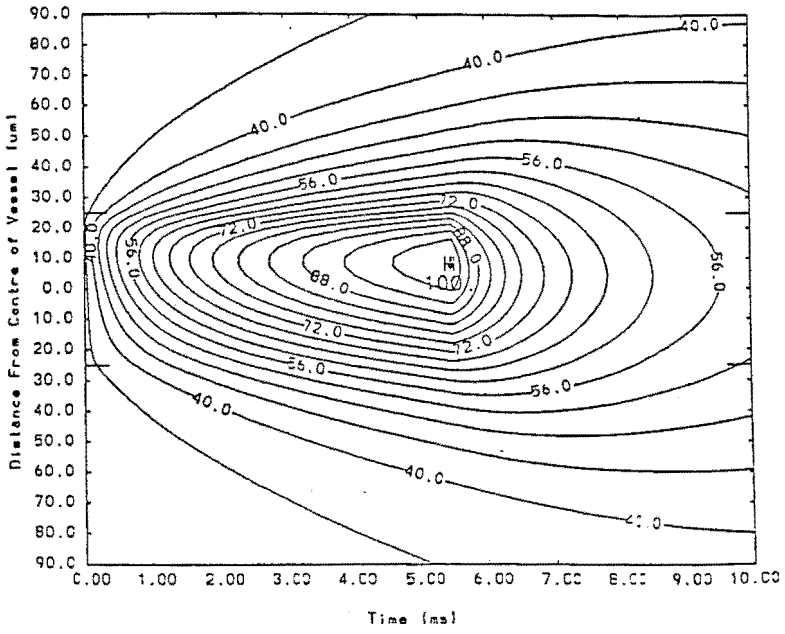

Figure 3. The time dependent isotherms of the vertical cross section of a 50um diameter vessel illuminated for 5.5ms with 2.9 J/cm² of 578nm light. The extent of the vessel is indicated by the extended graduations. The temperatures at 7ms corresponds to those through a central vertical axis of Figure 1.

3. Anderson, R.R. and Parish, J.A., *Microvasculature can be selectively damaged using dye lasers: A basic theory and experimental evidence in human skin*, Lasers Surg Med (1981), 1:263-276.

4. Gemert van, M.J.C., Kleijn de, W.J.A., Hulsbergen Henning J.P.., *Temperature behaviour of a model port-wine stain during argon laser coagulation*. Phys Med Biol (1982), 27:1089-1104.

5. Welch, A.J., Wissler, E.H., Priebe, L.A., *Significance of blood flow in calculations of temperature in laser irradiated tissue*. IEEE Trans Biomed Eng BME, (1980) 7:164-166.

6. Barsky, S.H., Rosen, S., Geer D.E., Noe, J.M., *The nature and evolution of port wine stains: A computer-assisted study*, J Invest Dermatol (1980), 74:154-157.

7. Barnes, F.S., *Applications of lasers to biology and medicine*, Proc IEEE, (1975), 63:1269-1278.

8. Jacques, S.L. and Prahl, S.A.*Modeling optical and thermal distributions in tissue during laser irradiation*, Lasers Surg Med (1987), 6:494-503.

9. Paul, B.S., Anderson, R.R., Jarve, J., Parrish, J.A.., *The effect of temperature and other factors on selective microvascular damage caused by pulsed dye laser*, J Invest Dermatol (1983), 81:333-336.

10. Searsc, F.W., Zemansky, M.W. and Young, H.D., University Physics (5th edition), Reading, Massachusetts.

11. Tan, O.T. and Stafford, J: *Treatment of port-wine stains at 577 nm: Clinical results*, Med Instru (1987), 21:218-221.

12. Noe, J.M., Barsky, S.H., Geer, D.E., Rosen, S., *Port wine stains and the response to argon laser therapy: Successful treatment and the predicative role of color, age, and biopsy*, Plast Recon Surg (1980), 65: 1130-136.

13. Ohmori, S. and Huang, C., *Recent progress in the treatment of portwine staining by argon laser: some observations on the prognostic value of relative spectro-reflectance (RSR) and the histological classification of the lesions*, Br J Plast Surg (1981), 34:249-257.

Appendix B WALKER ET AL. 1989

Walker EP, Butler PH, Pickering JW, Day W, Fraser R, and van Halewyn CN, (1989); *Histology of port wine stains after copper vapour laser treatment.* Br J Dermatol, **121**, 217-223.

British Journal of Dermatology (1989) **121**, 217–223.

Histology of port wine stains after copper vapour laser treatment

E.P.WALKER, P.H.BUTLER,* J.W.PICKERING,* W.A.DAY,† R.FRASER† AND C.N.VAN HALEWYN*

Milford Chambers, 249 Papanui Road, Christchurch, New Zealand, *Physics Department, University of Canterbury, Christchurch, New Zealand and †Christchurch Clinical School, University of Otago, Christchurch, New Zealand

Accepted for publication 10 February 1989

SUMMARY

We report histological changes in four patients with port wine stains treated with 578 nm yellow light from a high power copper vapour laser. Histology showed that selective damage occurred to the ectatic blood-vessels in the dermis, without haemorrhage and damage to non-vascular structures, and without scarring. The initial damage to the overlying epidermis was not permanent, and the damaged ectatic vessels returned to normal size or were completely necrosed and replaced by collagen.

Histological studies of the results of laser treatment have shown non-specific necrosis of all cutaneous tissue with use of the carbon dioxide laser,[1] or more specific damage to vascular tissue but accompanied often by an unacceptable level of scarring with the use of the argon ion laser.[1,2] More specific vascular damage has been shown to occur with short pulses of the 577 nm tunable dye laser.[1–4] We report the histological changes after the treatment of four patients with port wine stains with exposure to yellow 578 nm light from a copper vapour laser (Quentron™ QM90-51C).

The low ratio of melanin to haemoglobin absorption in the 560–580 nm range suggests that specific heating of ectatic blood-vessels will occur with light in these wavelengths.[5,6] Histological studies[1–4] support the use of yellow light over the wavelength produced by the argon ion laser (principally 488 nm and 514·5 nm), where there is considerably more melanin absorption.[5] Furthermore, the numerical models of van Gemert and co-workers[7–9] and our model[10] suggest that for the ideal damage to ectatic blood-vessels to be produced, the light must be delivered over a specific time interval and this is 1–10 ms.[8,10,11] Some tunable dye lasers delivering pulses with duration approaching this time interval have given good results,[1,2] but the exposure times using the carbon dioxide and argon ion lasers are 100 ms and often longer.

Correspondence: Mr J.W.Pickering, Department of Physics, University of Canterbury, Christchurch, New Zealand.

METHODS

Four Caucasian patients with port wine stains on the face, trunk and extremities were treated with 578 nm light from the copper vapour laser. This is a pulsed laser with a pulse length of 50 ns. However, unlike the pulsed dye lasers, the light is delivered by a large number of pulses in rapid succession (450–1500). The repetition rate is approximately 15 kHz, i.e. one pulse every 67 μs. The pulse train appears to be a very short pulse followed by a comparatively long period, about 1300 times the length of the pulse. Furthermore, each pulse delivers about 0·2 mJ of energy from the yellow light to the skin. This is much smaller than the 100 mJ or more from the single pulse use of the pulse dye laser.[1,4] The energy distribution is also different from the continuous wave laser where the distribution is independent of time.[1,2,12]

The light was focused onto a 1 mm diameter quartz optic fibre which was scanned by hand approximately 2 mm above the skin surface, thus producing a 1·3 mm diameter spot. All the patients were anaesthetized with a general anaesthetic before treatment, because of the large areas to be treated (average 392 cm^2). Light doses of 11–25 J/cm^2 were applied by 1·6–3·6 W of yellow light being scanned across the lesion at a rate of 6–9 s/cm^2. The power used is much higher than that of a continuous wave 577 nm dye laser.[12] The exact dose depended on when the skin first appeared to blanch, this minimal blanching being the endpoint.

Skin biopsies were taken prior to treatment and 24 h after treatment. Further biopsies were taken from the treated areas at 3 or 6 months. The biopsies were processed for light and electron microscopy (Table 1).

RESULTS

Light microscopy

Histology of the port wine stains in all the patients was that of the deeply located type,[13] with ectatic vessels at the junction of papillary and reticular dermis and throughout the reticular dermis. These vessels measured up to 150 μm in diameter.

The pathology of the skin biopsies 24 h following treatment showed an acute inflammatory infiltrate in the dermis, with a subepidermal blister. Parts of the papillary and reticular dermis

TABLE 1. The operating parameters and histologies performed for each biopsy

Patient	Age at biopsy (years)	Distribution of port wine stain	Area of port wine stain field cm^2	Type of microscopy	Pretreatment biopsy?	24 h post		3–6 months post	
						Scan rate s/cm^2	Dose J/cm^2	Scan rate s/cm^2	Dose J/cm^2
A	9	right-face, neck, shoulder, arm	371	light	yes	9	20	9	20
B	18	left-face, neck, lower leg	430	electron	yes	7	11	9	19
C	47	left-face, neck, cheek, forehead, leg, right-face, neck	115	electron	yes	6	17	No biopsy taken	
D	45	left-forearm, arm, neck, shoulder	570	light	yes	7	25	No biopsy taken	

FIGURE 1. Normal appearing hair follicle and sebaceous gland of patient D are adjacent to a coagulated ectatic vessel (E). (Original × 6·5).

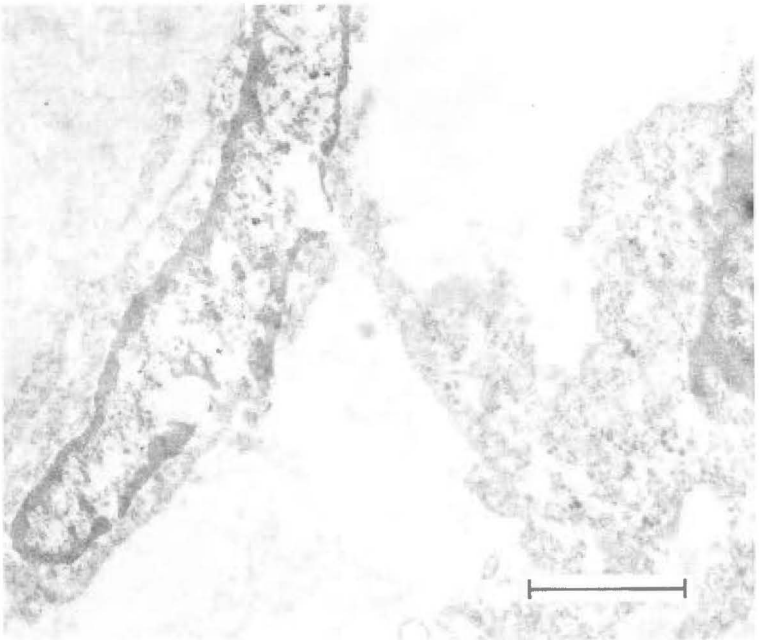

FIGURE 2. Disintegration of the nucleus of an endothelial cell of patient C at 24 h (magnification × 9912; bar indicates 2 μm).

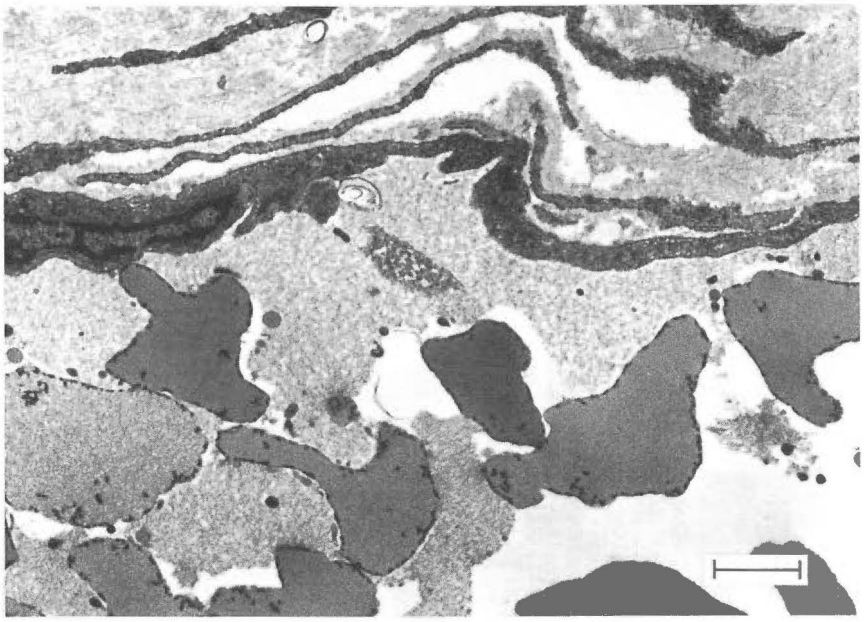

FIGURE 3. Thrombus of red blood cells within an ectatic vessel of patient B at 24 h. Dark spots within red blood cells indicate precipitates of iron (magnification × 5866; bar indicates 2 μm).

appeared to be degenerate and many of the ectatic vessels throughout the papillary and reticular dermis had necrotic endothelial cells, though they still contained red blood cells indicating blood flow. Several of these vessels were more damaged on their top outward facing side, rather than below. Some of these vessels contained a coagulum consisting of protein or neutrophils or both. There was no evidence of rupture of vessels or haemorrhage. Hair follicles, sweat and sebaceous glands appeared normal immediately adjacent to the damaged blood vessels (Fig. 1).

After 3 to 6 months, the epidermis was normal and there appeared to be a normal distribution of melanocytes. The papillary and reticular dermis appeared normal and there was clearance of ectatic blood-vessels. There was a slight increase in the number of normal sized capillaries. No haemosiderin was demonstrated in the dermis. The sweat glands and hair follicles appeared normal.

Electron microscopy

At 24 h after treatment, the endothelial cells showed marked damage, with disruption of the nuclei and considerable damage to the subcellular organelles (Fig. 2). The vessel walls showed degeneration with disruption of basal lamina, and there was destruction of pericytes and extension of the damage to the surrounding collagen fibrils. In some of the vessels there was thrombus with agglutinated red blood cells and there were a few platelets to be found on the walls of some of the larger vessels. A few red blood cells showed evidence of rupture, while others appeared to contain precipitates of iron (Fig. 3). Small vessels were present without the degenerative changes as seen in the larger ones. The epidermis showed some necrosis.

At 3 to 6 months the epidermis appeared to be normal (Fig. 4). There was some increase in the

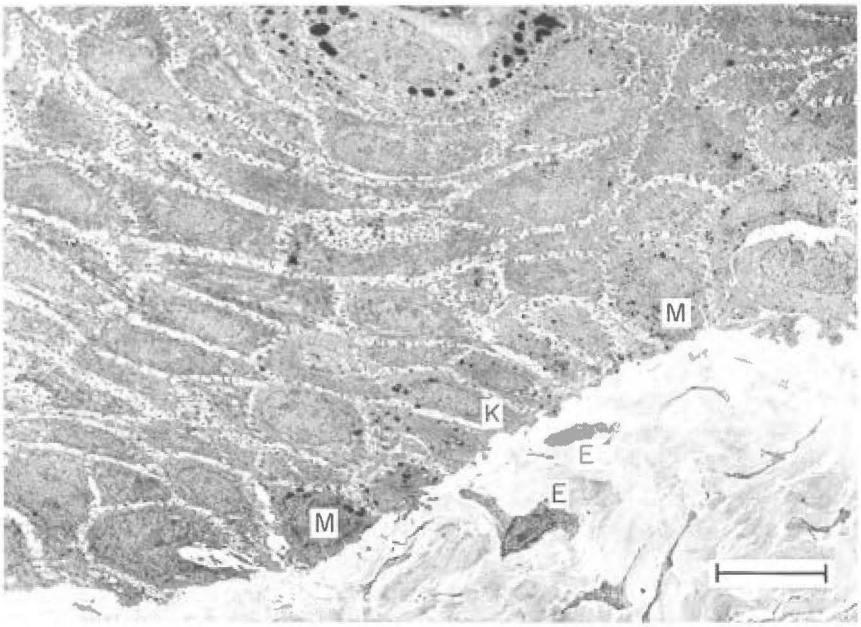

FIGURE 4. Normal epidermis with normal 1 to 7 distribution of melanocytes (M) to keratinocytes (K) of patient B at 6 months. Note the intact endothelial cells (E) apart from any blood-vessel (magnification × 1463; bar indicates 10 μm).

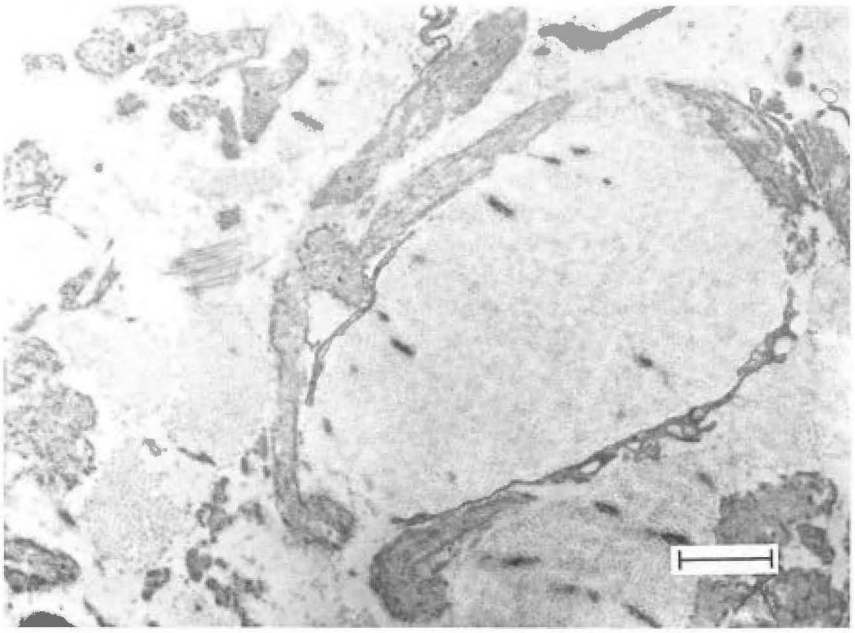

FIGURE 5. A large (approximately 100 μm diameter) blood-vessel that has been destroyed by laser treatment. This shows the vessel of patient B at 3 months completely filled with collagen (magnification × 595; bar indicates 20 μm).

fibrous connective tissue, though the collagen fibrils appeared normal. Some intact endothelial cells and remnants of basal lamina were seen, suggesting that following the occlusion of the ectatic vessels they had been replaced by fibrous connective tissue (Fig. 5). The vessels in the deeper dermis showed marked subendothelial fibrosis, some showing complete occlusion. Smaller vessels in the papillary dermis appeared normal. The endothelial cells of these vessels were often plump and contained normal organelles and many micropinocytotic vesicles.

DISCUSSION

When considering the interaction of light with tissue we need to consider the relationship between several timescales. First, the time over which the light is incident upon a blood-vessel, t_i; second, the pulse length if any of the laser delivering the light, t_p; third, the time required for a blood-vessel raised to a temperature above its immediate surroundings, to fall to a temperature midway between that temperature and the initial temperature of its surroundings: the blood-vessels' thermal relaxation time, t_v.

The argon ion laser is a continuous beam laser and is typically used with $t_i(Ar^+)$ of hundreds of milliseconds. The histology indicates marked epidermal damage[1,2] and diffuse dermal collagen coagulative necrosis to a depth in the dermis depending on the incident energy density.[2] Destruction of hair follicles, sweat glands and sebaceous glands has been shown to occur. Epidermal and dermal damage is often not repaired and as a result hypertrophic scars have often formed.[1,2] The pumped dye laser is a pulsed laser with pulse lengths in the range 300 ns $\leqslant t_p(577) \leqslant$ 360 μs. The common histological results are selective damage to blood vessels,[1-4] haemorrhage,[2-4] agglutination of red blood cells,[1-4] and some red blood cell rupture.[2,4]

Thermal relaxation times of blood-vessels varies according to size, and is independent of the incident light. For example blood-vessels with a 20 μm diameter have $t_v = 0{\cdot}15$ ms while those of 60 μm diameter have $t_v = 1{\cdot}3$ ms.[5] The copper vapour laser is a pulsed laser with very short pulses (50 ns) repeated very rapidly (15,000 per s—15 kHz). The high repetition rate means that even for the smallest ectatic vessels many pulses are absorbed by each vessel during the relaxation time t_v, and we are therefore able to consider the laser as operating in an essentially continuous mode. The illumination time t_i(Cu) is determined by the rate of scan of the light across the treated area; we operated with 30 ms $\leqslant t_i \leqslant$ 100 ms.

As with the argon laser, initial epidermal damage was seen to occur, consisting primarily of superficial blistering. However, unlike with the argon laser,[1,2] histology at 3 months indicated that this damage was not permanent. By the use of shorter illumination time scales, and because there is 30% less absorption by the melanin, considerably less heating was caused within the epidermis. Furthermore, the yellow light is four times more strongly absorbed by the haemoglobin than green light, so the outer crescent of ectatic vessels was heated most and hence the heating of the capillary wall was much more specific. Those vessels showing damage to their top side were a direct consequence of the strong absorption of yellow light.

The dye laser histologies[1-4] produced selective damage of blood-vessels similar to the present results with the copper laser. With the copper vapour laser the immediate observed response of the skin is blanching and it appears that damage was the result of heat conduction from the haemoglobin, causing thermal necrosis of endothelial cells and thermal damage to localized perivascular fibrous connective tissue. There was no visual or histological evidence of haemorrhage and only very little thrombosis or blood cell rupture. Rupture of blood cells and haemorrhaging is indicative of the very short (submillisecond) time-scale heating that occurs when the full dose of energy is applied essentially instantaneously, before the red blood cells are

able to thermally relax, the rapid supply of energy causing them to rise above 100°C. This seems to be the case with the 350 ns heating of Greenwald *et al.*[2] and 1·5 μs heating of Nakagawa *et al.*,[4] since their histologies indicate the possibility of some steam generation causing the cell to rupture. In both of these cases the target vessels were normal sized and when a red blood cell ruptures it may rupture the vessel wall as well. Short time scales may not maintain the red blood cells of an ectactic vessel at an elevated temperature long enough for conduction of heat to the endothelial cells to cause thermal necrosis.

We conclude from the histologies that a 100 ms illumination time with 11–19 J/cm^2 of 578 nm light from a copper vapour laser pulsed at 15 kHz produces satisfactorily specific ectatic blood vessel necrosis.

REFERENCES

1 Tan OT, Carney JM, Margolis R *et al.* Histologic responses of port-wine stains treated by argon, carbon dioxide and tunable dye lasers. *Arch Dermatol* 1986; **122:** 1016–22.

2 Greenwald J, Rosen S, Anderson RR *et al.* Comparative histological studies of the tunable dye (at 577 nm) laser and argon laser: the specific vascular effects of the dye laser. *J Invest Dermatol* 1981; **77:** 305–10.

3 Morrelli JG, Tan OT, Garden J *et al.* Tunable dye laser (577 nm) treatment of port wine stains. *Lasers Surg Med* 1986; **6:** 94–9.

4 Nakagawa H, Tan OT, Parrish JA. Ultrastructural changes in human skin after exposure to a pulsed laser. *J Invest Dermatol* 1985; **84:** 396–400.

5 Anderson RR, Parrish JA. The optics of human skin. *J Invest Dermatol* 1981; **77:** 13–19.

6 van Halewyn CN. Argon laser treatment of port wine stains. Undergraduate Project Report, University of Canterbury, 1985.

7 van Gemert MJC, de Kleijn WJA, Hulsbergen Henning JP. Temperature behaviour of a model port wine stain during argon laser coagulation. *Phys Med Bio* 1982; **27:** 1089–104.

8 van Gemert MJC, Welch AJ, Amin AP. Is there an optimal laser treatment for port wine stains? *Laser Surg Med* 1986; **6:** 76–83.

9 Lahaye CTW, van Gemert MJC. Optimal laser parameters for port wine stain therapy: a theoretical approach. *Phys Med Biol* 1985; **30:** 573–587.

10 van Halewyn CN. Laser treatment of port wine stains. *M.Sc. thesis*, University of Canterbury, 1987.

11 Pickering JW, Butler PH, Ring BJ, Walker EP. Thermal profiles of blood vessels heated by a laser. *Australasian Physical and Engineering Sciences in Medicine* 1989; **12:** 11–15.

12 Cotterill JA. Preliminary results following treatment of vascular lesions of the skin using a continuous wave tunable dye laser which emits at 577 nm. *Clin Exp Dermatol* 1986; **11:** 628–35.

13 Noe JM, Barsky SH, Geer DE, Rosen S. Port wine stains and the response to argon laser therapy successful treatment and the predictive role of colour, age and biopsy. *Plas Recon Surg* 1980; **65:** 130–6.

Appendix C PICKERING ET AL. 1989B

Pickering JW, Butler PH, Ring BJ, and Walker EP, (1989b); *Computed temperature distributions around ectatic capillaries exposed to yellow (578 nm) laser light.*, Physics in Medicine and Biology, **34**, 1247-1258.

Phys. Med. Biol., 1989, Vol. 34, No 9, 1247–1258. Printed in the UK

Computed temperature distributions around ectatic capillaries exposed to yellow (578 nm) laser light

John W Pickering†, Philip H Butler†, Brendan J Ring† and E Peter Walker†

† Physics Department, University of Canterbury, Christchurch, New Zealand
‡ Milford Chambers, 249 Papanui Road, Christchurch, New Zealand

Received 1 March 1989, in final form 18 May 1989

Abstract. We have numerically modelled the thermal effects of yellow (577 or 578 nm) light illumination on the ectatic blood vessels of port wine stains. We investigated the effect of the laser treatment parameters of light irradiance and illumination time on the extent of coagulation (coagulation thickness) of the endothelial cells of the ectatic vessels. We assumed that this coagulation is dependent on heating the cells to a critical temperature (coagulation temperature). We iteratively adjusted the treatment parameters so that the model vessels had a maximum temperature that did not exceed the boiling point of blood. Given the likely range of variation of coagulation temperature, coagulation thickness and vessel size, coagulation temperature was found to have the greatest effect on the treatment parameters. Variations in coagulation thickness had less influence, and the diameter of the ectatic vessel (typically in the 30–80 μm diameter range) had the least effect. The treatment parameters that have been shown clinically to cause purpura (e.g. 6–7 cm^{-2} in 360 μs) were also studied. The purpura seen by some workers using pulsed dye lasers is most likely to be the result of vaporisation of blood leading to the rupture of the vessel. We conclude that, in order to achieve coagulation with these short laser pulses, the choice of irradiance is critical.

1. Introduction

Port wine stains are congenital birthmarks consisting of ectatic dermal blood vessels. They are present in 0.3–0.5% of the population (Carruth and McKenzie 1986) and are often the cause of psychological problems. Until the advent of the argon ion laser, there was no successful method for removing these birthmarks.

Histological studies have classified port wine stains into four types (Noe *et al* 1980, Ohmori and Huang 1984): constricted, intermediate, dilated, and deeply located. Table 1 describes these classes in terms of their position within the dermis, their vessel size and their population distribution. The vessel size is normally uniform throughout a port wine stain, and the colour of the stain is correlated both with vessel size and with percentage fullness (Barsky *et al* 1980).

The clinical results of laser treatment depend on lesion colour, and the light pink lesions prevalent in children have been particularly difficult to treat (Noe *et al* 1980, Ohmori and Huang 1981, Cotterill 1986). However, some clinicians have found the deeper red or purple lesions difficult to treat (Garden *et al* 1988) and it is clear that the treatment depends on the technique used. In this paper, we present a theoretical model which helps to explain some of the reasons for this variation.

0031-9155/89/091247+12$02.50

Table 1. Port wine stain classification.

Type†	Vessel description†	% in population†	Vessel diameter‡ (μm)
Constricted	Larger than normal and in the subpapillary layer	41	$20 \leq 45$
Intermediate	Much larger than normal and in the subpapillary layer	29	45–55
Dilated	Considerably larger than normal and predominantly in subpapillary layer	25	≥ 55
Deeply located	As with dilated but spread throughout the dermis	5	≥ 55

† Ohmori and Huang (1981)
‡ Noe *et al* (1980)

Theoretical modelling (Anderson and Parish 1981, Lahaye and van Gemert 1985, van Gemert *et al* 1986), clinical practice (Anderson and Parish 1981, Tan and Stafford 1987, Garden *et al* 1988, Cotterill 1986) and histological findings (Greenwald *et al* 1981, Morelli *et al* 1986, Tan *et al* 1986, Walker *et al* 1989) have established that the ideal wavelength for the treatment is 570–585 nm. A wavelength in this range can be generated by either continuous or pulsed dye lasers at 577 nm, or by copper vapour laser at 578 nm. Some calculations based on preventing the 'iron heater' effect, i.e. the excessive heating of the dermis caused by too much heat being conducted from the epidermis, have established an ideal illumination time of 1–10 ms (Lahaye and van Gemert 1985, van Gemert *et al* 1986). The premise on which these models are based is that the ideal treatment will coagulate the ectatic blood vessels without damaging other cutaneous tissue. We also have based our model on this premise.

Depending on the treatment technique being used, the skin may respond visibly in either of two ways, namely blanching or purpura. In blanching, the skin turns white, which is indicative of protein denaturation. Purpura, by definition the extravasation of blood into tissue, appears as a dusky blue-grey colour, and is indicative of the breaching of the endothelial cells.

Many clinicians use the appearance of blanching as the end point for treatment (e.g. Cotterill 1986). Normally, the blanching end point is used with light from an argon laser, a continuous wave dye laser or a quasi-continuous copper vapour laser. Usually, a striping or mechanically pulsed technique is used for applying the light, with some variation in detail. Blanching appears immediately on application of the light, whereas purpura normally appears only after some 5–15 minutes (Garden *et al* 1988). Clinicians using the purpura end point apply the light in a submillisecond pulse.

The purpose of our model is to study the treatment conditions that result in each of these two clinical end points. We have assumed that the endothelial cells will coagulate at a temperature of around 60–70 °C. We have postulated that allowing the blood to boil will breach the endothelial cells, and that one should avoid this vaporisation to ensure sufficient coagulation.

In §2.2, we discuss the requirements of our model for coagulation of the endothelial cells. It is desirable to coagulate the cells in a time short with respect to the characteristic time for heat conduction and with the lowest energy dose that produces the desired coagulation. This will minimise the extent of thermal damage to dermal collagen or other cutaneous structures at a distance from the ectatic vessels.

In §3.1, we present the treatment parameters of illumination time and irradiance

which, according to our assumptions, result in the coagulation of endothelial cells. In §4.1, we discuss the effects that the choice of coagulation temperature and thickness have on these parameters.

To investigate the purpuric end point, we used the numerical model presented in §2.2 in order to model the treatment parameters that have been shown clinically to produce purpura (Tan and Stafford 1987). These parameters produce thermal profiles which differ from the profiles necessary for blanching. The purpuric profiles are illustrated in §3.2. In §4.2, we describe the processes which lead to purpura.

2. Methods

2.1. Assumptions

The tissue parameters presented in table 2 are constants for our model. They are the same as those used for other models (Anderson and Parish 1981, van Gemert *et al* 1982, 1986) and assume only that the heat capacity, density and conductivity for blood and other cutaneous tissue are all equal. The absorption coefficient for blood, α, is the same as that used by van Gemert *et al* (1986) for 577 nm light, and is based on Beer's law. We have ignored scattering within the blood because it is negligible compared with absorption at 578 nm.

Table 2. Tissue parameters.

Parameters	Values
Density (ρ)	10^3 kg m^{-3}
Heat capacity (C_v)	3.5×10^3 J kg^{-1} °C^{-1}
Thermal conductivity (η)	0.62 W m^{-1} °C^{-1}
Absorption coefficient of blood (α_{577nm})	430 cm^{-1}
Skin and blood temperature (T_o)	35 °C

Absorption of light by haemoglobin will result in heating of the blood and thermal conduction from the blood to the surrounding tissue. The quantity of light that is available to be absorbed by a vessel depends on a multitude of factors. These include: the irradiance at the top surface of the skin, the quantity of light that is absorbed by the melanin within the epidermis, the scattering properties of the epidermis and dermis, the depth of the blood vessel below the skin surface, the distribution of other blood vessels and the width of the incident beam.

There is no doubt that the dermis and epidermis are strongly scattering at 578 nm. Therefore an incident collimated beam would quickly lose its collimation, and the flux within the tissue may be greater than the incident flux (Wilson and Patterson 1986, Jacques and Prahl 1987, Star *et al* 1988). The directional distribution of the light within the skin is not accurately known, although there is some evidence that the incident light is mainly forward scattered (Bruls and van der Leun 1984, Jacques and Prahl 1987).

The ectatic capillaries of a port wine stain, which occupy up to 8% of the dermis (Barsky *et al* 1980), will markedly affect the distribution of light within the dermis because they absorb a high fraction of the light (at 578 nm) incident upon their surfaces.

In our model we have not attempted to include the scattering within the skin. Our histological results (Walker *et al* 1989) suggest that the majority of damage to the ectatic capillaries occurs at their upper surface (that is the surface that faces the skin surface). Thus we have used a simple model of collimated light (of infinite width) that is incident, with uniform irradiance, on the upper surface of the vessel. This allows us to investigate the relative effects of vessel size, coagulation temperature and coagulation thickness on the illumination time and irradiance.

Because the vessels we have modelled are considerably larger than red blood cells, we may assume that there is a homogeneous distribution of haemoglobin within the vessels. With heating on a subsecond time scale, there is negligible heat loss through blood flow (Welch *et al* 1980). As a consequence of the above assumptions, we were able to model the blood vessel in two spatial dimensions by looking only at a transverse cross section of the vessel.

For short time scales, less than 10 ms, we were able to ignore the effect of heat conduction from the epidermis for ectatic vessels at the average depth (300 μm below the dermal–epidermal junction, van Gemert *et al* 1986).

Endothelial cells are 4–6 μm thick (Barsky *et al* 1980) and it is not known for certain what proportion of a cell needs to be thermally damaged for necrosis to occur. We have assumed that it is sufficient to model the coagulation thickness at the top of the vessel alone, because the endothelial cells tend to wind themselves in a helical fashion along the length of the blood vessel. We have modelled various coagulation thicknesses (0–9 μm).

The temperature required to coagulate the endothelial cells is also uncertain. Jacques and Prahl (1987) performed a number of experiments on thermal coagulation of mouse skin and found a threshold temperature range for coagulation of 60–70 °C. Barnes (1975) gives the temperature range at which 37% of illuminated egg white survives as 65–72 °C, but this is dependent on pulse width. Anderson and Parish (1981) and van Gemert *et al* (1986) based their models on a temperature for irreversible damage of 70 °C. We have modelled both 60 and 70 °C, and have found the treatment parameters that make these the maximium temperature that the endothelial cell will reach at a given coagulation thickness.

Finally, the blood will begin to vaporise above 100 °C, and once this temperature is reached, further energy input will result in more vaporisation rather than a higher temperature. We have not attempted to incorporate the details of this process into our numerical model.

2.2. The numerical model

The temperature, T, for any point (x,y) within the bounds of the model will vary according to time, t, depending on the light absorbed and the heat conducted to or from that point.

Neglecting scattering within the vessel, the rate at which energy is absorbed at any point (x,y) within the vessel depends exponentially on the length of blood $d(x,y)$ through which the light has travelled to reach that point. For our simple model $d(x,y)$ is the distance from the upper surface of the vessel (figure 1). This is a consequence of our simplification that collimated light of irradiance I_o is incident across the whole upper surface of the vessel. This light is incident for a time t_{illum}. Thus we have that the rate at which heat is absorbed per unit volume, H_{abs}, is given by

$$H_{\text{abs}} = \alpha I_o \exp[-\alpha d(x, y)] \tag{1}$$

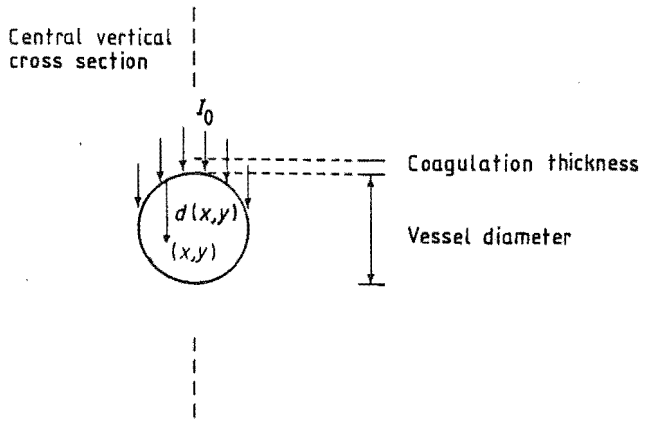

Figure 1. Our model of an ectatic blood vessel. The distance through which the light travels through the vessel before absorption is $d(x,y)$. The irradiance incident on the upper surface of the vessel is I_o and is assumed to be collimated and perpendicular to the skin surface. The distance above the vessel, on the central vertical axis, for which the coagulation temperature is just reached, is called the coagulation thickness.

inside the vessel and when $0 < t < t_{\text{illum}}$, and is zero otherwise.

The equation describing thermal conduction is

$$\rho C_v \frac{\partial T(x,y,t)}{\partial t} = H_{\text{abs}} + \eta \nabla^2 T(x,y,t). \tag{2}$$

This equation was solved by a finite difference method using a FORTRAN program run on a VAX 8350 computer. Simple first-order differences in a square grid were used for the derivatives. The grid was chosen to be 80×80. The vessel was situated at the centre of the grid and occupied, at most, 10% of the grid points. Increasing the distance of the square's boundary from the blood vessel by a factor of ten caused a less than 1% change in the resultant temperatures. Our program allowed us to compute a temperature profile for a vessel cross section at any time during or after illumination.

We required the temperature throughout the vessel to be always below 100 °C and designated the coagulation temperature (60 or 70 °C) at a designated coagulation thickness (0, 3, 6 or 9 μm). In order to obtain the illumination time for each of the eight conditions we interpolated between profiles of differing illumination time but with identical fluence. This provided us with the unique time that gave the required ratio between the increase in temperature at the coagulation thickness and the increase in temperature of the vessel. Once the illumination time was found a simple linear extrapolation of irradiance gave the coagulation temperature at the coagulation thickness. This procedure was repeated for a variety of vessel diameters (15, 30, 50, 80 and 100 μm).

We also used the fluence and illumination time of Tan and Stafford (1987) in our model in order to investigate the conditions which result from those treatment parameters that have produced purpura clinically.

3. Thermal profiles

3.1. Endothelial cell coagulation

Figure 2 shows the isotherms for a cross section of an 80 μm diameter vessel immediately after the end of the illumination time. In this case, the treatment parameters heated a point 6 μm above the vessel lumen (the coagulation thickness) to 70 °C (the coagulation temperature). Because of the nearly circular symmetry of a profile such as figure 2, we were able to represent its key elements by giving its vertical cross section. We then plotted the temperature along this central vertical cross section as a function of time. This is illustrated in figure 3, where we plotted the profile of an 80 μm diameter vessel illuminated with the treatment parameters that created the profile of figure 2, namely 410 Wcm^{-2} of light for 5.0 ms.

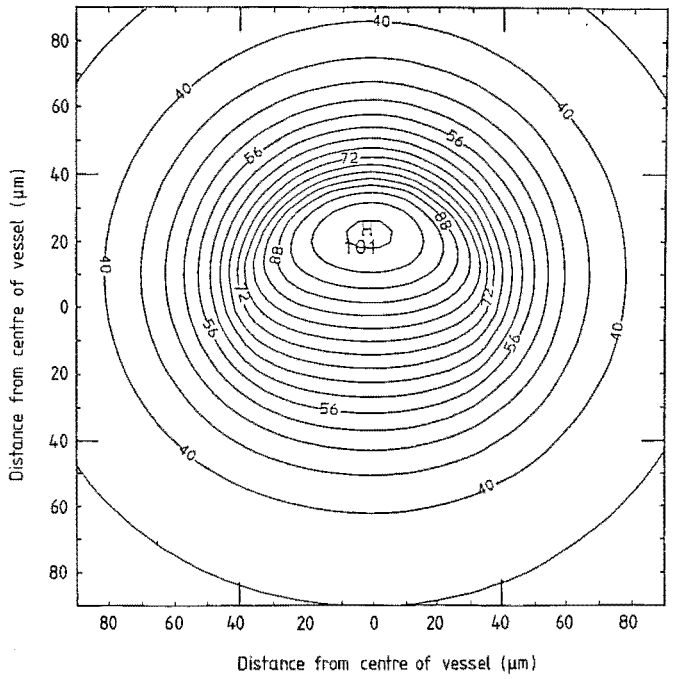

Figure 2. The thermal profile of the cross section of a 80 μm diameter vessel, illuminated from above, immediately after the end of its illumination time. The irradiance was 410 W cm^{-2}, the illumination time 5.0 ms, the coagulation thickness 6 μm and the coagulation temperature 70 °C. The isotherms are marked in degrees celsius and are at 4 °C intervals. The extent of the vessel is shown by the extended gradations on each of the four sides of the figure. The hottest part of the vessel is indicated by an H and is accompanied by the temperature at this point.

Table 3 gives the treatment parameters for 15, 30, 50, 80 and 100 μm diameter vessels. The 15 μm diameter vessel is much smaller than most ectatic vessels within port wine stains, but its inclusion illustrates how a low light absorption within, and a high heat loss from, a small vessel affect the treatment parameters. The treatment parameters are given for the assumed coagulation temperature (60 or 70 °C). The final variable is the coagulation thickness above the vessel lumen at which these temperatures are reached.

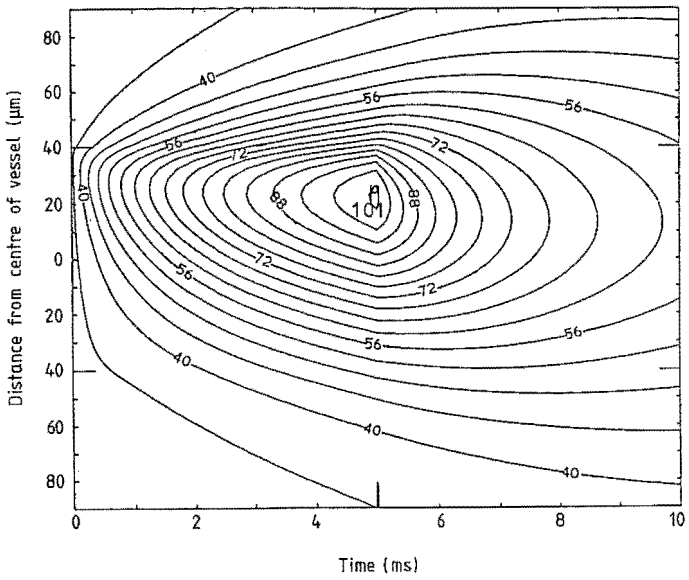

Figure 3. A time-dependent thermal profile of the same vessel under the same illumination and assumed coagulation conditions as figure 2. A vertical line through this figure at 5.0 ms is identical to a vertical line through the central axis of figure 2. The isotherms are again at 4 °C intervals. The extent of the vessel is shown by the extended gradations on each of the two vertical sides of the figure. The hottest part of the vessel is indicated by an H and is accompanied by the temperature at this point. The illumination time is indicated on the botttom axis of the figure by the extended gradation.

Table 3. Treatment parameters.

Vessel diameter (μm)	Temperature °C	Coagulation thickness (μm) 0 W cm^{-2}	ms	3 W cm^{-2}	ms	6 W cm^{-2}	ms	9 W cm^{-2}	ms
15	60	4400	0.4	3000	1.3	2800	2.0	2300	4.5
	70	3000	1.2	2300	4.3	2100	8.8	1800	22
30	60	4900	0.15	1400	1.0	980	2.0	760	4.0
	70	1300	1.1	780	4.0	740	5.9	640	11
50	60	5400	0.14	1200	1.0	800	2.0	550	3.8
	70	1200	1.0	570	3.8	520	5.5	420	10
80	60	6200	0.12	1800	0.50	950	1.3	700	2.0
	70	1100	0.90	480	3.5	410	5.0	350	7.3
100	60	6200	0.12	2200	0.42	1100	1.0	790	1.6
	70	1200	0.90	530	2.9	390	5.0	330	7.0

3.2. A purpuric profile

Tan and Stafford (1987) typically obtained purpura with a total fluence of 6–7 Jcm^{-2} incident on the skin. Loss of light from the beam will occur between the skin surface and the top of the vessel, both due to absorption by melanin in the epidermis and to scattering out of the beam. A figure of 70% will overestimate this loss, especially since scattering will give some increase in flux due to the mechanism discussed in §2.1. Figure 4 is the time-dependent thermal profile for a 50 μm diameter vessel illuminated in 360 μs

with 2.1 Jcm^{-2} of 577 nm light incident on the model vessel. The figure illustrates that even with this underestimated fluence, two thirds of the vessel reaches a temperature in excess of 100 °C. We have not numerically modelled the effect of the vaporisation that will result from heating the blood above 100 °C, so the computed thermal profile of figure 4 will not accurately reflect the situation after the central temperature reaches 100 °C. Instead of a continued temperature rise, rapid vaporisation will occur for as long as the haemoglobin continues to absorb the light. The associated pressure shock waves and large volume changes will breach the endothelial cell and thus give rise to purpura.

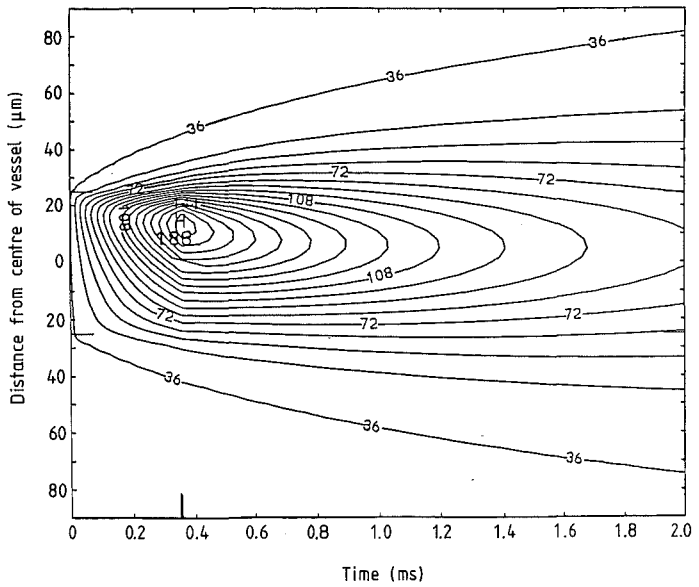

Figure 4. A time-dependent thermal profile of a 50 μm diameter vessel under purpura-producing illumination conditions, 2.1 J cm^{-2} in 0.36 ms incident on the vessel surface. Parts of the lumen reached the vaporisation temperature of 100 °C after less than half of the illumination period. The isotherms are at 9 °C intervals. The extent of the vessel is shown by the extended gradations on each of the two vertical sides of the figure. The hottest part of the vessel is indicated by an H and is accompanied by the temperature at this point. The illumination time is indicated on the bottom axis of the figure by the extended gradation.

4. Discussion

4.1. Coagulation conditions

It is important that the designated coagulation temperature be reached in a time short with respect to the characteristic time for heat conduction and with a minimum total energy dose, in order to minimise the amount of heating at a distance from the vessel. Excessive heating of dermal collagen or other cutaneous structures will accentuate undesirable side effects. However, the constraint of keeping the blood temperature below 100 °C gives a minimum illumination time.

As can be seen from table 3, for most port wine stain vessel sizes (30–80 μm diameter), the present model indicates that there is little difference in the ideal treatment parameters. The ideal treatment heats the endothelial cells to the designated temperature at the designated thickness in a minimum time. For example, for this range of vessel sizes, a point 6 μm from the lumen can be heated to 70 °C, with an irradiance at the vessel surface of between 740–410 Wcm^{-2} applied for 5.9–5.0 ms. (Note that there is considerable uncertainty about the irradiance required at the skin surface because of the uncertainty in the scattering parameters, and because of variations in melanin content.)

Heating endothelial cells to a lower critical temperature (60 °C compared with 70 °C) is better achieved by a higher irradiance and a shorter illumination time. Likewise a higher irradiance and a shorter illumination time are indicated for a smaller coagulation thickness. (This is because decreasing the coagulation thickness is equivalent to decreasing the coagulation temperature at the larger coagulation thickness.)

The ideal illumination time is shorter for larger vessels. The total energy (fluence) required decreases with increasing vessel size. The large vessels absorb more of the incident light and the heat conducts away more slowly than with the small vessels. Thus the coagulation time may be reached more quickly and with less total energy.

4.2. Purpura

Paul *et al* (1983) produced purpura in normal skin of volunteers using a 300 ns pulse from a dye laser tuned to 577 nm. The fluence at the skin surface was 2 J cm^{-2}.

A single red blood cell, when approximated as a 5 μm diameter sphere, has a thermal relaxation time of approximately 6 μs. That is the time the temperature of the sphere takes to fall to a point midway between its maximum temperature and the temperature of the cell's surroundings. If we assume that red blood cells occupy 45% of the blood by volume then to raise the temperature of this sphere to 100 °C, over an illumination time much shorter than the thermal relaxation time of the sphere, requires approximately 0.3 J cm^{-2} of yellow light. If we estimate that 30% of the light incident on the skin's surface reaches the vessel, then 2 J cm^{-2} of light incident on the skin surface (as used by Paul *et al* 1983) would vaporise about one eighth of the fluid within the cell. As we have discussed previously the assumed fluence incident on the cell is almost certainly an underestimate. The steam generated would most likely cause haemolysis. Nakagawa *et al* (1985) reported histological evidence of steam generation. Vaporisation within red blood cells would contribute to the vessel rupture reported by Nakagawa *et al* (1985) and Greenwald *et al* (1981). This rupture is the purpura which is seen as a dusky blue-grey colour a few minutes after illumination.

Purpura has also been reported with much longer pulses (360 μs; Tan and Stafford 1987, Garden *et al* 1988) where the thermal relaxation time of the red blood cells suggests that an isolated cell would not reach 100 °C. However, the red blood cells are not thermally isolated on this time scale. When we modelled these longer pulses, we found that the temperature of the entire lumen exceeds 100 °C, and we must assume that the energy that is incident after this temperature is reached causes some vaporisation of the blood. The vaporisation and associated shock waves would be expected to lead to the extravasation of blood which is the cause of purpura. However, there is one anomaly in the literature: Garden *et al* (1988) state that their histologies showed no extravasation of blood at purpura threshold doses for pulse durations from 1.5 to 360 μs. At higher than purpura threshold doses, they reported that there was

no extravasation of red blood cells for the longer pulse durations only. Note that the absence of extravasation is contrary to the standard definition of purpura (e.g. Miller and Keane 1987).

Clinical results have been improved by increasing the pulse lengths from 300 ns (Paul *et al* 1983) to 360 μs (Garden *et al* 1988).

Heating over a short time scale results in a rapid rise in temperature of the blood within the lumen. We have shown that, with such heating, the endothelial cells cannot be coagulated by the conducted energy without the blood vaporising. It would seem clinically (Garden *et al* 1988) that the irradiance must be precisely the correct amount to cause the kind of damage that results in a satisfactory treatment. If too low an irradiance is used, there will not be sufficient heat conducted in the short illumination time in order to raise the endothelial cell temperature significantly. If too high an irradiance is used, too much vapourisation occurs. Garden *et al* (1988) found it necessary to determine the irradiance for each individual patient empirically. The procedure used is to produce purpura on the volar forearm within 5 minutes of exposure and then to use twice this irradiance on the port wine stain.

5. Summary

We have numerically modelled the absorption of yellow (577 or 578 nm) light by ectatic blood vessels. Our premise, as with all previous models of the treatment of port wine stains, is that causing part of some of the endothelial cells to coagulate is sufficient to damage the vessel irreversibly. The physical requirements for this coagulation are not known precisely. We modelled the coagulation temperature as 60 or 70 °C and the coagulation thickness above the top of the vessel lumen as between 0 and 9 μm. For the blanching end point, vaporisation of the blood was avoided by finding the values of the parameters (illumination time and irradiance) that avoid heating the blood above 100 °C, while attaining the designated coagulation temperature and thickness.

The range of coagulation temperatures and coagulation thicknesses produced a wide range of treatment parameters for each vessel size. The choice of coagulation temperature had the most marked effect, with the ideal illumination time being about five times longer at 70 °C than at 60 °C.

Each vessel size required different treatment parameters. However, for vessels within the average size for port wine stains (30 to 80 μm), the variation in these parameters was not significant compared with the uncertainties in the coagulation parameters.

The purpura used as an end point by some clinicians is most likely the result of vaporisation of blood caused by heating over a short time scale. With short pulses, a small variation in the irradiance will lead to large variations in the damage done to the endothelial cells.

Acknowledgments

J W Pickering was supported by a fellowship provided by the Medical Research Council of New Zealand.

Résumé

Calcul des distributions de température autour de capillaires dilatés exposés à de la lumière laser jaune (578 nm).

Les auteurs ont effectuè une modèlisation numériques des effets thermiques de l'illumination en jaune (577 ou 578 nm) des vaisseaux sanguins dilatés de taches de vin. Ils ont étudié l'influence des paramètres du traitement au laser, l'éclairement énergétique et la durée de l'illumination sur l'importance de la coagulation (épaisseur de la coagulation) des cellules endothéliales des vaisseaux dilatés. Ils ont supposé que cette coagulation dépend de l'échauffement des cellules jusqu'à une température critique (température de coagulation). Ils ont effectué un ajustement itératif des paramétres du traitement de maniére à ce que les vaisseaux du modéle atteignent une température maximale qui n'excéde pas le point d'ébulition du sang. Considérant la gamme probable de variation de la température de coagulation, de l'épaisseur de coagulation, et de la taille des vaisseaux, on en a déduit que la température de coagulation est le paramétre qui conditionne le plus les paramétres du traitement. Les variations de l'épaisseur de coagulation ont une influence moindre, le diamétre des vaisseaux dilatés (typiquement dans la gamme de diamétres compris entre 30 et 80 μm) ayant l'influence la plus faible. Les paramétres de traitement qui sont reconnus cliniquement comme générateurs de purpura (par exemple 6–7 J cm^{-2} en 360 μs) ont également été étudiés. Le purpura observé par quelques expérimentateurs utilisant des lasers à colorant pulsés est le plus probablement lié à la vaporisation du sang conduisant à la rupture du vaisseau. Les auteurs concluent que, afin de réaliser la coagulation avec ces lasers à impulsions bréves, le choix de l'éclairement énergétique est critique.

Zusammenfassung

Berechnete Temperaturverteilungen um ektatische Kapillaren bestrahlt mit gelbem (578 nm) Laserlicht.

Die thermischen Effekte gelber (577 oder 578 nm) Laserlichtbestrahlung von ektatischen Blutgefäßen in Feuermalen wurden numerisch modelliert. Der Einfluß der Bestrahlungsstärke und der Bestrahlungszeit bei der Laserbehandlung auf die Stärke der Koagulation (Koagulationsdicke) endothelialer Zellen von ektatischen Blutgefäßen wurde untersucht. Dabei wurde angenommen, daß diese Koagulation abhängig ist von der Erwärmung der Zellen auf eine kritische Temperatur (Koagulationstemperatur). Die Behandlungsparameter wurden schrittweise so angepaßt, daß di Modell-Blutgefäße eine maximale Temperatur unterhalb des Siedepunktes für Blut hatten. Unter Annahme einer gewissen Variationsbreite für die Koagulationstemperatur, die Koagulationsdicke und die Gefäßgröße, stellte sich heraus, daß die Koagulationstemperatur den größten Einfluß auf die Behandlungsparameter hatte. Schwankungen der Koagulationsdicke hatten weniger Einfluß und der Durchmesser der ektatischen Gefäße (typischerweise im Bereich 30–80 μm) hatte am wenigsten Einfluß. Die Behandlungsparameter (z.B. 6–7 J cm^{-2} in 360 μs), bei denen klinisch Purpura festgestellt wurden, wurden ebenfalls untersucht. Die Purpura, die bei einigen Beschäftigten, die mit gepulsten Dyelasern arbeiten festgestellt wurden, sind wahrscheinlich das Ergebnis der Verdampfung von Blut, was zu einer Ruptur der Gefäße führt. Es wird gefolgert, daß, um mit diesen kurzen Laserpulsen eine Koagulation zu erreichen, die Wahl der Bestrahlungsstärke kritisch ist.

References

Anderson R R and Parish J A 1981 Microvasculature can be selectively damaged using dye lasers *Lasers Surg. Med.* **1** 263–76

Barnes F 1975 Applications of lasers to biology and medicine *Proc. IEEE* **63** 1269–78

Barsky S H, Rosen S, Geer D E and Noe J M 1980 The nature and evolution of port wine stains: A computer assisted study *J. Invest. Dermatol.* **74** 154–7

Bruls W A G and van der Leun J C 1984 Forward scattering properties of human epidermal layers *Photochem. Photobiol.* **40** 231–42

Carruth J A S and McKenzie A L 1986 *Medical Lasers* (Bristol: Hilger)

Cotterill J A 1986 Preliminary results following treatment of vascular lesions of the skin using a continuous wave tunable dye laser which emits at 577 nm *Clin. Exp. Dermatol.* **11** 628–35

Garden J M, Polla L L and Tan O T 1988 The treatment of port-wine stains by the pulsed dye laser *Arch. Dermatol.* **124** 889–96

Greenwald J, Rosen S, Anderson R R, Harrist T, MacFarland F, Noe J and Parrish J A 1981 Comparative histological studies of the tunable dye (at 577 nm) laser and argon laser: The specific vascular effects of the dye laser *J. Invest. Dermatol.* **77** 305–10

Jacques S L and Prahl S A 1987 Modelling optical and thermal distributions in tissue during laser irradiation *Lasers Surg. Med.* **6** 494–503

Lahaye C T W and van Gemert M J C 1985 Optimal laser parameters for port wine stain therapy: a theoretical approach *Phys. Med. Biol.* **30** 573–87

Miller B F and Keane C B (eds) 1987 *Encyclopedia and Dictionary of Medicine Nursing and Allied Health* (Philadelphia: Saunders)

Morelli J G, Tan O T, Garden J, Margolis R, Seki Y, Boll J, Carney J M, Anderson R R, Furumoto H and Parish J A 1986 Tunable dye laser (577 nm) treatment of port wine stains *Lasers Surg. Med.* **6** 94–9

Nakagawa H, Tan O T and Parish J A 1985 Ultrastructural changes in human skin after exposure to a pulsed laser *J. Invest. Dermatol.* **84** 396–400

Noe J M, Barsky S H, Geer D E and Rosen S 1980 Port wine stains and the response to argon laser therapy: Successful treatment and the predicative role of color age and biopsy *Plast. Reconstr. Surg.* **1** 130–5

Ohmori S and Huang C 1981 Recent progress in the treatment of portwine staining by argon laser *Br. J. Plast. Surg.* **34** 249–57

Paul B S, Anderson R R, Jarve J and Parish J A 1983 The effect of temperature and other factors on selective microvascular damage caused by pulsed dye laser *J. Invest. Dermatol.* **81** 333–6

Star W M, Marijnissen S P A and van Gemert M J C 1988 Light dosimetry in optical phantoms and in tissues: I. Multiple flux and transport theory *Phys. Med. Biol.* **33** 437–54

Tan O T, Carney J M, Margolis R, Seki Y, Boll J, Anderson R R and Parish J A 1986 Histological responses of port wine stains treated by argon, carbon dioxide and tunable dye lasers *Arch. Dermatol.* **122** 1016–22

Tan O T and Stafford T J 1987 Treatment of port wine stains at 577 nm: Clinical results *Med. Instrum.* **21** 218–21

van Gemert M J C, de Kleijn W J A and Hulsbergen Henning J P 1982 Temperature behaviour of a model port-wine stain during argon laser coagulation *Phys. Med. Biol.* **27** 1089–104

van Gemert M J C, Welch A J and Amin A P 1986 Is there an optimal laser treatment for port wine stains? *Lasers Surg. Med.* **6** 76–83

Walker E P, Butler P H, Pickering J W, Day W A, Fraser R and van Halewyn C N 1989 Histology of port wine stains after copper vapour laser treatment *Br. J. Dermatol.* In press

Welch A J, Wissler E H and Priebe L A 1980 Significance of blood flow in calculations of temperature in laser irradiated tissue *IEEE Trans. Biomed. Eng.* **BME-27** 164–6

Wilson B C and Patterson M S 1986 The physics of photodynamic therapy *Phys. Med. Biol.* **31** 327–60

Appendix D PICKERING ET AL. 1990A

Pickering JW, Butler PH, Ring BJ, and Walker EP, (1990a); *Copper vapour laser treatment of port wine stains: a patient questionnaire.*, Lasers in Medical Science, accepted October 1989.

This paper has yet to be printed and is presented here in the style of Lasers in Medical Science.

Copper Vapour Laser Treatment of Port Wine Stains: A Patient Questionnaire.

JOHN W. PICKERING, PHILIP H. BUTLER, BRENDAN J. RING, E. PETER WALKER[a]

Physics Department, University of Canterbury, Christchurch, New Zealand

[a] *Milford Chambers, 249 Papanui Road, Christchurch, New Zealand*

Abstract. Two hundred and forty two questionnaires were sent to patients who had undergone treatment with yellow light (578 nm) from a copper vapour laser for a port wine stain (PWS), for facial telangiectasia (FT), or for a spider naevus (SN). Seventy three percent of the patients replied. The questionnaire covered the social implications of the lesion, the physical appearance of the lesion after treatment and the patient's judgement of how the treatment has affected them.
83% PWS, 74% FT and 81% SN patients felt there had been an improvement in their appearance compared with 2.5% PWS, 14% FT, and 7.5% SN patients who felt that their appearance had changed for the worse. The overall impression of the treatment was also very positive, especially with PWS patients, 91% would recommend the treatment to others, 84% would have the treatment again and 60% indicated their feelings regarding their overall treatment and the effect it had on their lives was very good.

INTRODUCTION

Since the mid 1970's the argon ion laser has been established as the treatment of choice for port wine stains and other vascular malformations (1-5). However, recently yellow light at 577 or 578 nm has been shown through histological study (6-9), clinical trials (10-12), and theoretical argument (13,14) to be superior to the blue/green 488-514 nm light from the argon laser. The reasons for the preferred use of yellow light is twofold. First, less light is absorbed by the melanin at 577/578 nm than at 488-514 nm and consequently there is less epidermal heating. Second, more light is absorbed by haemoglobin at 577/578 nm than at 514 nm. This results in cutaneous damage that is specific to the ectatic blood vessels, rather than widespread damage throughout the epidermis and upper dermis. Yellow light may be produced by either a pulsed dye (6-8,11,12), a continuous wave dye (10), or a copper vapour (9) laser. Since 1986 we have conducted over 1300 vascular lesion treatment sessions with yellow (578 nm) light from a copper vapour laser. This laser is distinct from

both kinds of dye lasers as it produces a rapid train of short low energy pulses rather than a single high energy pulse or a continuous wave.

As these lesions are potential causes of psychological morbidity, the success of the treatment can not be assessed entirely by physical measurements such as change in lesion size or colour. The patient's own assessment of the outcome of the treatment is very important. Their assessment depends in part on their self perception before and after the treatment and on their expectations for the treatment. Dixon et al (15) used a patient questionnaire in 1984 to assess the argon laser treatment of port wine stains, decorative tattoos and essential telangiectasia of the legs. This paper presents the results of a similar questionnaire mailed to patients treated with the copper vapour laser for either a port wine stain (PWS), facial telangiectasia (FT) or spider naevus (SN). We were interested in obtaining a broad perspective of the treatment from the patients and rather than assess patients only after they had completed their treatment we chose to assess patients at a time when some had completed their treatments and some were part way through their course of treatment.

Since the inception of the questionnaire we have treated additional patients. The clinical results of 236 PWS patients have undergone analysis and a paper detailing these results is in preparation.

MATERIALS AND METHOD

We distributed a similar questionnaire to that of Dixon et al (15). Thirty two questions were asked covering :

- Patient's perception of how they and others regard the lesion.
- The effect the lesion has had on their social interactions.
- Reasons for entering therapy.
- Pain and healing processes after their first and after their most recent treatment.
- Present physical colour and texture of the lesion.
- Satisfaction with the treatment.
- The effect the treatment has had on their social interactions.

Most questions were constructed with a bipolar scale allowing a choice of at least four answers. We collated the responses to these questions as numerical information on a data base (Superbase™ Professional on an Amiga™ B2000). From this information a mean and standard deviation were calculated separately for four age

Table 1: Age groups of questionnaire responders.

Age	Class	*% in each lesion group* PWS	FT	SN
< 12	Children	19	0	11
12-20	Adolescent	19	9	30
21-50	Adult	58	64	50
> 50	Older Adult	4	27	9

groups (see Table 1) and collectively over all the age groups for each question. There were also a number of questions that requested a written response.

A total of 242 patients were sent questionnaires. Of these 143 were PWS, 58 FT and 41 SN. Initial non-responders were sent another questionnaire after three weeks. Replies were received from 79% PWS, 59% FT and 66% SN patients. For young patients (under 12 years) the parents were asked to assist in answering the questionnaire. The response as a function of age group is given by Table 1. The distribution of ages in this table is very similar to the distribution of ages of all our patients. Females comprised 65% of PWS, 83% of FT and 90% of SN patients. Only 5% of the PWS who replied to the questionnaire had completed their course of treatment and been discharged.

The copper vapour laser used in all cases was a Quentron™ QM91C which produces a train of short, 50 ns, pulses at a rate of 16 kHz. PWS and FT patients were treated using a scanning strategy (9) with a 1 mm diameter quartz optical fibre which produced a 1.3 mm diamater spot on the skin when held 2 mm above the skin surface. The strategy was to move the spot back and forth in single scans which do not overlap. There results a small gap (less than 0.5 mm) between each scan. Preferably these scans are approximately parallel to Langer's lines. On second and subsequent treatments (at least three months apart) the scans were such as to treat any gaps left by the previous treatment. The rate of scan was such as to produce minimal blanching (the point at which the skin just appears to blanch). Typically the fibre was scanned at a rate of 3 to 10 s/cm^2 with a dose of 20 to 30 J/cm^2. A full course of treatment involves three to eight treatments to the same area for PWS and one to three treatments for FT. Children or patients with lesions greater than 60 cm^2 in area are treated under general anaesthetic. Otherwise a non-vasoconstricting local anaesthetic, 2% plain Xylocaine™ is used. Normally the entire lesion is treated during each treatment session except in the cases of lesions that cover a large portion of the body. In these cases, we treat only those areas that the patient wishes to be treated. Usually this is the face and neck down to the clavical and possibly the arms up to where a short sleeved shirt may cover the lesion.

SN were treated by initially blanching the central "body" of the naevus. This usually required less than one second of illumination with three or more watts of

light. When required this was followed by treating the "legs" individually. Often when the SN were very small, we used no anaesthetic because such a short illumination time was required that the discomfort associated with the light was comparable with that of the local anaesethetic injection.

Prior to receiving the questionnaire all patients had recieved at least one treatment to the entire area of lesion that they wished to be treated (i.e. excluding any test treatments). Furthermore, if they had received only one treatment, they were sent a questionnaire only if they had sufficient time (taken as three months after treatment) in which to evaluate their response to treatment.

RESULTS

Perception of appearance and social implications

The first four questions were concerned with how patients and other people regarded their lesion. The two categories were noticeability and unattractiveness.

The mean patient response and one standard deviation each side of the mean for each of the three lesion groups is indicated on each diagram. For the purpose of statistical analysis the descriptive responses on each questionnaire were also numbered. The responses for noticeability are:

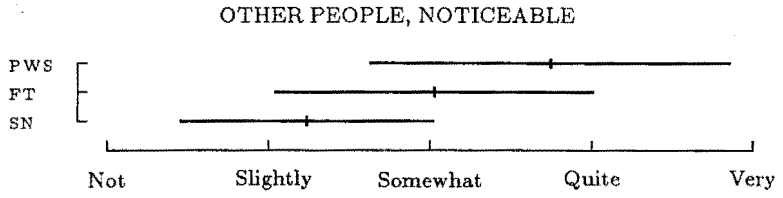

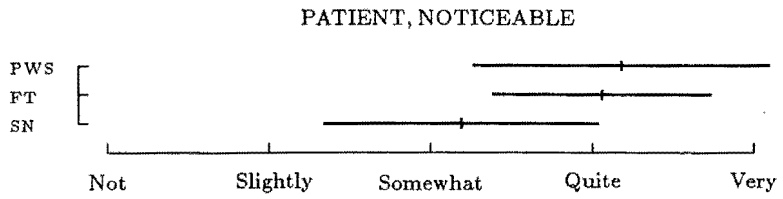

These results are consistent with the size and colour of the lesion. The SN being the smallest lesion, whilst the PWS is often larger and nearly always more red that FT. The extent of FT is also often dependent on room and body temperature conditions.

The responses for unattractiveness were similar, but with the lesions less unattractive than they were noticeable. The difference in the statistical means was half to one response unit.

Patients were asked how the lesion affected their education, employment, and social relationships with members of the same gender and the opposite gender. For most patients the lesion was at most a very slight disadvantage in each of the above situations except for relationships with members of the opposite gender.

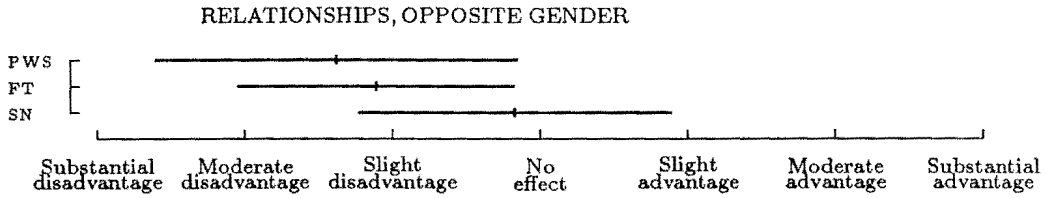

The PWS and FT patients found their lesion to be more of a disadvantage than did the SN patients. This again may reflect on the relative sizes of the lesions with SN much smaller than most PWS or FT. This also correlates with the patients' perception of the effect of their lesion on life in general.

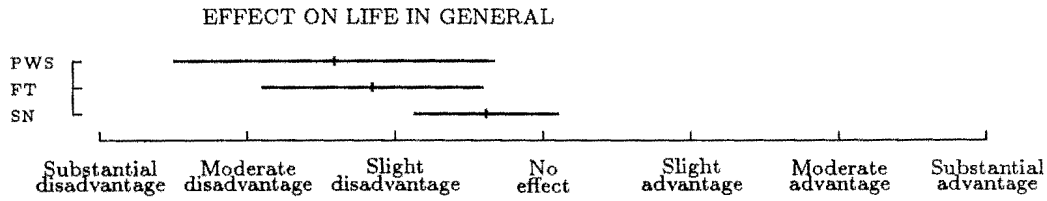

Reasons for undertaking treatment

The question asking for the patients reason for undertaking treatment was open-ended. The four themes :

- embarrassment in public.
- personal unattractiveness.
- self-consciousness.
- difficulties with makeup.

occured most often. Indeed nearly 40% of PWS patients stated a desire to avoid public embarrassment. Personal unattractiveness and self consciousness were the other two primary reasons. With FT all four of the listed reasons were stated equally as often. However for SN the principle reason was difficulties with makeup (40%).

Although a large number of patients indicated that the lesion hindered their relationships with members of the opposite gender, only five PWS and one FT patient indicated that a desire to improve personal relationships was a reason for undertaking treatment.

The treatment

Patients assessed their first and their most recent (at least three months previous to receiving their questionnaire) treatments with respect to pain and the healing cycle.

The most pain was felt during anaesthetic injections, with 70% of FT and SN, and 59% of PWS registering mild or moderate pain. Some pain was also felt during the application of the laser light.

This pain was normally the result of the failure of the local anaesthetic to sufficiently anaesthetise small parts of the lesion (often near the periphery of the lesion). Any patient's indication of pain due to the laser was rectified by additional local anaesthetic before continuing treatment. Some SN were treated without anaesthetic when the lesion was small. During the healing process, from immediately after the treatment to beyond four weeks, there was very little pain reported. What pain was reported was described as akin to severe sunburn and lasted for the first 20 to 30 minutes after the anaesthetic wore off. There was also very little difference in the patients' perception of pain, between the first and most recent treatment.

Immediately after treatment the skin feels normal to the touch. We dress the skin with a soothing burn cream. PWS and FT patients experienced a mild to moderate amount of blistering, scabs and discharge. Scab formation was reported as being slightly more severe than the other reactions. Normally the blisters appear 6-12 hours after the treatment and are followed by some discharge. Additionally, when the treatment is near an eye the eye may swell up over the first 24 hours post treatment. The discharge and swollen eyes last for two or three days. After three days, the treated area drys and scabs form. These separate off after 10 days to two weeks. In addition 9 PWS and 3 FT patients complained of swelling and 6 PWS of bleeding and grave itching. Only 3 PWS and 2 FT indicated any scar formation had taken place. This is consistent with our records of 236 PWS (including those surveyed) which indicate an incidence of scarring of $3.5 \pm 1.4\%$ (mean$\pm$sd) per patient. We define a scar clinically as the presence of a permanent hypertrophic or atrophic mark of any size.

Colour and texture

We asked questions concerning the present texture and size of the treated area.

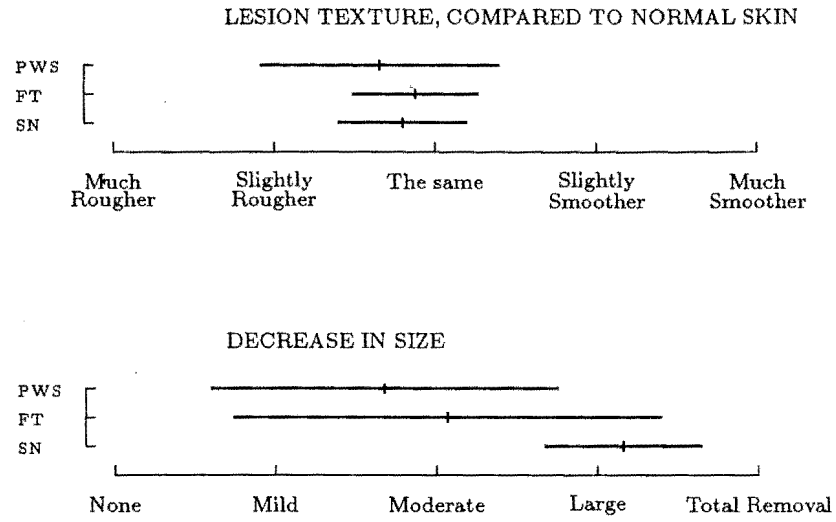

Our clinical measurements of the PWS area treated indicate a percentage reduction in area that is greatest after the first treatment and is on average 20±19% (mean±sd) for the first treatment. Normally the lesion resolves first at its edge.

Some mild striped appearance on PWS and FT may be visible after the first one or two treatments due to the scanning technique. Especially susceptible are FT because of their normally superficial nature. The stripes in these cases are the result of complete resolution of the lesion (to the extent of looking like normal skin) with the first treatment. Thus the stripes are the difference between treated normal looking skin and the untreated gaps between the treated skin. We usually find that the striped appearance disappears after the second or third treatment. FT patients indicated that the striping was only mild and PWS even less mild.

Most patients experience some browning during the healing cycle which normally takes three to four months to resolve. However, when asked if the treated area was the colour of normal skin, or if it was paler or browner than normal skin, all three groups gave an even preference for normal or paler than normal colour. Less than 25% indicating browner than normal. Our clinical results give an incidence of hyperpigmentation (or permanent browning) of 1.4±0.5%.

Changed appearance

All groups felt their appearance had improved.

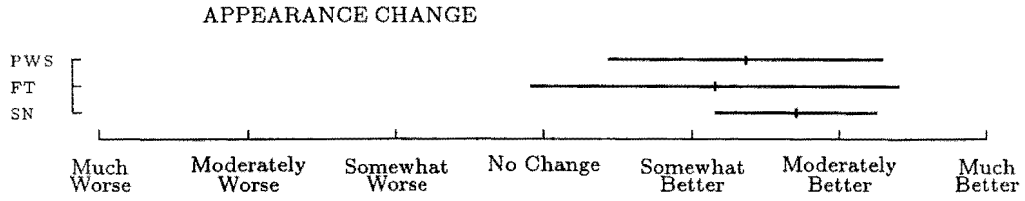

Only two patients (both FT) indicated a much or moderately worse change, while 3 FT and 4 PWS a somewhat worse change. Of these 5 FT, 1 returned for futher treatment and only two had negative overall feelings towards the treatment (see section Overall). However 14 (45%) of FT indicated a much or moderately better change. 3 of the 4 PWS probably or definitely would recommend the treatment to others, and the fourth PWS definitely would not recommend the treatment and was the only PWS to have a negative response to the treatment overall (section Overall).

Most patients also expressed satisfaction with the present appearance.

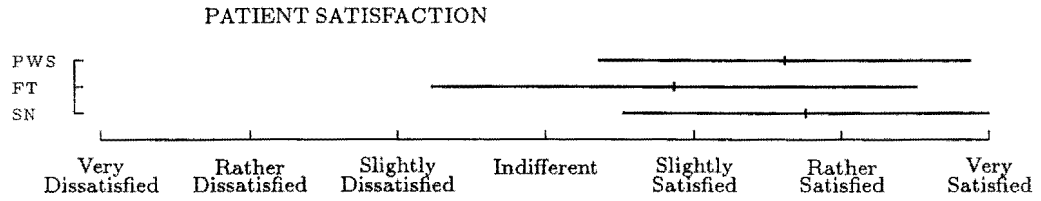

The patients reported that their family and friends had a similar degree of satisfaction with the treated area. Patients indicated that these results were what they had expected from the treatment.

All groups indicated a slight improvement in their social interactions with both family and friends and with strangers. Similarly they felt their self esteem, consciousness and acceptance, by themselves and by others, had all improved slightly.

When asked in an open ended question if there had been any change in wardrobe or makeup due to the treatment, 30% of FT, 25% of SN and 25% of PWS responded that they now used no or less makeup. In addition 15% of PWS patients said they were less restricted in their choice of hairstyle and clothing. We should remind the reader that at the time of the questionnaire, only 5% of the PWS patients who responded had completed their course of treatment to their satisfaction and been discharged, and that there was a two to one ratio of females to males treated.

Overall

PWS patients were the most likely to recommend the treatment to someone else (91%), and a number stated they already had.

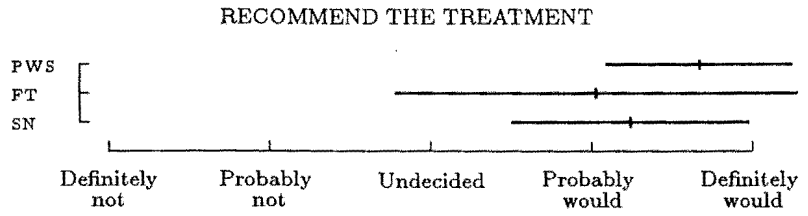

Similarly patients in retrospect would still have undergone treatment. 84% of PWS, 64% of FT and 81% of SN said they probably or definitely would.

As a final assesment of the treatment, patients were asked to express how they felt about the treatment taking into account all the physical and social affects the treatment had had upon them.

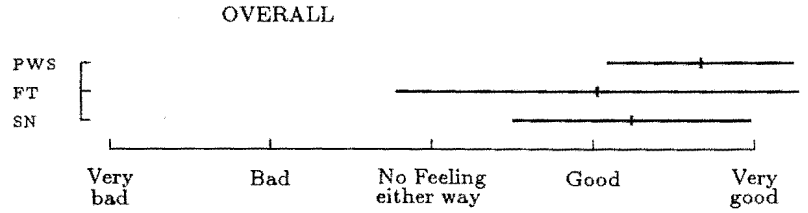

Only 2% of PWS, 5% of FT and 12% of SN answered negatively compared to 60% of PWS, 48% of FT and 39% of SN who answered very good.

DISCUSSION

Statistical reliability

The questionnaire was answered by 79% PWS, 59% FT, and 66% SN of those sent the questionnaire. Of the total of 67 non responders 17 questionnaires were returned "address unknown", and the other 50 chose not to answer the questionnaire for one reason or other. Therefore, we need to give an estimate of the accuracy of the means presented in each of the above diagrams. If we take the largest standard deviation of any question for each of the patient classes and calculate a 95% confidence interval for the means, based on sampling statistics without replacement (16), we have for PWS mean$\pm$0.15 of a division, for FT mean$\pm$0.40 of a division, and for SN mean$\pm$0.87 of a division.

The psychology of PWS

Most patients indicated that they found their lesion unattractive and that it had to some degree affected their social relationships. A recent and much more comprehensive psychological analysis of patients with PWS by Lanigen and Cotterill (17) indicated that patients suffer from psychological distress which is not apparent in their normal social interactions. Similarly to our results they found that pateints had difficulties with interpersonal relationships, particularly with members of the opposite gender. An interesting aspect of their survey was that older people were often more affected by their lesion than younger people, suggesting that there is little acceptance of the problem with increasing age.

Effect of age on PWS responses

Children (under 12) regarded their lesion as less noticeable and less unattractive than did the adults ($p < 0.01$). They also responded with more pain during the first 24 hours and a slightly rougher skin than the adults ($p < 0.05$). Other than this there was no significant difference between the responses of the differing age groups.

Comparison with argon laser

Our patients responded in a very similar manner to the questions concerning noticibility and unattractiveness as did the argon laser patients of Dixon et al. (15). In addition, Dixon et al. patients found similar hinderences with their social relationships and similar reasons for undertaking treatment. We conclude that the New Zealanders with PWS are similarly affected by their lesion as those in Utah.

The mean results for appearance, satisfaction, self perception after treatment and overall feelings were all more positive for our copper laser patients compared to Dixon et al's argon laser patients (which had all completed a treatment course). Dixon et al. do not present their data on standard deviations. However all of the Dixon et al. means were within one standard deviation of our copper laser means.

Our clinical experience has been that we are often able to remove a significant proportion of the lesion without adverse side efffects. Of all those patients who have now undergone 4 or more treatment sessions (approximately 100 patients); 21% have had removed greater than 70% of the lesion, 10% have had removed less than 30% of the lesion with at most only a slight colour change to the remainder of the lesion, whilst the remianing 69% of the patients have had an intermediate result and are still improving. Furthermore, 11% of those patients who are yet to have 4 treatments greater than 70% of the lesion has been removed. Our rate of scarring (3.5%), hypopigmentation and hypopigmentation (1.4% each) is low in comparisson to some argon laser treatments (2,4,15).

PWS, FT and SN

All groups responded with a positive overall judgement. The simplicity of treating the SN was probably a major factor in its positive overall result.

The PWS patients felt their lesion was more noticeable, more unattractive and more of a social hindrance than did FT or SN and as a consequence they had the "most to gain" from the treatment. There was little indication of an age dependent response to the questionnaire with PWS. Most patients felt the treatment was as expected and were satisfied with the result.

ACKNOWLEDGEMENTS

We wish to thank Dr John A. Dixon of Department of Surgery, Health Sciences Center, University of Utah, Salt Lake City for providing us with a copy of his questionnaire. John W. Pickering is supported by a postgraduate graduate scholarship from the Medical Research Council of New Zealand. Financial support has also been provided by Medical Laser Developments.

REFERENCES

1. Goldman L, Dreffer R, Rockwell RJ, Perry E. Treatment of Portwine Marks by an Argon Laser. *J Dermatol Surg* 1976, **2**:385-388
2. Cosman B. Experience in the Argon Laser Therapy of Port Wine Stains.*Plast Reconstr Surg* 1980, **65**:119-129
3. Arndt KA. Treatment technics in argon laser therapy.*J Am. Acad Dermatol* 1984, **11**:90-97
4. Touquet VLR and Carruth JAS. Review of the Treatment of Port Wine Stains with the Argon Laser.*Lasers Surg Med* 1984, **4**:191-199
5. Apfelberg DB, Smith T, Maser MR, Lash H and White DN. Dot or Pontillistic Method for Improvement in Results of Hypertrophic Scarring in the Argon Laser Treatment of Portwine Hemangiomas. *Lasers Surg Med* 1987, **6**:552-558
6. Anderson RR and Parish JA. Microvasculature can be selectively damaged using dye lasers. *Lasers Surg Med* 1981, **1**:263-276
7. Greenwald J, Rosen S, Anderson RR, Harrist T, Macfarland F, Noe J and Parish JA. Comparitive Histological Studies of the tunable Dye (at 577nm) laser and Argon Laser: The Specific Vascular Effects of the Dye Laser. *J Invest Dermatol* 1981, **77**:305-310
8. Tan OT, Carney M, Margolis R, Seki Y, Boll J, Anderson RR and Parish JA. Histological responses of Port-wine Stains treated by Argon , Carbon Dioxide, and Tunable Dye lasers. *Arch Dermatol* 1986, **122**:1016-1022
9. Walker EP, Butler PH, Pickering JW, Day WA, Fraser R and van Halewyn CN. Histology of port wine stains after copper vapour laser treatment. *Br J Dermatol.* 1989, **121**:216-23

10. Cotterill JA. Preliminary results following treatment of vascular lesions of the skin using a continuous wave tunable dye laser which emits at 577nm. *Clin Expt Dermatol* 1986, **11**:628-635

11. Tan OT and Stafford JS. Treatment of Port-Wine Stains at 577nm: *Clinical Results Med Instru* 1987, **21**:218-221

12. Garden JM, Polla LL, Tan OT. The Treatment of Port-wine Stains by the Pulsed Dye Laser *Arch Dermatol* 1988, **124**:889-896

13. Anderson RR and Parish JA. The optics of human skin. *J Invest Dermatol*, 1981, **77**:13-9

14. Lahaye CTW and van Gemert MJC. Optimal laser parameters for port wine stain therapy: a theoretical approach. *Phys Med Biol*, 1985,**30**:573-87

15. Dixon JA. Patient's Evaluation of Argon Laser Therapy of Port Wine Stain, Decorative Tattoo, and Essential Telangiectasia. *Lasers Surg Med* 1976, **4**:181-190.

16. Winkler RL and Hays WL. *Statistics* (2nd ed.). 1975, Holt, Rinehart and Winston, New York

17. Lanigen SW and Cotterill JA. Psychological disabilities amongst patients with port wine stains. *Br J Dermatol* 1989, **121**:209-15

Key words:

Copper vapour laser, Argon ion laser, port wine stains, telangiectasia, spider naevi, questionnaire.

Appendix E PICKERING ET AL. 1990B

Pickering JW, Walker E,P Butler PH, and van Halewyn CN, (1990b); *Copper vapour laser treatment of port wine stains and other vascular malformations.*, British Journal of Plastic Surgery, accepted November 1989.

This paper is yet to be printed and is presented here in the style of the British Journal of Plastic Surgery.

Copper vapour laser treatment of port wine stains and other vascular malformations

J. W. PICKERING[1], E. P. WALKER[2], P. H. BUTLER[1], C. N. VAN HALEWYN[3]

[1]*Physics Department, University of Canterbury, Christchurch, New Zealand.*
[2]*Milford Chambers, 249 Papanui Road, Christchurch, New Zealand.*
[3]*Physics Department, University of Canterbury, Christchurch, New Zealand.*
Present address Banque Indosuez, P.O.Box 10-112, Wellington, New Zealand.

Summary–Over a two year period more than 1350 treatment sessions have been conducted with yellow 578 nm light from a copper vapour laser on a variety of vascular malformations. Of these sessions half were of port wine stains, from 297 patients.
The light is applied by scanning a 1mm optical fibre approximately 2mm above the lesion along the lines of Langer. We use a maximum scan rate of 3 s/cm^2, which is the highest rate at which minimal blanching can be produced. Up to 6.5 watts of light has been used, and a typical energy fluence is 20 to 30 J/cm^2.
Topical melanin suppressing creams are used before and after treatment, in order to maximise the effectiveness of the treatment. Non-vasoconstricting anaesthetics are always used. Repeat treatments are three months apart.
The scan rate we used was directly correlated with the light intensity. The degree to which the colour of the port wine stains lightened after the first treatment was also well correlated with the scan rate ($p < 0.0005$). The faster the scan rate, the greater the colour reduction. This provides some supporting evidence for the short illumination time that theoretical models have indicated as "ideal".
The lightening was more marked for patients whose lesion colour was initially dark ($p < 0.0005$). Those whose skin had a high melanin content, (Maori, Polynesian and Asian) responded more slowly than others.
Thirty six patients have had a greater than 70% reduction in the size of their lesions after an average of four treatments. Ten patients have responded poorly after at least four treatments (10% of all those who have had four or more treatments). The occurrence of scarring, hyperpigmentation and hypopigmentation was low in comparison to previous reports of the green light results from argon ion laser treatments.

Port wine stains are congenital vascular lesions consisting of ectatic capillaries. They are present in 0.3 to 0.5% of the population (Carruth and McKenzie, 1986), and often cause psychological problems. During the 1970's, Leon Goldman developed a successful treatment method using the argon ion laser (Goldman *et al.* , 1976). A variety of other vascular malformations, such as spider naevi, telangiectasia and

strawberry naevi have been treated with lasers (see for example Craig *et al.* 1985, Dixon 1987).

Yellow (570 to 585nm) light can on theoretical grounds be expected to produce a better result than the blue/green (488 to 514nm) light of the argon ion laser (Anderson and Parish, 1981; van Gemert *et al.*, 1982). This is so because melanin absorbs less yellow light than blue or green light, and because yellow light corresponds to an absorption peak of haemoglobin.

The clinical use of yellow light has been limited mostly to tunable dye lasers tuned to 577nm in either pulsed (Paul *et al.*, 1983; Garden *et al.*, 1988) or low-power continuous wave (Cotterill, 1986) modes. This practice has been justified by histological studies (Nakagawa *et al.*, 1981; Tan *et al.*, 1986) which illustrates that yellow light is more selectively absorbed by ectatic vessels within the skin than is blue or green light.

Since 1986 we have been using the yellow 578nm light from a Quentron™ QM91C copper vapour laser. A histological study has shown that the copper vapour laser, like the dye lasers, produces damage that is specifically concentrated on the ectatic vessels, rather than non specifically throughout the dermis (Walker *et al.* 1989). Prior to this we had treated patients with an argon laser at 514nm (from 1982 to 1986) and briefly in 1986 a dye laser tuned to 577nm.

We have treated port wine stains in 64% of the sessions, telangiectasia in 16%, spider naevi in 9% and a variety of other lesions such as strawberry naevi, venous flares, and venous lake in the remaining 11% of the sessions.

This paper presents information on three aspects of the treatment of vascular malformations. The first is the treatment technique used with the copper vapour laser. Because of the number of variables involved, anyone wishing to reproduce our treatment will require the details of our technique which we present in the materials and method section.

The second aspect of the treatment is a detailed study of port wine stain patients after the first treatment to their whole lesion. This study allows us to explore the effects of age, initial lesion colour, skin pigmentation, laser power and illumination time (the time the laser is on any one point on the lesion). Furthermore, because of the changes in the illumination times we have used, we are able to provide some clinical evidence that supports the theoretical models (Anderson and Parish 1981, van Gemert *et al.* 1982, 1986 and Pickering 1989a, 1989b) which suggest a short 1 to 10ms "ideal" illumination time.

The third part to this paper is the presentation of the results of port wine stain patients who have completed treatment. These are patients who have either responded well, to the extent of removing at least 70% of the lesion, or have not noticeably responded after four treatments.

Materials and method

Equipment

The copper laser produces a train of 50 ns pulses of light at a rate of approximately 16 kHz. Two wavelengths of light are produced: green 511 nm and yellow 578 nm. This laser differs in its delivery of light from that of the dye lasers, which are either continuous wave or single pulsed (300 ns to 450 μs pulse length). For all vascular lesions, we filter out the green light and use only the yellow. We have used up to 6.5 watts of 578 nm light.

The light is delivered to the lesion via a 1 mm diameter quartz optical fibre. The end of this fibre protrudes from a pen-shaped handpiece, and has been ground flat and roughly polished. Light delivery is controlled by a pneumatic foot switch.

For eye protection the surgeon and assistants are provided with goggles or glasses containing Schott™ BG36 filter lenses. These lenses contain a mixture of rare earth elements that absorb yellow 578 nm light, but allow essentially unimpaired colour vision at all other wavelengths (van Halewyn *et al.* 1989).

The patient's eyes are covered with red perspex shields which are opaque to yellow light. However, when treating lesions close to the eye, we use a contact lens-shaped Medishield™ eye shield, which is also opaque to yellow light. This shield is inserted under the eyelid after anaesthetising the eye with 4% ophthalmic Xylocaine™ (Lignocaine Hydrochloride 43 mg/ml, Astra Pharmaceutical).

Preparation of patients

In the majority of the cases we treat, the lesion has been exposed to sunlight. For this reason we prescribe ultraviolet block factor 15 (UV Ultrablock, ICI, 8% octyl dimethyl para aminobenzoic acid; 2% butyl methoxydibenzoylmethane; 5% benzophenone–3) and 3% hydroquinone topical creams for application 5 to 6 weeks before treatment. The ultraviolet block reduces the stimulation of melanocytes, whilst the hydroquinone chemically suppresses the production of melanin (Kligman and Willis, 1975; Engasser and Maibach, 1981; Boyle and Kennedy, 1985). These simple precautionary procedures can increase the optical window for the transmission of laser light to the underlying dermis and vascular plexus. Both creams are used between treatment sessions and for 3 months after treatment in order to maintain a low level of melanin production and to reduce the risk of hypopigmentation and hyperpigmentation. Maillard and Geinoz (1985) have reported that the post-treatment use of an ultraviolet block reduces the incidence of hyperpigmentation.

Congestion may be induced to increase the volume of the haemoglobin within the lesion.

For young patients, or for those with extensive lesions (usually greater than 60 cm^2), a general anaesthetic is used in order to minimise distress. Distress is undesirable not only from the patient's point of view, but also for the treatment,

because it can cause the vessels to constrict through endogenous adrenalin production. In other cases, we anaesthetise locally with injections of 2% plain Xylocaine™ (Lignocaine Hydrochloride B.P. 2.13%, Astra Pharmaceutical) by block anaesthesia or local infiltration. The amount of haemoglobin within the lesion will affect the amount of light absorbed. The greater the amount of haemoglobin present, the shorter the time period needed for the application of enough light to damage the blood vessels. As a consequence, there will be less time for heat to be conducted away from the vessel and possibly to cause unwanted damage. Hence, to maintain the volume of haemoglobin within the lesion, the local anaesthetic must be non–vasoconstricting. Plain Xylocaine™ has a mild vaso-dilating effect which enhances blood volume. For the rare instances when patients become distressed, we keep on hand a rapidly acting sublingual tranquilizer (Ativan™).

The treatment

On the basis of clinical observation, each patient is assigned to a particular class of vascular abnormality. The periphery of the area to be treated is marked with a green pen, which contrasts with the colour of the lesion. The green outline provides a finishing point for the scan because the true edge of the lesion is not easily discerned when the scanning is rapid. The fibre optic handpiece is scanned across the area about 2 mm above the skin surface. Normally, the scans follow the lines of Langer. This minimises the uneveness in blanching which is sometimes noticeable after the first treatment. Individual scans are typically up to 10 cm in length, depending on the size and shape of the lesion. Part-length scans are used to feather the area in cases where the grain of the skin broadens (Fig. 1). On second and subsequent treatments we scan so as to fill the gaps between scans of the original treatment. The striped look is usually no longer apparent after two or three treatments (Fig. 2). We have assumed that sufficient damage has been caused if the skin just blanches (minimal blanching). We start treatment at a point on the lesion near the periphery and if possible at a point normally not exposed (for example under the hair line). We establish the scan rate to achieve minimal blanching within one or two scans and use this rate throughout the lesion. As we can interactively assess the lesion colour and degree of blanching during treatment we are able to make any adjustments to the scan rate if necessary.

With the copper vapour laser, up to 6.5 watt of light is available from the fibre as measured by an integrating sphere. We have found with this power 3 s/cm^2 is the fastest rate at which scanning can be done reliably by hand. The fluence may vary between patients from up to 50 J/cm^2 to below 10 J/cm^2, but is typically between 20 and 30 J/cm^2. Figure 3 illustrates the relationship between power and scan rate, and illustrates the consistency of treatment achieved by using the same scanning strategy for all patients.

This treatment technique applies in broad outline to all vascular lesions, but in

Figure 1: The scanning strategy is illustrated by the white lines (indicating minimal blanching) on this nine year old boy. The scanning is in the lines of Langer. This is the first treatment to the boy's face and the second to his neck.

Figure 2: The same nine year old boy as in figure 1 after four treatments. The striping effect in figure 1 is not apparent. The lesion has undergone a marked decrease in colour. Note the complete removal of parts of the lesion above the eye.

particular to port wine stains. However, some lesion-specific strategies are used.

For spider naevi the central vessel, the "body" of the spider, is completely blanched to prevent re-establishment. The radiating capillaries, the "legs", are scanned individually, since they can remain ectatic even when the pressure from the central vessel has been relieved. Treatment of spider naevi "bodies" seldom requires more than 1 second of illumination with 3 or more watts.

Telangiectasia are usually marked out and treated in the same manner as port wine stains. Particular emphasis is placed on maintaining congestion by having a high ambient room temperature, applying warmth, positioning of the patient horizontally and sometimes light slapping of the lesion. For female patients with mild telangiectasia (or with rosacea), an area above the cheekbones where blush makeup may normally be applied, may be left untreated if desired.

Post–treatment

Immediately after treatment, the skin feels normal to the touch. For the patient's comfort, the area is dressed with a soothing Silverzine™ burn cream (Silver Sulphadiazine 1%, Chlorohexidine gluconate 0.25%, Smith and Nephew).

On recovering from the anaesthetic, patients notice a warm sensation akin to severe sunburn. This sensation lasts for only 20 or 30 minutes and needs no analgesics. Some hours later, the damaged endothelium leaks plasma, causing fine blisters at the epidermal/dermal interface. One day later, the Silvazine dressings are changed. The dressings are finally removed by the patient on the third day, usually by washing off, and the areas allowed to dry and to form fine scabs which are shed over a period of 10 days to 2 weeks. As soon as the scabs separate, the patient again begins to apply the ultraviolet block and 3% hydroquinone creams. The lesion continues to fade over the ensuing 6 to 12 weeks. Normally, patients return for another treatment after approximately 3 months, which is enough time for any erythema or hyperpigmentation to disappear. Histology show the epidermis to be normal and permanent damage to be confined to the ectatic vessels (Walker *et al.* 1989).

Assessment

All power measurements were made by the use of an integrating sphere. The area of the lesion and total exposure time were measured. From these the scan rate was calculated.

The colour of the treated areas was assessed by comparing photographs taken before each treatment. This was carried out by a single observer who was familiar with the treatment. A four-point scale ranging from light/salmon pink to dark red/purple (Table 1) was used to grade the initial colour of the lesion. A four-point scale ranging from poor (no change) to excellent (substantially closer to normal skin) (Table 2) was used to grade the change in colour after the first treatment.

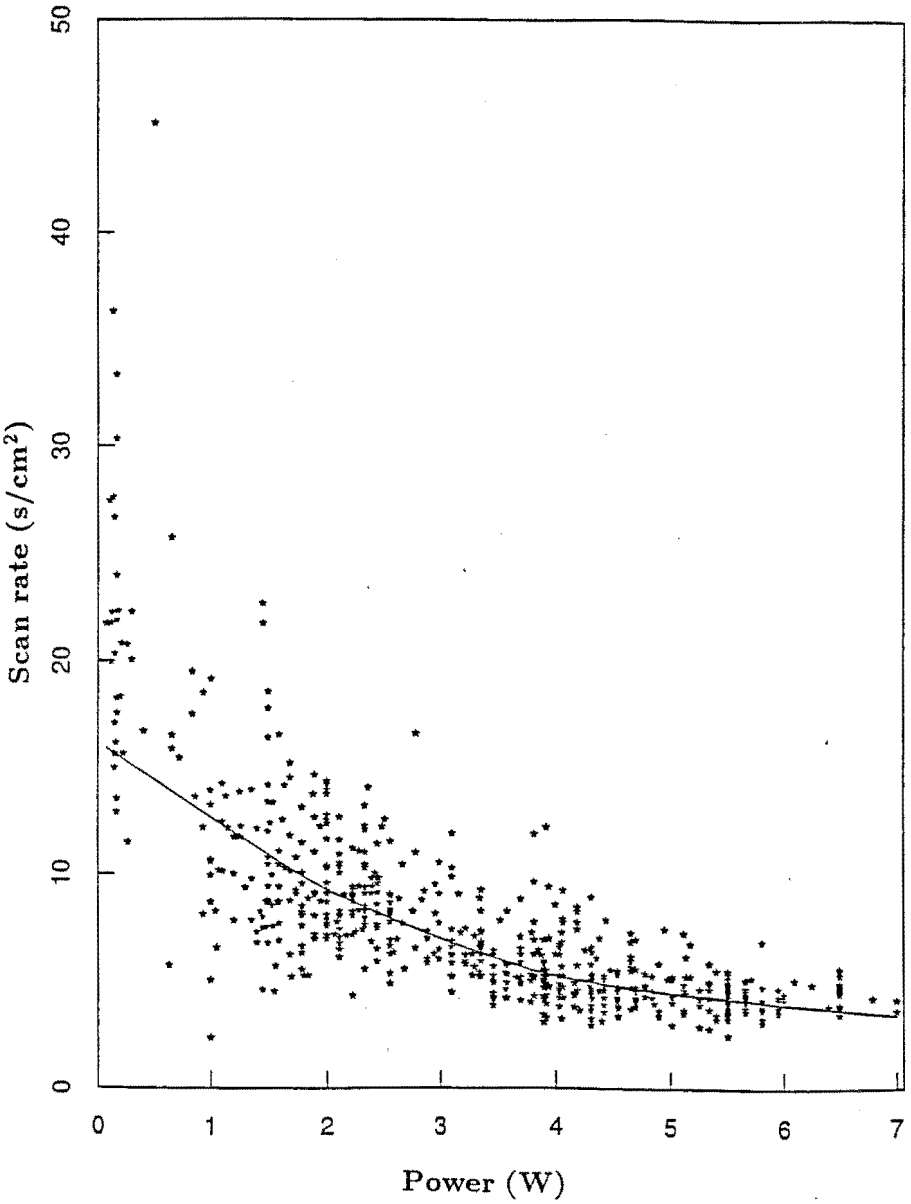

Figure 3: Scatter diagram of the scan rates and powers used for each treatment. The decrease in scan rate for higher powers is indicative of the consistency of the minimal blanching end-point of the treatment.

In the completed patients' section, we use Quaba's (1989) five-point colour change scale (Table 3). Quaba's scale takes into account both hypo- and hyper-pigmention and is a measure of the colour change from the initial colour to the colour at the time of assessment after a number of treatments.

Although we have presented some of our results statistically, these results must be regarded in the context of hypothesis formulation rather than hypothesis testing. This is because of the exploratory rather than the experimental nature of the investigation. As we have mentioned above, there has been a great deal of consistency between the treatments, both in the method of treatment (minimal blanching for all patients) and in the analysis of results. Thus, for some of the apparently conclusive results, we have presented a probability value (p) as if we were attempting to show that we could not disprove a hypothesis. We used the t test when comparing groups of measured data such as age or area, and the χ^2 test for testing of independence when comparing two sets of information, such as the dependence of colour change on power.

Results and discussion

The first treatment.

A group of one hundred and seventy four patients were evaluated after their first treatment. The average decrease in area after the first treatment was 19 $\pm$ 20% (mean $\pm$ sd). This decrease represents the area that has changed colour to the extent that it now resembles normal skin and no longer needs to be treated. This is normally at the periphery of the lesion. Most of the lesions (61%) also showed some lightening (grade 1 to 3, Table 2) of the remaining area.

(i) The effect of power (or scan rate). The level of power used had no effect on the percentage area reduction. However, it is evident that the higher power levels, with their correspondingly faster scan rates, produced a consistently greater colour change ($p < 0.0005$, Table 4). The faster scan rates correspond to a shorter illumination time, with the fastest scan rate (3 s/cm^2) corresponding to an illumination time of approximately 40 ms. This is still at least a factor of four longer than the ideal illumination times suggested by the theoretical models. However, it is evident that our improved results with shorter illumination times provide some clinical evidence for the models.

(ii) The effect of age and initial lesion colour. The average age of all patients was 27 $\pm$ 15 years. The average age for those showing no colour change (grade 0) was 21 $\pm$ 15 years, whereas for those exhibiting an excellent colour change (grade 3) was 36 $\pm$ 13 years. This suggests that better results are obtained with older patients.

It is well known that the light pink lesions are prevalent in children, and that lesions darken with age (Barsky *et al.* , 1980). (This was certainly true for our patients.) By comparing initial colour and first colour change we find that darker

Table 1:

Grade	*Definition*
0	light/salmon pink
1	pink
2	red
3	dark red/purple

Table 2:

Grade	*Description*	*Definition*	*Approximate % Change*
0	poor	no change	0%
1	fair	slight lightening	< 25%
2	good	obvious lightening	25–60%
3	excellent	near normal skin	> 60%

Table 3:

Grade	*Definition*	*Approximate % change*
−1	↑↓ pigmentation	
0	Nil – Slight change	0%+
1	Moderate lightening	50%
2	Marked lightening	75 to 80%
3	Total blanching	100%

Table 4:

Colour change	*Power (watts)*		
	low	*medium*	*high*
	< 2	*2 - 4*	*> 4*
0	0.55	0.25	0.08
1	0.26	0.30	0.24
2	0.15	0.38	0.33
3	0.04	0.08	0.35

lesions (initial colour grade 2 or 3) are more likely to result in a good or excellent colour change ($\chi^2_{3df} = 91.3$, $p < 0.0005$). This has also been the case with argon lasers (Cosman 1980 and Ratz 1987). However Garden *et al.* 1988 commented that the darker red lesions did not respond as well as other lesions to the yellow light from a pulsed dye laser. Figure 4 shows a good colour change (grade 2) from a patient with an initial colour of red (grade 2).

It is notable that the average power and scan rate were reasonably consistent for all initial lesion colours .

(iii) Changes in area and colour. Patients who showed a good colour change (grade 2 or 3) tended to exhibit a greater change in percentage area than those whose colour changes were poor ($p < 0.005$).

(iv) Non-Caucasian patients. Thirteen Maori, Polynesian, or Asian patients were treated. Their average age (23 $\pm$ 12 years) and initial colour distribution were consistent with those of the other patients, and they showed the same distribution of colour change. However, the average change in percentage area after the first treatment, at 6.6%, was less than that for Caucasian patients. The abundance of overlying melanin in non-Caucasians means that less light will reach the ectatic vessels. Satisfactory results are obtainable, however, as illustrated by figures 5 and 6. These photographs of a 38 year old Maori woman are pre-therapy and post the fifth treatment session respectively (patient 24 of table 5).

Completed treatments

(i) Good and poor results In tables 5 and 6 we have presented detailed assessment of 46 patients from a group of 236 patients (which includes the 174 patients which we assessed after their first treatment) out of the total of 297 patients. The other 61 patients treated have had only one treatment, the results of which have not been assessed. This group contains additional patients to the group assessed after their first treatment because with this group the assessment was carried out at a later date.

The 236 patients have had on average 3.3 treatments. Of the two assessing parameters, area change and colour, the measurement of area change is objective within the limits of area measurement. On the other hand the colour change is a subjective measurement. However, we have attempted to remain as true to Quabba's colour change parameters (Table 3) as possible.

Thirty six patients have completed treatment to the extent of removing at least 70% of the lesion (Table 5). As our experience shows that repeat treatments can continue to remove the lesion, several of these patients are undergoing further treatment (indicated in the table by a + symbol after the % area reduction). Figures 7 and 8 are before and after photographs of patient 28 of table 5. Ten other patients have received at least four treatments with a less than 30% reduction in area and slight or no colour change. All other patients are continuing treatment and fall

Figure 4: A good result (grade 2) on the clavical of this 55 year old women is seen in contrast to the original colour of the lesion on the untreated shoulder (initial colour 2). The treatment parameters were 2.7 watts at a scan rate of 11 s/cm^2. The area on the neck has received two treatments.

Figure 5: A 38 year old Maori woman shown prior to therapy. The lesion has a red initial colour (grade 2). This is patient 24 of table 5.

Figure 6: The same patient as figure 5 after 4 treatments. Her lesion has shrunk by 70% and has considerably faded in colour (Grade 2 on Quabba's scale). However the difficulties with pigmented skin are illustrated by a small 1 cm by 0.5cm hypertrophic scar on the lower left jaw bone. This patient was satisfied with the treatment at this point and has been discharged.

Table 5:

Patient	*Age (years)*	*Area (cm^2)*	*Initial colour*	*Number sessions*	*Area loss (%)*	*Col change (Quabba)*	Comments
1	5	47	1	5	83+	1	
2	11	18	1	3	100	3	
3	13	5	1	4	80+	1	
4	13	36	1	3	97+	2	0.5 cm^2 hypertrophic scar
5	15	84	0	1	85+	0	
6	16	4	3	2	100	3	some previous TiO_2 tattoo
7	18	135	1	4	70+	1	
8	21	18	2	5	92+	2	
9	21	31	2	5	74+	2	
10	21	33	2	5	95	2	
11	22	55	3	3	70+	2	Neck - removed, face - col decrease
12	23	2	1	2	75+	0	
13	23	12	1	3	75	2	
14	26	14	2	3	100	3	slight hollow
15	27	52	2	9	78+	2	
16	29	28	2	3	100	3	
17	31	33	2	4	80+	2	
18	31	71	2	5	86+	2	
19	33	4	3	3	75+	2	
20	33	36	0	3	100	3	
21	36	20	2	4	75+	2	
22	38	21	1	3	75+	1	
23	38	188	3	5	85	2	
24	38	66	2	4	70	2	Pigmented skin. 0.5 cm^2 hypertrophic scar
25	40	12	2	4	79+	2	
26	41	50	2	5	100	2(3-1)	slight hypopigmentation.
27	45	16	2	4	94+	2	
28	45	42	2	2	87+	2	
29	46	66	1	4	85+	1(2-1)	slight hypopigmentation.
30	54	58	3	3	70+	2	
31	55	28	2	3	100	3	
32	58	85	2	5	77	1	
33	64	31	2	4	77+	2	Test Argon had left 2 hypopigmented marks.
34	64	71	2	5	70+	2	
35	67	29	3	4	71+	2	
36	75	200	1	8	88+	1	

Table 6:

Patient	*Age (years)*	*Area (cm^2)*	*Initial colour*	*Number sessions*	*Area loss (%)*	*Col change (Quabba)*	Comments
1	8	7	2	4	29+	0	
2	14	101	1	4	0	0	
3	15	6	0	5	16+	0	
4	16	150	1	4	0	0	Maori
5	17	175	1	7	0	0	
6	18	49	1	6	18	0	
7	20	24	1	6	16	0	
8	20	4	0	6	25	0	
9	21	7	1	4	29+	0	
10	32	9	1	6	22	0	

somewhere between the good results (Table 5) and the poor results (Table 6) at this stage of their treatment.

The obvious difference between the good and poor results is that the age and initial colour distribution of the poor results is lower than that of the good results. Of all the patients who had undergone four or more treatments 10% responded poorly and 21% fall into the good catogory. The other 68% of patients are still undergoing treatment, some of which may yet have a good result. In addition 11% of those who have yet to undergo four treatments have already had 70% or more of their lesion removed.

We find that most of the colour and area reduction occurs with the first few treatments and thereafter the lesion becomes more difficult to treat. This is probably because of the deeper nature of the ectatic vessels.

The poorest results were from spongy/salmon-pink stains that had a tendency to blanch quickly (particularly patients 1,3,7 and 9 in table 6). In some cases there was no detectable change in colour. These also had small areas and although some area change is evident, visually it is not a significant change. Ratz 1987 suggests that these lesions, which blanch quickly yet do not produce a good result, are likely to have faster flowing blood and hence a less effective "target" for the light.

(ii)Adverse effects Adverse effects have been recorded; six cases of scarring, two cases of hyperpigmentation (excessive browning) and two cases of hypopigmentation (excessive whitening). In all six cases of scarring, only a small fraction of the treated area (less than 5%) was affected. Table 7 gives the percentages for the adverse effects per patient and per treatment. The $3.5 \pm 1.4\%$ patient scarring rate is less than the 5 to 30% rates for argon ion lasers (Cosman 1980; Dixon *et al.*, 1984; Apfelberg *et al.*, 1987).

(iii)Comparison with argon laser The clinical results from the copper vapour laser for the treatment of port wine stains show a marked improvement in most patients.

Figure 7: A 45 year old Caucasian man shown prior to therapy. The lesion has a red initial colour (grade 2). (patient 28, table 5.)

Figure 8: The same patient as figure 7 after 2 treatments. The treatable area has shrunk from 42 cm^2 to 9 cm^2 and has considerably lightened in colour (grade 2). This patient is continuing treatment.

Table 7:

Effect		*% ± s.d.*
Scar	per patient	3.5±1.4
	per treatment	1.2±0.8
Hyperpigmentation	per patient	1.4±0.5
	per treatment	0.5±0.3
Hypopigmentation	per patient	1.4±0.5
	per treatment	0.5±0.3

Our own experience was that these results were better than those we had obtained with the argon ion laser. However, because of differences in treatment technique and laser parameters between ourselves and other treatment centres it is difficult to make a statistically significant comparison between the two laser systems.

Discussion

We have found the change in percentage area of port wine stains to be independent of the treatment parameters of power and scan rate. We have observed that lesions tend to be resolved from the outside in, and suggest that this may be so because the outside of a lesion is often thiner than its center, that is "saucer-shaped".

The greater colour change in the darker lesions is indicative of a greater absorption of light.

The adverse effects of treatment with the copper vapour laser are few compared to those associated with argon treatments, and although the number of patients was insufficient to confirm our suspicion that fewer adverse effects occur with higher levels of power, we nevertheless postulate that this may be the case. The physical reason for such a phenomenon would be that, at high levels of power, the exposure times are shorter and the heat is contained within the immediate surroundings of the ectatic vessels.

We have also described the difficulty we encountered in treating non-Caucasian patients, which was due primarily to the blocking of light to the capillaries by the overlying melanin.

The theoretical work (Anderson and Parrish 1981; van Gemert *et al.*, 1982; van Gemert *et al.*, 1986; Pickering *et al.*, 1989) suggests that the optimal exposure time is in the range of 3–10 ms. Our shortest exposure time is 40 ms, while the longest pulsed dye laser is about 0.45 ms. Our direct correlation between high power (or fast scan rate) and colour change seems to confirm this theoretical work.

Acknowledgements

Our thanks go to Dr. Graham Wood of the Mathematics Department, University of Canterbury for his help with the statistics, and to Medical Laser Developments and the Medical Research Council of New Zealand for their financial assistance.

References

Anderson, R. R. and Parrish, J. A. (1981). Microvasculature can be selectively damaged using dye lasers: A basic theory and experimental evidence in human skin. *Lasers in Surgery and Medicine*, **1**, 263.

Apfelberg, D. B., Smith, T., Maser, M. R., Lash, H. and White, D. N. (1987). Dot or pointillistic method for improvement in results of hypertrophic scarring in the argon laser treatment of portwine hemangiomas. *Lasers in Surgery and Medicine*, 6, 552.

Barsky, S.H., Rosen, S., Geer, D.E. and Noe, J.M. (1980). The Nature and evolution of port wine stains: A computer assisted study. *The Journal of Investigative Dermatology*, **74**, 154.

Boyle, J. and Kennedy, C.T.C. (1985). Leucoderma induced by monomethyl ether of hydroquinone. *Clinical and Experimental Dermatology*, **10**, 154.

Carruth, J. A. S. and McKenzie, A. L. (1986). *Medical lasers.* Bristol, Adam Hilger Ltd.

Cosman, B. (1980). Experience in the argon laser therapy of port wine stains. *Plastic and Reconstructive Surgery* , **65**, 119.

Cotterill, J. A. (1986). Preliminary results following treatment of vascular lesions of the skin using a continuous wave tunable dye laser which emits at 577nm. *Clinical and Experimental Dermatology*, **11**, 628.

Craig, R.P., Purtser, J.M., Lessells, A.M. and Hufton A.P. (1985). Argon laser therapy for cutaneous lesions. *British Journal of Plastic Surgery*, **38**, 148.

Dixon, J. A., Rotering, R. and Huether, S. (1984).Patient's evaluation of argon laser therapy of port wine stain, decorative tattoo, and essential telangiectasia. *Lasers in Surgery and Medcine*, **4**, 181.

Dixon, J. A., Huether, S. and Rotering, R. (1984). Hypertrophic scarring in argon laser treatment of port-wine stains. *Plastic and Reconstructive Surgery*, , **73**, 771.

Engasser, P.G. and Maibach, H.I. (1981). Cosmetics and dermatology: Bleaching creams. *Journal of the American Academy of Dermatology*, 5, a43.

Garden, J. M., Polla, L. L., and Tan, O. T. (1988). The treatment of port-wine stains by the pulsed dye laser. *Archives of Dermatology*, **124**, 889.

Goldman, L., Dreffer, R., Rockwell, R. J. and Perry, E. (1976). Treatment of portwine marks by an argon laser. *Journal of Dermatological Surgery*, **2**, 385.

van Gemert, M. J. C., de Kleijn, W. J. A. and Hulsbergen Henning, J. P. (1982). Temperature behaviour of a model port-wine stain during argon laser coagulation. *Physics in Medicine and Biology*, **27**, 1089.

van Gemert, M. J. C., Welch, A. J. and Amin, A. P. (1986). Is there an optimal treatment for port wine stains? *Lasers in Surgery and Medicine*, **6**, 76.

van Halewyn, C.N., Miles, C., Butler, P.H., Holdsworth, J. and Walker, E.P. (1989) Rare-earth doped eyewear provide for safer laser surgery. *British Journal of Dermatology*, **120**, 470.

Kiligman, A.M. and Willis, I. (1975). A new formula for depigmenting human skin. *Archives of Dermatology.* **111**, 40.

Maillard, G.F. and Gienoz, J. (1985). Argon laser photocoagulation of various angiomas. *British Journal of Plastivc surgery*, **38**, 156.

Nakagawa, H., Tan, O. T. and Parrish, J. A. (1985). Ultrastructural changes in human skin after exposure to a pulsed laser. *Journal of Investigative Dermatology* , **84**, 396.

Paul, B. S., Anderson, R. R., Jarve, J. and Parrish, J. A. (1983). The effect of temperature and other factors on selective microvascular damage caused by pulsed dye laser. *Journal of Investigative Dermatology*, **81**, 333.

Pickering, J. W., Butler, P. H., Ring, B. J. and Walker, E. P. (1989). Thermal profiles of blood vessels heated by a laser. *Australasian Physical and Engineering Sciences in Medicine*, **12**, 11.

Pickering, J. W., Butler, P. H., Ring, B. J. and Walker, E. P. (1989). Computed temperature distributions around ectatic capillaries exposed to yellow (578 nm) laser light. *Physics in Medicine and Biology*, **34**, 1247.

Quaba, A. A. (1989). Results of argon laser treatment of port wine stains: A method of assessment. *British Journal of Plastic Surgery*, **42**, 125.

Ratz, J.L. (1987) Laser applications in dermatology and plastic surgery. *Surgical Application of Lasers (ed. Dixon, J.A.).* Chicago, Year Book Medical Publishers, **Ch. 9**, 160.

Tan, O. T., Carney, J. M., Margolis, R., Seki, Y., Boll, J., Anderson, R. R., and Parrish, J. A. (1986). Histologic responses of port-wine stains treated by argon, carbon dioxide, and tunable dye lasers. *Archives of Dermatology*, **122**, 1016.

Walker, E. P., Butler, P. H., Pickering, J. W., Day, W. A., Fraser, R., and van Halewyn, C. N. (1989). Histology of port wine stains after copper vapour laser treatment. *British Journal of Dermatology*, **121**, 217.

Appendix F THERMAL RELAXATION TIME CALCULATIONS

The thermal relaxation time of a structure is an estimate of the time required for that structure to release a certain fraction of the heat within it. In the case of blood vessels this time is normally defined as:

> *The time it takes for the central temperature to fall to half way between its peak temperature and the temperature of the structures surroundings.*

To calculate this time we begin with the fundamental law of heat conduction (in one dimension):

$$\frac{dQ}{dt} = -\eta A \frac{dT}{dx} \tag{F.1}$$

where

Q is the heat within the structure,

t is the time,

η is the thermal conductivity,

A is the area through which the heat is conducted,

T is the temperature (K), and

x is the path length of the conducted heat.

In the case of a blood vessel we have a cylindrical structure of length l and radius r. The heat contained within this structure when at a temperature ΔT above its surroundings is:

$$\begin{aligned} Q &= m C_v \Delta T \\ &= \rho \pi r^2 l \Delta T \end{aligned} \tag{F.2}$$

If we approximate the temperature gradiant $(\frac{dT}{dx})$ as $-\frac{\Delta T}{r}$ and allow the vessel length to be long in comparison to the radius so that most of the heat conducts through the vessel walls, then by substituting into equation F.1, we have for a 50% drop in the relative peak temperature a thermal relaxation time (τ) of:

$$\begin{aligned} \tau &= \frac{1}{2}\frac{\rho C_v \pi r^2 l \Delta T}{\eta 2\pi r l \frac{dT}{dx}} \\ &= \frac{1}{4}\frac{\rho C_v}{\eta} \end{aligned} \tag{F.3}$$

This illustrates the approximate nature of the thermal relaxation time. This equation, with the values for ρ, C_v, and η from table 1 Pickering *et al.* 1989a, gives a thermal relaxation time for a 30 μm diameter vessel of 0.3 ms, and a 100 μm diameter vessel of 3.5 ms.

Similarly we may calculate the thermal relaxation time of a sphere. This is:

$$\tau_{sphere} = \frac{1}{6}\frac{\rho C_v}{\eta} \tag{F.4}$$

In particular if we approximate erythrocytes and melanosomes as spheres then we have a thermal relaxation time for a 5 μm diameter erythrocyte of 0.006 ms and for a 0.7 μm diameter melanosome of 0.0001 ms.

The calculation of the thermal relaxation time is most useful if it happens to be considerably longer than the illumination time. In this case we may estimate that most of the energy absorbed within the structure will result in a temperature rise or phase change, rather than be conducted away from the structure.

Two applications of this principle are particularly important. The first is with pulsed dye lasers with pulse lengths much shorter than 0.006 ms (usually 0.0003 ms, 0.001 ms, or 0.0015 ms). An erythrocte has a mass of approximatey 6.5×10^{-11} gm. Thus, with a heat of vaporisation of 2274 J gm^{-1}, 1.5×10^{-7} J of energy would need to be absorbed at the boiling point of the haemoglobin in order to vaporise the cell totally. If we approximate this erythrocyte as a disk of 5 μm diameter and a volume the same as a sphere of this diameter, approximately 27% of the incident light will be absorbed. To raise the sphere to a temperature of 100 °C would require approximately 0.3 J/cm^2. Any excess energy would therefore result in vaporisation of some of the haemoglobin within the cell. The resulting rapid expansion of the steam is likely to cause cell and vessel wall rupture. This phenomenon has been observed at these illumination times.

The second application of the thermal relaxation time of a structure uses a similar argument to above but with respect to melanosomes. This suggests that at 351 nm and with a pulse length much shorter than 0.0001 ms, approximately 0.04 J/cm^2 will heat the melanosome to 100 °C. Additional energy would result in some of the melanosome vaporising. The skin surface threshold fluence for melanosome degradation at this wavelength is 0.12 J/cm^2 (Murphey *et al.* 1983).

The other potential use for considering thermal relaxation times is when assessing for some heating time scale whether structures are thermally isolated from each other

or not. If the illumination time is much longer than the thermal relaxation time of the structure then during its heating a considerable amount of heat will be conducted away and surrounding structures can be expected to be heated. However, what is of major importance is the separation between structures. Close, or in contact, structures such as erythrocytes within blood vessels are unlikely to be thermally isolated, except on the shortest of illumination times when the total heat generated is small. Yet, structures such as blood vessels are thermally isolated except with the very long (hundreds of milliseconds) illumination times. For example we find that for a 50 μm diameter vessel, a 30 ms illumination time, and a maximum blood temperature of 100 °C that the maximum temperature at a distance of 95 μm above the vessel lumen is 35.9 °C. The average inter-vessel distance (Barsky *et al.* 1980) is 120 μm. Thus, we conclude that for all but the longest illumination times that the vessels are, on average, thermally isolated from one another. However, some vessels may be exceptionally close to one another, or may be sufficiently close to the epidermis, for them not to be thermally isolated.

Appendix G ACKNOWLEDGEMENTS

It is difficult to know where to start when there are so many people to thank for their help and support. Perhaps if I start with a disclaimer and thank all those people who I may forget to mention by name.

First I must thank my late Grandma Pickering who encouraged me to choose the study of lasers in surgery as my PhD topic.

My wife, Jane, has been a continual source of encouragement and has helped with the proof reading of this manuscript, thank you Jane. My parents and the rest of my family have also given me great support.

My most sincere thanks go to my supervisor, Phil Butler. Phil, your optimism, guidance, and drive have been invaluable to me, it has been a real pleasure working with you.

It has also been a pleasure working with our plastic surgeon Peter Walker. I have enjoyed your company in the operating theatre and have been most fortunate to be able to learn so much from you. I'm sure you will the agree that quality of the nurses and anaesthetists (principally Bill Barlow) at St Georges Hospital have added considerably to the treatment.

I have also had the pleasure of working with pathologists Tony Day and Robin Fraser. Thank you both for your help with the histology.

I have received considerable assistance from my fellow students who have worked with me on this project. Namely, Chris van Halewyn, Brendan Ring, and Derek Smithies. The technical staff within the Physics Department have been outstanding, especially Stephen Hemmingsen, Crispin Maclean, and Bernie Mentink. Without these people the research would have stagnated many times.

On the academic side I have also received help from Drs Graeme Wood and Rod Claridge.

Like any research there are financial costs. I have been very fortunate in the assistance I have had. Medical Laser Developments provided me with a scholarship for the first year of this research. Not only for this assistance but for the considerable input into the laser, the scanner system, and the many other aspects of the research I thank the directors of this company for their courage, commitment, and vision.

Since January 1988 it has been a pleasure to be a Medical Research Council of New Zealand Postgraduate Fellow. The MRC have been generous in their support, not only with this fellowship, but also with a grant to travel to the 8th Congress of the International Society of Lasers in Surgery and Medicine in Taipei in November 1989. I also wish to thank the Rotary Club of Hornby for their generosity in supporting my travel to this conference. This conference was invaluable to me.

I also received travel funds from the Canterbury branch of the Royal Society of New Zealand. These funds assisted my travel to the annual conference of Engineering and Physical Sciences in Medicine, Brisbane, August 1988.

The organisers of these two conferences also deserve thanks. I am most grateful for the opportunity to present papers and meet with other researchers.

Two special thanks need to be made. First to my friends Claire and Lloyd Carpenter. Thanks guys for the support, especially the chance to drop out of (or was it drop into) normallity occasionally. Your generosity in helping me make the Taiwan conference was incredible. Second my thanks go to my brother-in-law Marty Stone. Marty your cartoons are brilliant, I'll be the first to buy a book of them!

Finally I thank the tea-room students and staff. It's often extremely supportive to hear that yours isn't the only computer program that fails, or to be able to wonder aloud, why?

Thanks all.

JP